

RESPONSE SPECTRA OF COUPLED ACOUSTICAL  
RESONATORS TO TRANSIENT EXCITATION

By

NARAYANA N. REDDY

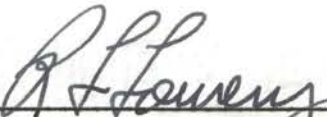
Bachelor of Engineering  
University of Mysore  
Mysore, India  
1960

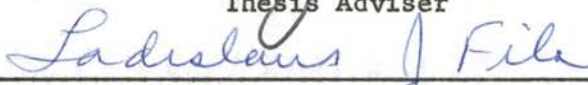
Master of Engineering  
Indian Institute of Science  
Bangalore, India  
1962

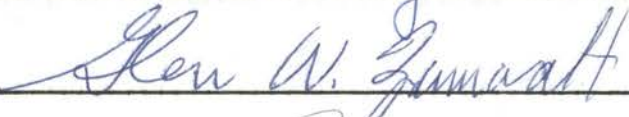
Submitted to the faculty of the Graduate College  
of the Oklahoma State University  
in partial fulfillment of the requirements  
for the degree of  
DOCTOR OF PHILOSOPHY  
May, 1967


RESPONSE SPECTRA OF COUPLED ACOUSTICAL  
RESONATORS TO TRANSIENT EXCITATION

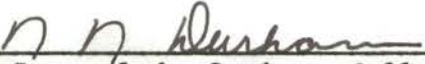
Thesis Approved:

  
\_\_\_\_\_  
Thesis Adviser

  
\_\_\_\_\_

  
\_\_\_\_\_

  
\_\_\_\_\_

  
\_\_\_\_\_  
Dean of the Graduate College

JAN 16 1968

### ACKNOWLEDGMENTS

I wish to express my sincere regards and appreciation to Dr. R. L. Lowery for his encouragement given throughout my graduate studies at Oklahoma State University and his interest and guidance in conducting this investigation.

I am particularly indebted to Professor L. J. Fila for his encouragement and helpful suggestions given during the conduct of this research. Thanks are due Drs. G. W. Zumwalt and J. R. Norton for serving as members of my advisory committee. I am thankful to Mr. G. D. Whitehouse for his general assistance in this investigation and to Dr. M. N. Reddy for his suggestions in mathematical analysis.

I wish to give particular recognition to my brother Muni Reddy and his wife Kamala for their encouragement to continue my higher education.

## TABLE OF CONTENTS

Chapter	Page
I. INTRODUCTION . . . . .	1
Definition of the Problem . . . . .	3
Purpose and Scope of the Study . . . . .	5
II. PREVIOUS INVESTIGATIONS . . . . .	8
III. MATHEMATICAL MODEL . . . . .	13
Limitations of Lumped Parameters for Acoustical Resonators . . . . .	13
Consideration of Damping in Acoustical Resonators . . . . .	15
Pressure Response of Double Acoustical Resonators . . . . .	17
Transmission of Energy from one Resonator to the Other . . . . .	28
Merits and Demerits of Analog Computer . . . . .	30
IV. THEORETICAL RESULTS . . . . .	31
Governing Equations . . . . .	32
Uncoupled and Coupled Frequencies of the System . . . . .	33
Damped Acoustical Resonator . . . . .	35
Mechanical System . . . . .	55
V. EXPERIMENTAL MODEL AND INSTRUMENTATION . . . . .	63
Description of the Model . . . . .	63
Simulation of Sonic Boom and Other Types of Transient Pressures . . . . .	66
Testing and Instrumentation . . . . .	68
VI. EXPERIMENTAL PROCEDURE AND RESULTS . . . . .	72
Natural Frequency and Damping Measurements . . . . .	72
Pressure Response in Time Domain . . . . .	76
VII. CONCLUSIONS AND RECOMMENDATIONS . . . . .	85
BIBLIOGRAPHY . . . . .	89

Chapter	Page
APPENDICES . . . . .	92
A. Response Solution of the Double Acoustical Resonator for Transient Excitation Pressures . .	92
B. Calibration and List of Major Instrumentation . .	111
C. FORTRAN Programs for the Response of the Double Acoustical Resonator . . . . .	114

LIST OF TABLES

Table	Page
I. Natural Frequencies of Typical Acoustic Structures . . . . .	36
II. Theoretical and Experimental Natural Frequencies of Resonators . . . . .	74
III. Microphone Sensitivity Comparison . . . . .	112

## LIST OF FIGURES

Figure	Page
1. Pressure Records Inside Buildings . . . . .	2
2. Double Acoustical Resonator . . . . .	4
3. Acoustical Network . . . . .	5
4. Simple Acoustical Resonators Used by Helmholtz (Spherical Cavities) . . . . .	9
5. Equivalent Mechanical System for Double Acoustical Resonator . . . . .	18
6. Excitation Pressure of Sine Pulse on Neck $N_1$ . . . . .	22
7. Excitation Pressure Made up of Straight Lines . . . . .	26
8. Building Structure That Can be Idealized as a Double Acoustical Resonator . . . . .	35
9. Pressure Beatings in a Double Acoustical Resonator . . . . .	37
10. Pressure Response Spectra in $V_2$ for a Constant Coupling Frequency (Effect of $f_1$ on Undamped Resonator) . . . . .	45
11. Pressure Response Spectra in $V_2$ for a Constant Coupling Frequency (Effect of $f_1$ ) . . . . .	46
12. Pressure Response Spectra in $V_2$ for a Constant $f_2$ (Effect of $f_1$ and $f_{12}$ ) . . . . .	47
13. Pressure Response Spectra in $V_2$ for a Constant $f_2$ (Effect of $f_2$ and $f_{12}$ ) . . . . .	48
14. Pressure Response Spectra in $V_2$ (Effect of $f_{12}$ ) . . . . .	49
15. Pressure Response Spectra in $V_1$ for Constant $f_{12}$ and $f_2$ (Effect of $f_1$ ) . . . . .	50
16. Pressure Response Spectra in $V_1$ for Constant $f_{12}$ and $f_2$ (Effect of $f_2$ and $f_{12}$ ) . . . . .	51

Figure	Page
17. Pressure Response Spectra in $V_2$ for Constant $f_{12}$ (Effect of $f_1$ With Damping Factors, $\xi_1=\xi_2=0.05$ ) . . .	52
18. Pressure Response for Constant $f_{12}$ (Effect of $f_1$ and Damping Factors) . . . . .	53
19. Pressure Response Spectra in $V_2$ for Constant $f_{12}$ (Comparison Response to Saw Tooth and N-wave Type Excitation) . . . . .	54
20. Mechano-Acoustic System . . . . .	56
21. Displacement Response Spectra of Two Degrees-of- freedom System (Mass $M_1$ is Excited by a Force of Sine Pulse) . . . . .	59
22. Displacement Response Spectra of Two Degrees-of- freedom System (Both the Masses are Excited by the Forces of Sine Pulses in the Opposite Direction) . . . . .	60
23. Displacement Response Spectra of Two Degrees-of- freedom System (Both the Masses are Excited by the Forces of Sine Pulses in the Same Direction) .	61
24. Configuration of Test Resonator (Double Acoustical Resonator) . . . . .	64
25. Test Resonator Assembly . . . . .	65
26. Test Resonator Mounted in Wooden Frame . . . . .	65
27. Plane Wave Tube . . . . .	67
28. Resonator Arranged With Plane Wave Tube . . . . .	67
29. Block Diagram of the Instrumentation . . . . .	69
30. Arrangement of the Resonator to Test the Effect of Loading Due to the Impedance of the Plane Wave Tube . . . . .	70
31. Arrangement of Microphones With Plane Wave Tube for Comparative Calibration . . . . .	70
32. Free Pressure Oscillations in the Resonator of 11.75 Inches Diameter, (Neck: 1 Inch Diameter and 1.25 Inches Length) . . . . .	75



Figure	Page
33. Free Pressure Oscillations in the Resonator of 4.25 Inches Diameter, (Neck: 0.5 Inches Diameter and 6 Inches Length) . . . . .	75
34. Pressure Response in Cavity $V_1$ . . . . .	79
35. Pressure Response in Cavity $V_2$ . . . . .	80
36. Time Response Measurements . . . . .	81
37. Response Pressures From Idealized Sine Pulse . . . .	82
38. Response Pressures by Straight Line Approximation. .	83

## LIST OF SYMBOLS

$A_1, A_2$	Cross sectional areas of the resonator necks
$A_0$	Absolute maximum value of the excitation pressure
$c$	Velocity of sound
$c_1, c_2$	Viscous damping coefficients in the resonator
$f_1, f_2$	Uncoupled natural frequencies of the system ( $2\pi p_1, 2\pi p_2$ )
$f_{12}$	Coupling frequency of the system ( $2\pi p_{12}$ )
$l_1, l_2$	Lengths of the resonator necks
$l_{e1}, l_{e2}$	Effective lengths of the resonator necks
$p_1, p_2$	Uncoupled circular natural frequencies of the system
$p_{12}$	Coupling circular frequency of the system
$p_+$	Higher coupled circular natural frequency of the system
$p_-$	Lower coupled circular natural frequency of the system
$P_1, P_2$	Pressures in the cavities $V_1, V_2$
$R$	Radius of the resonator neck
$x$	particle displacement
$\dot{x}, \ddot{x}$	First and second derivative of $x$ with respect to time (particle velocity, particle acceleration)
$X$	Volume displacement
$\dot{X}, \ddot{X}$	First and second derivative of $X$ with respect to time (volume velocity, volume acceleration)
$\alpha$	Correction factor for the length of the resonator
$\gamma$	Ratio of specific heats of air ( $c_p / c_v$ )

$\tau$	Period of excitation pressure
$\omega$	Circular frequency of excitation pressure ( $2\pi/\tau$ )
$\xi_1, \xi_2$	Damping factors in the system
$\rho_0$	Mass density of the air per unit volume

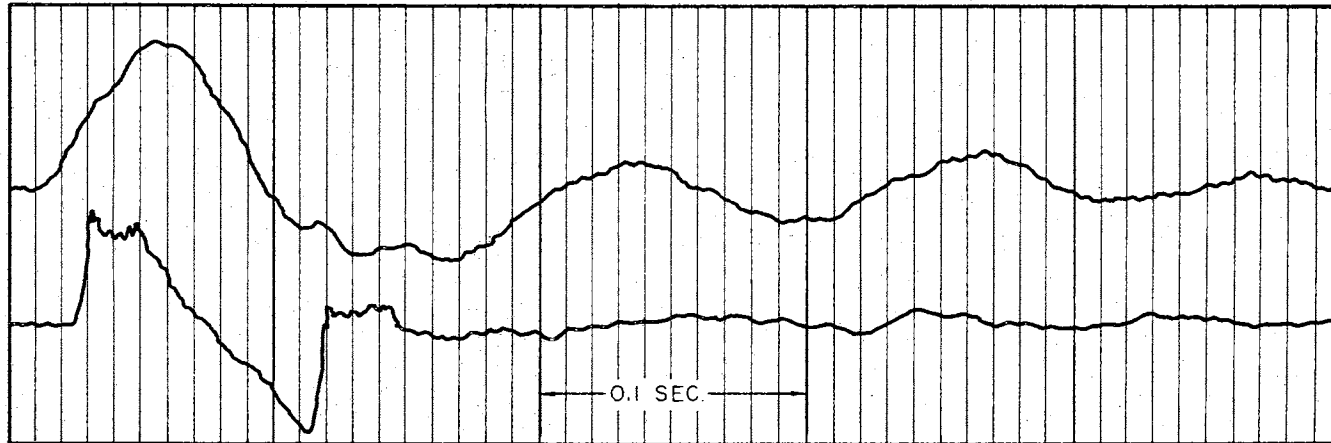
## CHAPTER I

### INTRODUCTION

The dynamics of acoustical or mechano-acoustical systems have been the object of the attention of engineers and scientists for the last few years. Many structures may behave as multiple acoustical resonators coupled together and exposed to acoustical excitation pressures. Typical structures which constitute coupled multiple acoustical resonators are domestic buildings with several rooms, connecting passage ways, doors and windows. In some cases the windows, with distributed mass and elasticity, coupled to a simple Helmholtz resonator behave as a multiple dynamic system with mechanical and acoustical elements coupled together. The pressure response measurements made inside a sonic boom test house and Kinney shoe store at Oklahoma City, Oklahoma (Figure 1), indicate that there is a considerable amount of damping in such structures. Because of this mechanism of energy dissipation, the pressure oscillations are not present for a long span of time. This shows the need for the consideration of damping in the response analysis of acoustic systems.

It has been a great concern to many investigators whether sonic booms will be acceptable to people. This important factor depends on the strength of the sonic boom and the structural response to finite duration excitation pressures like those of sonic booms. Whether the result of dynamic effect or not, the unintentional pressure

SONIC BOOM RECORD AT OKLAHOMA CITY - TEST HOUSE NO. 1 - FLT. 1 - 10 FEBRUARY 64



FREE PRESSURE OSCILLATIONS INSIDE KINNEY SHOE STORE AT OKLAHOMA CITY

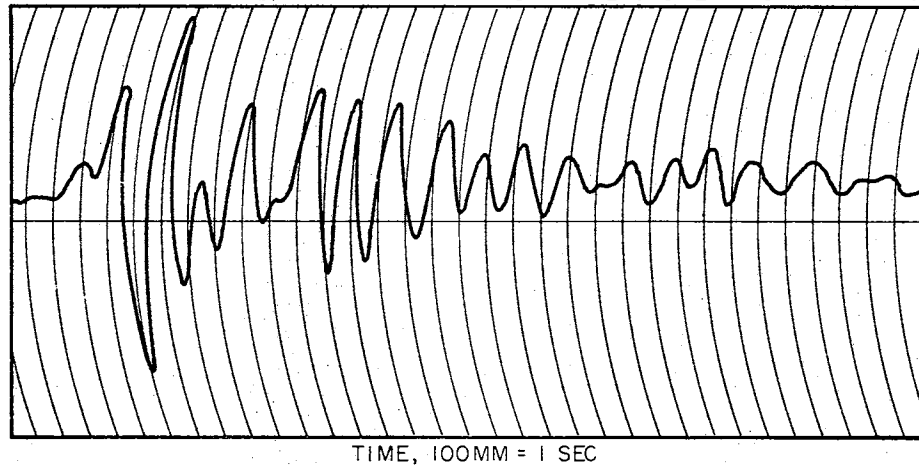


Figure 1. Pressure Records Inside Buildings

magnifications inside the buildings are the undesirable environments to be tolerated. These increased pressures can be the primary cause of damage to the structural components such as the windows and the doors in the buildings.

It is important to note that structural damage is simply an instantaneous consequence of the dynamic response of multiple acoustical resonators to transient excitation; the inadvertent discomfort of people due to pressure magnifications in buildings exposed to excitation pressures, such as blast pressures, gusts produced by storms, and noise generated by rocket launchings, is also substantial.

These considerations lead to a marked need for an understanding of the dynamic response of acoustical or mechano-acoustical systems to various types of pressures or force excitations. Recognition, isolation, and understanding of the parameters pertinent to the phenomenon of the system can provide a sound basis for design concepts.

#### Definition of the Problem

The total energy of a conservative system remains constant at all times. In the case of a dynamic system with multiple degrees-of-freedom this energy is distributed among the different natural modes and among various elements.

In a multiple acoustical resonator, the pressure magnification in each of the cavities or the magnification of the particle displacements at the necks depends on the type of coupling and the various system parameters. The following are the important system parameters which affect the response of acoustical networks:

1. Conductivities of various necks,

2. Relative volumes of the cavities, and
3. Damping in the system.

A double acoustical resonator consisting of two enclosed volumes,  $V_1$  and  $V_2$ , and two necks,  $N_1$  and  $N_2$  (Figure 2), is very common among the existing structures (4). When this system is excited with transient pressures on neck  $N_1$ , the pressures inside the cavities may be higher than the excitation pressures due to the dynamic effect of the system. If there is no dissipation of energy, and the two natural frequencies are nearly equal, the pressure oscillations will exhibit the beating phenomenon due to transfer of energy from one resonator to the other.

It is necessary to investigate the factors influencing the pressure magnification and the effect of various system parameters of a coupled resonator to a finite duration and aperiodic excitation.

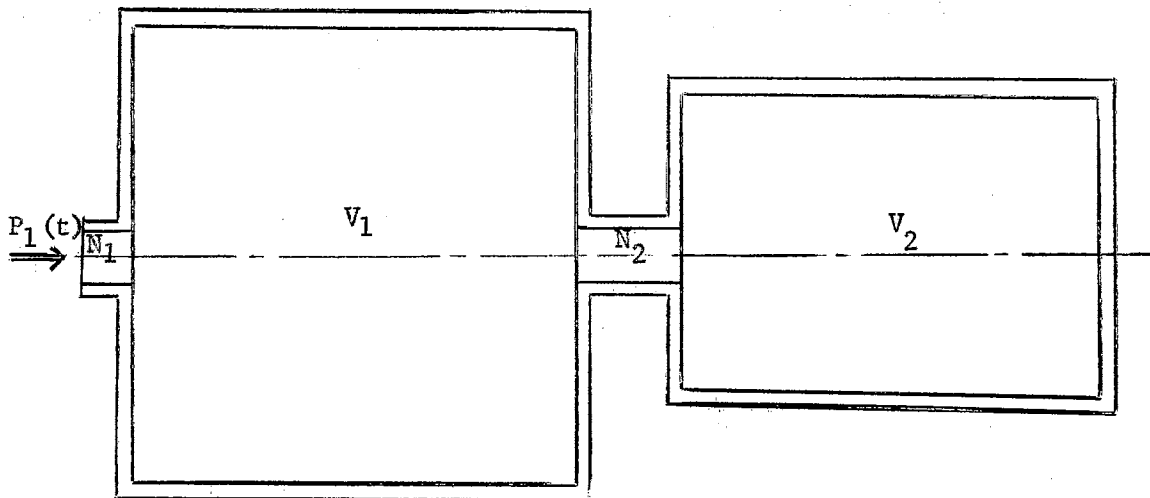


Figure 2. Double Acoustical Resonator

### Purpose and Scope of the Study

In general, any acoustical system is a continuous dynamic system. Under certain restrictions in a case like the acoustical resonator, it is possible to approximate the continuous system by lumping the parameters so that the response problem is amenable to mathematical treatment. It has been proven in the literature (3, 16) that the lumped parameter model is a good approximation for the Helmholtz resonator if the largest dimension is very small compared to the wave length in the steady state case. Also, Simpson (4) has established that the frequency limitations necessary for the lumped parameter assumption are less severe in the case of transient response of Helmholtz resonator than in steady state response. The lumped parameter approximation is valid even in the case of the acoustical network shown in Figure 3 provided that the largest dimension of any component is small compared to the wave length at resonance.

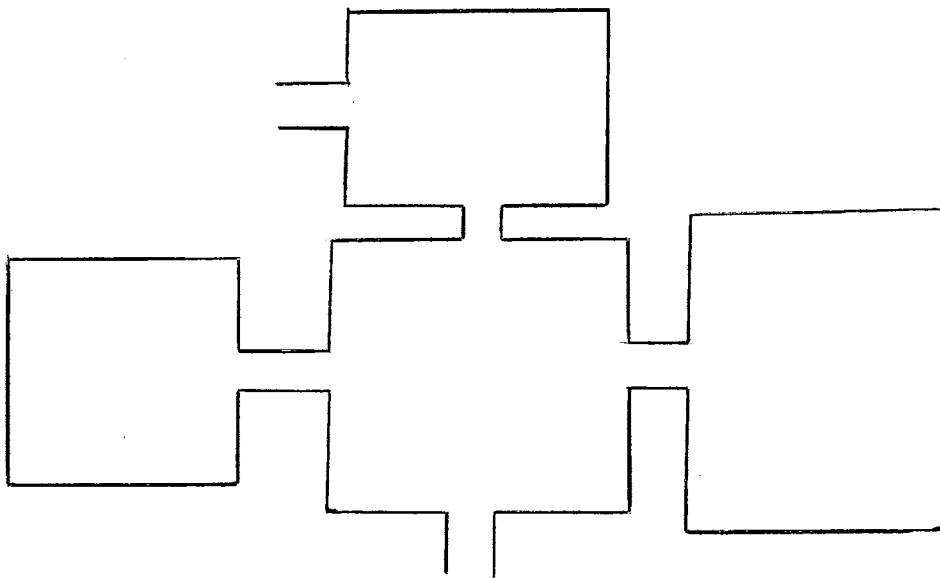


Figure 3. Acoustical Network



The purpose of this study is to investigate the pressure magnification and the response of double acoustical resonators coupled together for finite duration transient pressure excitations like N-shaped, saw tooth and sine pulse waves. The study consists of both theoretical and experimental phases. The results of this investigation are helpful in better understanding the mechanism of energy feedback in a coupled acoustical system subjected to transient excitations and thereby permitting the determination of the effect of the system parameters such as frequencies and damping on maximum pressures in the cavities. The other important application is in the area of dynamic response of various structures in excitation pressures like sonic booms, blast pressures, wind gusts, noise produced by rocket launchings, and random excitation.

The scope of the theoretical study consisted of deriving the differential equations of motion and solving for the natural frequencies of the double acoustical resonator. The transfer function of the system has been derived using the Laplace Transformation notation. Response of the system in both the frequency and time domain has been investigated for transient excitations such as finite duration pressure loadings. Numerical techniques and high speed digital computers have been used in computing and investigating the transient response. An attempt was made to use the techniques of analog computers to solve for the response. Equivalent viscous damping was assumed in the analytical treatment to approximate the various damping mechanisms in the system. The following major assumptions were made in the mathematical treatment of the problem:

1. The wave length corresponding to the natural frequency

is 16 or more times greater than the largest dimension of the resonator;

2. The pressure at all points inside the cavity is the same; and
3. All the walls of the resonator are rigid.

The principal object of the experimental investigation was to substantiate the validity of the assumptions made in deriving the mathematical model. Therefore, the scope of the experimental phase of the study was to design and build a double acoustical resonator with rigid walls, satisfying frequency limitations for the lumped parameter assumption, to excite it with transient pressure pulses, and to measure the pressure response in both cavities of the resonator as a function of time. The plane wave tube in the acoustical laboratory was used as an acoustical delay line to excite the resonator with finite duration transient excitation pressures. Instrumentation was developed to produce the excitation pressure pulses and to measure and record the input pressure and pressure response in both the cavities.

## CHAPTER II

### PREVIOUS INVESTIGATIONS

The primary investigation has been done in the area of acoustical networks from the stand point of musical tones and acoustical wave filters. The acoustical resonators used by Helmholtz (16) in his research on the quality of musical notes were almost completely closed vessels with an aperture (Figure 4) and were used to intensify effect of a simple tone produced in the neighborhood of the resonator. This intensification is the result of vibrations of the air enclosed by the resonator. Rayleigh (2) solved for the steady state response of a vessel containing air, which communicates with the external atmosphere by a narrow aperture or a neck. He assumed that the kinetic energy of the air due to its velocity can be neglected except in the vicinity of the neck or aperture. The potential energy can be calculated by treating the density of the air in the interior of the vessel as being uniform. These assumptions are valid if the space through which the kinetic energy is sensible is reasonably small in comparison with the length of the wave.

The stiffness of a Helmholtz resonator depends on the volume of the cavity and areas of the necks, and the modes of the vibration are dependent on the inertia of the air in the vicinity of all the apertures. Thus the fundamental frequency of a Helmholtz resonator with more than one neck is different from that of the simple resonator. When two

or more interconnected vessels communicate with each other, and with external air, then the inertia of the air in a connecting passage is as great as that of the channel which communicates with the external air. By assuming lumped parameters, the system is treated as a finite, multidegree-of-freedom system. Many investigators (1, 3, 6, 7) have attempted to solve for the steady state response of multiple resonators with application to wave filters, but very little work has been done in the field of transient response.

Simpson (4) has investigated the transient response of a simple Helmholtz resonator for a sonic boom type of excitation. He established the validity of the lumped parameter description of an undamped acoustical resonator for the transient pressure excitations, and has shown theoretically that the frequency limitations necessary in the transient response of a Helmholtz resonator are less severe than those associated with the steady state response.

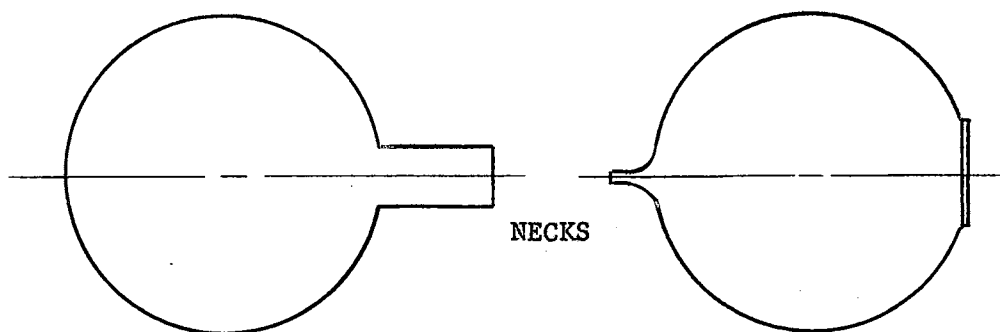


Figure 4. Simple acoustical Resonators used by Helmholtz (Spherical Cavities)

Rayleigh (2) described briefly the method to obtain the differential equations for the particle motion of two acoustical resonators coupled together and derived expressions for the natural frequencies of a particular configuration. McGinnis and Albert (1) have investigated an analytical method to obtain the equations of motion and natural frequencies of different configurations of multiple Helmholtz resonators assuming lumped parameters. They compared the theoretically obtained frequencies with the experimental results and found them to be in good agreement. Paris (9) in 1925 investigated the double Helmholtz resonator with a particular interest to the designing of a sensitive acoustical receiver used to measure the sound amplitudes. He found that increased magnification can be obtained by the use of an acoustical system with double resonance. He demonstrated the influence of loose coupling and tight coupling on pressure response of the system. In his analytical work, he took into account the damping due to viscosity and radiation.

Christian (11) examined the response of an undamped multiple resonator for steady state sinusoidal excitation and free vibrations. He derived a functional relationship of coupling parameters of a double acoustical resonator.

Olson (3) derived expressions for the frequency response spectrum of the multiple resonators which behave as low pass, high pass, band pass, and band elimination wave filters. He used the analogy of electrical filters and the impedance method to derive attenuation expressions. No explanation was given for the energy transfer from one resonator to the other through coupling. He indicated that the simple Helmholtz resonator can be treated as a single degree of freedom system

even for transient cases.

Ingles (21) investigated the effect of the pressure (at the equilibrium condition) on the response spectrum of Helmholtz resonator formed by two cavities and a neck. In this form of Helmholtz resonator, the variation in pressure changes both the mass of air in the neck and the volume of the air in the cavities. Thus, the resonant frequency of the system varies with the pressure. He also investigated the effect of temperature on the resonant frequency.

Morse (5) discussed a statically coupled mechanical system with two degrees-of-freedom, but mention has not been made about the transient response of coupled dynamic system.

Wein (10) examined different kinds of coupling in a two degrees-of-freedom system. He developed a relation showing the effect of various coupling parameters on free vibrations of the system.

Andrews Associates (18) in their final report on "The Studies of Structural Response to Sonic Booms" analyzed a simple oscillator for an N-wave excitation and found that the structure can be arrested from oscillations if the relationship between the natural period and duration of the pulse is at a critical value. For an N-wave, the maximax response is 2.05 times the static response.

Jacobsen and Ayre (3) have solved for the maximax response of an undamped simple mechanical oscillator for different types of transient excitation forces. The maximax response is defined as the maximum absolute displacement, velocity or acceleration of the oscillator occurring at any time as a result of the action of the forcing function. They also stated that the transient response of an undamped two degrees-of-freedom mechanical system can be solved by a classical solution of

simultaneous differential equations for particular cases; but the conditions for maximax response are not discussed.

Ormondroyd and Den Hartog (28) have given a design criterion for a vibration absorber. They discussed the conditions under which only smaller mass will have a considerable displacement when the bigger mass of the two degrees-of-freedom is driven by a steady state harmonic force. The effect of damping has also been included in their discussion.

Kryter (33) has done laboratory investigation on the relative noisiness and loudness of sonic booms having different wave fronts, the reactions of people to booms as an auditory experience, and their startling reactions to acoustic stimuli. The following statement is one of the conclusions from his investigations: "The sound heard in a house subjected to sonic booms are judged to be noisier or more unwanted than the sonic boom heard outdoors, probably because of rattles and other secondary sounds that result from vibration of the house." After this study, it appears that the pressure inside the house can be much higher for certain configurations due to dynamic acoustic effects rather than to rattles and vibrations of the house itself.

## CHAPTER III

### MATHEMATICAL MODEL

The response of a double acoustical resonator to transient excitation, as represented by an electrical or mechanical analog, depends on the frequency limitations, dimensions of the system, and the mechanism of damping in the system.

#### Limitations of Lumped Parameters for Acoustical Resonators

The assumption of a lumped parameter model for the acoustical system depends mainly on the critical dimension, which is defined as the largest dimension of the system (4).

In many cases the various elements of the acoustic structures are small in dimension compared with the wave length of sound. When this restriction is fulfilled, the behavior of sound or pressure pulse in the structure is analogous to the behavior of electric current in a circuit with lumped elements or to the behavior of the displacement in a mechanical system with lumped parameters. When the dimensions of the elements of the structure are not small relative to the wave length, the electric analog is a transmission line and the mechanical analog is an elastic continuous system.

In the case of a simple Helmholtz resonator (Figure 4), the velocity attained by the air within the volume is diminutive when compared to the velocity attained by the air particles in the neck of



the resonator. If the neck or constriction is very small as compared to the wave length, the compressibility of air in that part is negligible. The air in the constriction has a total mass of  $A\ell_e\rho_0$ , where  $A$  is the cross sectional area and  $\ell_e$  is the effective length of the neck. The effective length has to be used in the analysis to include mass of the air beyond the ends of constriction which moves along with the air in the neck. Thus, the kinetic energy is due only to the motion of the effective mass of air in the neck and the potential energy is only due to the compression and expansion of the air in the cavity of the system.

The correction factor to be added to the actual length of the neck depends on the wave length and shape of the neck. This has been derived in the literature (2, 5) by considering impedance of the open end of the tube. For a circular cross section, if the open end is fitted with a flange that is wide compared to the wave length, the approximate value of specific acoustic impedance at the open end is given by,

$$Z_{\ell} = \frac{\rho_0 R^2 \omega^2}{2c} + j \omega \frac{8\rho_0 R}{3\pi} \quad \text{for wave length, } \lambda > 8\pi R, \text{ and}$$

$$Z_{\ell} = \rho_0 c + \frac{j}{\omega} \frac{2\rho_0 c^2}{\pi R} \quad \text{for wave length, } \lambda < 8\pi R;$$

where  $R$  = radius of the tube.

Open tubes having cross sectional parameters much smaller than the wave length are, therefore, nearly as successful hoarders of energy as closed tubes, for only a small percent of the stored energy can be radiated away in a period of one oscillation. From the above equations it is apparent that the reactive term is mass load equal to mass of air,

$8\rho_0 R/3\pi$ , for small cross sectional area of the neck. When there is no flange on the end of the tube or when the flange dimension is negligible, the reactance is reduced to some extent in magnitude changing from  $8\rho_0 R/3\pi$  to approximately  $0.6\rho_0 R$ . Therefore, the correction factor,  $\alpha$ , to be used for the effective length of the neck should be in between the limits  $0.6\rho_0 R$  and  $8\rho_0 R/3\pi$ .

#### Consideration of Damping in Acoustical Resonators

Energy dissipation would be inevitable in any physical dynamic system. It is necessary to understand the various mechanisms of losses in order to incorporate damping in the response analysis. In acoustical systems the significant damping is due to: 1) viscosity and heat conduction, 2) anomalous gaseous absorption due to thermal relaxation, and 3) mechanical wall vibrations.

Energy dissipation due to friction in the neck is a function of the exposed area and the roughness of the neck. This dissipation can be reduced by making the surface of the neck smooth. In general, dissipation of energy due to radiation is more important when compared to that of friction in the neck, provided the resonator is so situated that it can radiate. However, when the aperture of resonator is small or the length of the neck is long enough, then the dissipation due to friction is predominant. If the walls are rigid enough, then the losses due to the vibrations of the walls can be relinquished. At low frequencies, where there is little thermal relaxation, the energy loss due to thermal relaxation can be neglected. Therefore, for a resonator with rigid walls at low frequencies, the losses that are sizeable are those due to radiation and friction in the neck.

The damping coefficient due to radiation of the resonator is derived by Crandall (17) and is given as,

$$C_R = \frac{\rho_o \omega^2}{4\pi c};$$

where

$\rho_o$  = mass density of air/unit volume,

$\omega$  = driving frequency in radians/second,

$c$  = velocity of sound, and

$C_R$  = damping coefficient, energy/unit volume velocity.

Damping due to friction at the walls is given by the complex function,

$$C_F = \sqrt{\frac{\rho_o \omega \mu}{2}} (1 + j) \quad (1)$$

where  $\mu$  = viscosity coefficient of the fluid.

The imaginary quantity  $\sqrt{\frac{\rho_o \omega \mu}{2}}$  is in phase with the acceleration; therefore, it has the nature of a mass reactance. This gives the effect of virtually increasing the mass density of air which corresponds to lowering of the natural frequency of a vibrating system by loading it with added mass. However, this may be taken into consideration equally well by adding the correction factor to the length of the neck to obtain the effective length.

The equivalent viscous damping coefficient for the resonator has been derived (31) by using the criterion of equivalent energy dissipation per cycle:

$$C_{eq} = C_n \omega^{n-1} X^{n-1} Y_n, \quad (2)$$

where

$n$  = the power of the velocity for which the actual damping coefficient is proportional, and

$X$  = the maximum amplitude.

### Pressure Response of Double Acoustical Resonators

The critical dimension of the resonator is assumed to be very small when compared to the wave length corresponding to the natural frequencies of the system. Since the temperature gradients are small and the process of compression and rarification are rapid, it is reasonable to assume the process of compression and expansion in the cavities (Figure 2) is adiabatic; therefore, the pressure and the volume are related to each other by the relation,

$$PV^{\gamma} = \text{constant}. \quad (3)$$

Differentiation of equation (3) yields the expression for a change in pressure as,

$$dP = - \frac{\gamma P_0}{V} dV; \quad (4)$$

where  $P_0$  is the original pressure.

Assuming that the air in the necks behave as masses and that in the enclosed volumes as springs, the mechanical analog can be derived as shown in Figure 5. If  $x_1$  and  $x_2$  are the displacements of masses  $M_1$  and  $M_2$  (air masses at necks  $N_1$  and  $N_2$ ), respectively, then the forces acting on each of the masses are given below:

Force on neck  $N_1$ :

$$\text{Inertia force} = \rho_0 l_{e1} A_1 \frac{d^2 x}{dt^2},$$

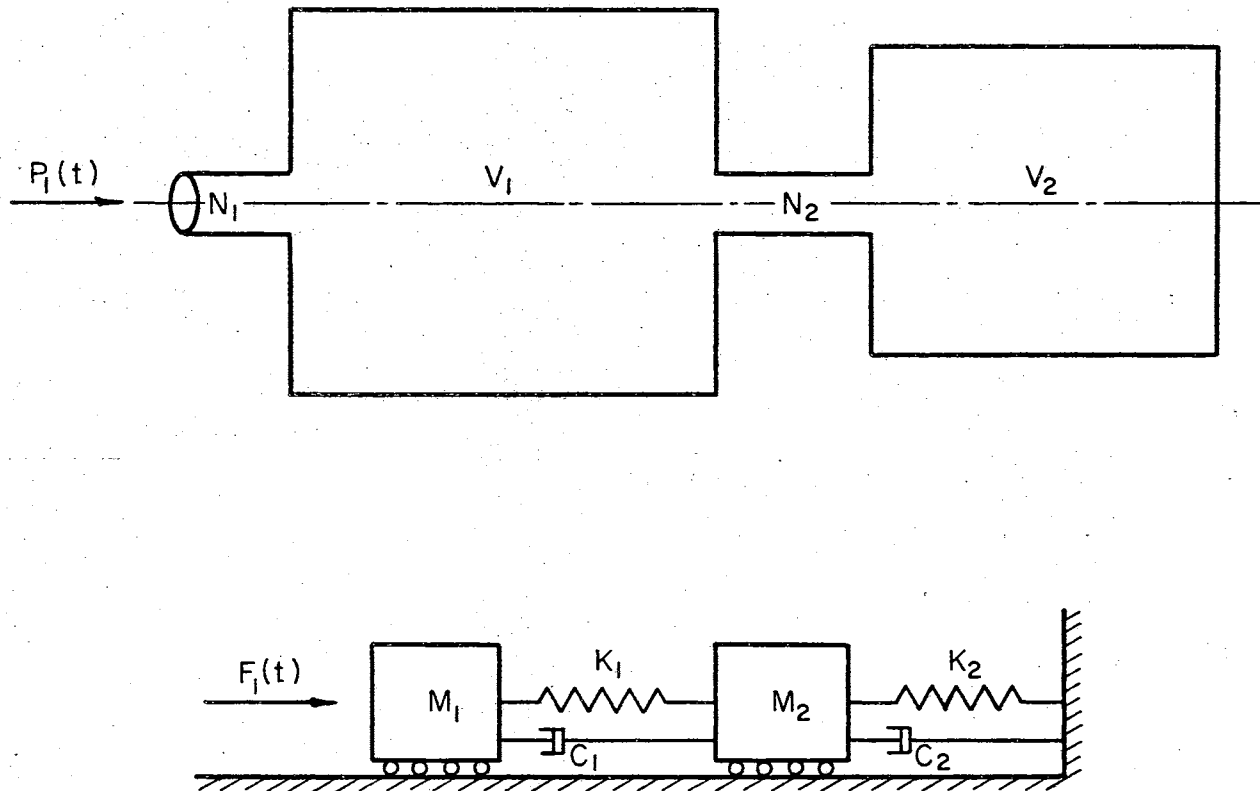


Figure 5. Equivalent Mechanical System for Double Acoustical Resonator

Restoring force due to volume,  $V_1 = -A_1 dP = \frac{\gamma P_0}{V_1} A_1 (A_1 x_1 - A_2 x_2)$ ,

Dissipating force due to damping =  $c_1 A_1^2 \frac{dx_1}{dt}$ , and

External force =  $P_1 A_1$ ; and (5)

Force on neck  $N_2$ :

Inertia force =  $\rho_0 l e_1 A_1 \frac{d^2 x_1}{dt^2}$ ,

Restoring force due to volume,  $V_1 = \frac{\gamma P_0}{V_1} A_2 (A_2 x_2 - A_1 x_1)$ ,

Restoring force due to volume,  $V_2 = \frac{\gamma P_0}{V_2} A_2 (A_2 x_2)$ ,

Dissipating force due to damping =  $c_2 A_2^2 \frac{dx_2}{dt} + c_1 \left( A_2 \frac{dx_2}{dt} - A_1 \frac{dx_1}{dt} \right) A_2$ , and

External force =  $P_2 A_2$ . (6)

By Newtonian force balance on air masses of each of the necks, the following simultaneous differential equations of motion may be obtained,

$$\rho_0 l e_1 A_1 \frac{d^2 x_1}{dt^2} + c_1 A_1 \left[ A_1 \frac{dx_1}{dt} - A_2 \frac{dx_2}{dt} \right] + \frac{\gamma P_0}{V_1} A_1 (A_1 x_1 - A_2 x_2) = P_1 A_1, \quad (7a)$$

and

$$\rho_0 l e_2 A_2 \frac{d^2 x_2}{dt^2} + c_1 A_2 \left[ A_2 \frac{dx_2}{dt} - A_1 \frac{dx_1}{dt} \right] + c_2 A_2^2 \frac{dx_2}{dt} + \frac{\gamma P_0}{V_1} A_2 (A_2 x_2 - A_1 x_1) + \frac{\gamma P_0}{V_2} A_2^2 x_2 = P_2 A_2. \quad (7b)$$

The equations of motion may be reduced to the following form by

dividing equation (7a) by  $A_1$  and equation (7b) by  $A_2$  and replacing  $P_o \gamma$  by its equivalent  $\rho_o c^2$ ,

$$\frac{\rho_o l e_1}{A_1} \ddot{x}_1 + c_1 (\dot{x}_1 - \dot{x}_2) + \frac{\rho_o c^2}{V_1} (x_1 - x_2) = P_1, \text{ and} \quad (8)$$

$$\frac{\rho_o l e_2}{A_2} \ddot{x}_2 + c_2 \dot{x}_2 + c_1 (\dot{x}_2 - \dot{x}_1) + \frac{\rho_o c^2}{V_2} x_2 + \frac{\rho_o c^2}{V_1} (x_2 - x_1) = P_2 ;$$

where

$X_1 = A_1 x_1 =$  volume displacement at neck  $N_1$ ,

$X_2 = A_2 x_2 =$  volume displacement at neck  $N_2$ ,

$P_1 =$  external pressure on neck  $N_1$ , and

$P_2 =$  external pressure on neck  $N_2$ .

The transformation of linear simultaneous differential equations (8) into complex frequency domain by the Laplace transformation with zero initial conditions, yields the following simultaneous algebraic equations:

$$\left[ \frac{\rho_o l e_1}{A_1} s^2 + c_1 s + \frac{\rho_o c^2}{V_1} \right] X_1(s) - \left[ c_1 s + \frac{\rho_o c^2}{V_1} \right] X_2(s) = P_1(s),$$

and

$$\left[ \frac{\rho_o l e_2}{A_2} s^2 + (c_1 + c_2) s + \frac{\rho_o c^2}{V_1} + \frac{\rho_o c^2}{V_2} \right] X_2(s) - \left[ c_1 s + \frac{\rho_o c^2}{V_1} \right] X_1(s) = P_2(s).$$

$$X_1(s) = P_2(s). \quad (9)$$

The solution of these equations gives the response of the system in complex frequency domain as,

$$X_1(s) = \frac{P_1(s) \frac{\rho_0 l e_2}{A_2} \left[ s^2 + 2p_2 (\xi_2 + \xi_{12}) s + p_2^2 + p_{12}^2 \right]}{\Delta} + \frac{P_2(s) \frac{\rho_0 l e_1}{A_1} \left[ 2\xi_1 p_1 + p_1^2 \right]}{\Delta},$$

and

$$X_2(s) = \frac{P_2(s) \frac{\rho_0 l e_1}{A_1} \left[ s^2 + 2\xi_1 p_1 + p_1^2 \right]}{\Delta} + \frac{P_1(s) \frac{\rho_0 l e_2}{A_2} (2\xi_1 p_1 s + p_1^2)}{\Delta} \quad (10)$$

where

$p_1, p_2$  are the uncoupled natural frequencies,

$p_{12}$  is the coupling frequency, and

$\Delta$  = characteristic determinant of equations (9) (Appendix A).

Response in the time domain can be obtained by factoring the complex expressions of equation (10) by partial fractions and transforming from complex frequency domain using inverse Laplace transformation.

The excitation pressure on neck  $N_2$ ,  $P_2(t)$  is assumed to be zero.

Then equation (10) simplifies to

$$X_1(s) = \frac{P_1(s) \frac{\rho_0 l e_2}{A_2} \left[ s^2 + 2p_2 (\xi_2 + \xi_{12}) s + p_2^2 + p_{12}^2 \right]}{\Delta},$$

and

$$X_2(s) = \frac{P_1(s) \frac{\rho_0 l e_2}{A_2} \left[ 2\xi_1 p_1 s + p_1^2 \right]}{\Delta} \quad (11)$$

The response solution is obtained for two important types of transient excitation pressures on neck  $N_1$ : one cycle of sine wave and



a wave made of straight lines with finite duration and finite number of discontinuities.

Case 1. Response of double acoustical resonator for an excitation of one cycle of sine wave:

This excitation pressure can be illustrated graphically as in Figure 6 and expressed mathematically as,

$$\begin{aligned} P_1(t) &= A_0 \sin \omega t, & \text{for } 0 \leq t \leq \frac{1}{2\pi\omega} ; \\ P_1(t) &= 0, & \text{for } t < 0 \text{ and } t > \frac{1}{2\pi\omega} ; \text{ and} \\ P_2(t) &= 0, & \text{for all } t. \end{aligned} \quad (12)$$

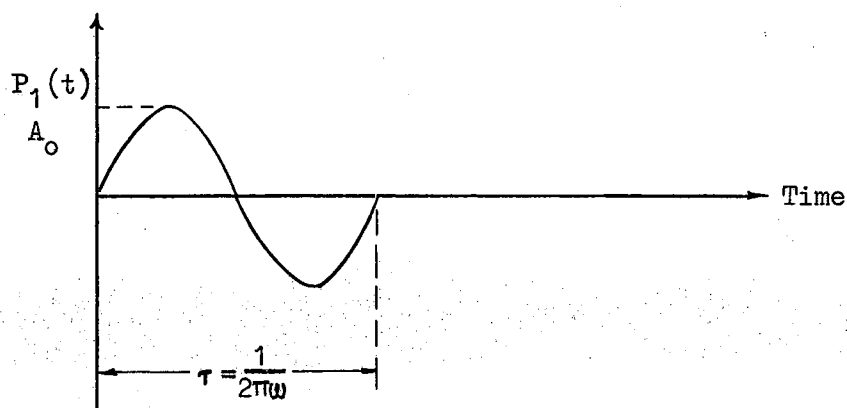


Figure 6. Excitation Pressure of Sine Pulse on Neck  $N_1$

The volume displacement response of the system which may be obtained by inverse Laplace transformation are (Appendix A),

$$\begin{aligned} X_1(t) &= \frac{A_0 \omega}{\frac{\rho_0 l e_1}{A_1}} \left\{ [a_1 \cos \omega t + \frac{b_1}{\omega} \sin \omega t + \frac{e^{at}}{b} (\Phi_1 \sin bt + \Phi_2 \cos bt)] \right. \\ &\quad \left. + \frac{e^{ct}}{d} (\Psi_1 \sin dt + \Psi_2 \cos dt) \right] u(t) - [a_1 \cos \omega(t-\tau)] \end{aligned}$$

$$+ \frac{b_1}{\omega} \sin \omega(t - \tau) + \frac{e^{a(t-\tau)}}{b} (\Phi_1 \sin b(t - \tau) + \Phi_2 \cos b(t - \tau)) + \frac{e^{c(t-\tau)}}{d} (\Psi_1 \sin d(t - \tau) + \Psi_2 \cos d(t - \tau)) \Big] u(t - \tau) \Big\} ,$$

and

$$X_2(t) = \frac{A_0 \omega^2 p_1^2}{\frac{\rho_0 l e^2}{A_2}} \left\{ \left[ a_2 \cos \omega t + \frac{b_2}{\omega} \sin \omega t + \frac{e^{at}}{b} (\Phi_3 \sin bt + \Phi_4 \cos bt) + \frac{e^{ct}}{d} (\Psi_3 \sin dt + \Psi_4 \cos dt) \right] u(t) - [a_2 \cos \omega(t - \tau) + \frac{b_2}{\omega} \sin \omega(t - \tau) + \frac{e^{a(t-\tau)}}{b} (\Phi_3 \sin b(t - \tau) + \Phi_4 \cos b(t - \tau)) + \frac{e^{c(t-\tau)}}{d} (\Psi_3 \sin d(t - \tau) + \Psi_4 \cos d(t - \tau))] u(t - \tau) \right\} ; \quad (13)$$

where the coefficients  $a_1, b_1, \dots, \Psi_3, \Psi_4$  are given by equations (15) in Appendix A.

The pressures in the cavities may be expressed in terms of volume displacements from equations (12) as,

$$P_1 = \frac{\rho_0 c^2}{V_1} (X_1 - X_2) , \text{ and}$$

$$P_2 = \frac{\rho_0 c^2}{V_2} X_2 .$$

These pressures can be normalized with respect to the amplitude of the excitation pressure  $A_0$ , and can be derived as a function of uncoupled frequencies,  $p_1$  and  $p_2$ , coupling frequency  $p_{12}$ , and the damping factors  $\xi_1, \xi_2$  as (Appendix A),

$$\frac{P_1}{A_0} = p_1^2 \omega \left\{ A_x \cos \omega t + B_x \sin \omega t + \frac{e^{at}}{b} (C_x \sin bt + D_x \cos bt) \right\}$$

$$\begin{aligned}
& + \frac{e^{ct}}{d} (E_x \sin dt + F_x \cos dt) u(t) - [A_x \cos \omega(t - \tau) \\
& + B_x \sin \omega(t - \tau) + \frac{e^{a(t - \tau)}}{b} (C_x \sin b(t - \tau) + D_x \cos b(t - \tau)) \\
& + \frac{e^{c(t - \tau)}}{d} (E_x \sin d(t - \tau) + F_x \cos d(t - \tau))] u(t - \tau) \}
\end{aligned}$$

and

$$\begin{aligned}
\frac{P_2}{A_0} = & p_1^2 p_2^2 \omega^2 \left\{ [a_2 \cos \omega t + \frac{b_2}{\omega} \sin \omega t + \frac{e^{at}}{b} (\Phi_3 \sin bt + \Phi_4 \cos bt) \right. \\
& + \frac{e^{ct}}{d} (\Psi_3 \sin dt + \Psi_4 \cos dt)] u(t) - [a_2 \cos \omega(t - \tau) \\
& + \frac{b_2}{\omega} \sin \omega(t - \tau) + \frac{e^{a(t - \tau)}}{b} (\Phi_3 \sin b(t - \tau) + \Phi_4 \cos b(t - \tau)) \\
& \left. + \frac{e^{c(t - \tau)}}{d} (\Psi_3 \sin d(t - \tau) + \Psi_4 \cos d(t - \tau))] u(t - \tau) \right\}; \quad (14)
\end{aligned}$$

where

$$\begin{aligned}
A_x &= a_1 - a_2 p_{12}^2, \\
B_x &= \frac{1}{\omega} (b_1 - b_2 p_{12}^2), \\
C_x &= \Phi_1 - \Phi_3 p_{12}^2, \\
D_x &= \Phi_2 - \Phi_4 p_{12}^2, \\
E_x &= \Psi_1 - \Psi_3 p_{12}^2, \text{ and} \\
F_x &= \Psi_2 - \Psi_4 p_{12}^2. \quad (15)
\end{aligned}$$

In equations (12) and (14) the unit functions  $u(t)$  and  $u(t - \tau)$  indicate that the response expressions are valid for only  $t > 0$  and  $(t - \tau) > 0$ , respectively, which should be taken into account in evaluating pressures in the cavities at any time.

Since from this analysis it is rather difficult to understand the effect of various system parameters on the response, the analysis of the pressure response of the undamped system subject to an excitation pressure of sine pulse will predict the parameters involved. These pressures can be written as (Appendix A),

$$\frac{P_1}{A_0} = \frac{p_1^2}{(\omega^2 - p_+^2)(\omega^2 - p_-^2)} \left\{ [a_z \sin \omega t + b_z \sin p_+ t + c_z \sin p_- t] \cdot \right. \\ \left. u(t) - [a_z \sin \omega(t - \tau) + b_z \sin p_+(t - \tau) + c_z \sin p_- \cdot \right. \\ \left. (t - \tau)] u(t - \tau) \right\}, \quad \text{and} \quad (16)$$

$$\frac{P_2}{A_0} = \frac{p_1^2 p_2^2}{(\omega^2 - p_+^2)(\omega^2 - p_-^2)} \left\{ [\sin \omega t + b_y \sin p_+ t + c_y \sin p_- t] u(t) \right. \\ \left. - [\sin \omega(t - \tau) + b_y \sin p_+(t - \tau) + c_y \sin p_-(t - \tau)] u(t - \tau) \right\};$$

where

$$a_z = a_x - a_y p_{12}^2, \\ b_z = b_x - b_y p_{12}^2, \text{ and} \\ c_z = c_x - c_y p_{12}^2.$$

When the frequency of driving pressure,  $\omega$ , is the same as one of the coupled natural frequencies of the system,  $p_+$  or  $p_-$ , the denominator of equation (16) will be zero, which indicates that the pressures in the cavities may be infinite. But at these conditions, the numerator also becomes zero which makes the response mathematically indeterminate and leads to the use of the L'Hospital rule to find the pressure response. Since these expressions are complex functions of the un-

coupled frequencies,  $p_1$  and  $p_2$ , and of the coupling frequency,  $p_{12}$ , of the system, it is more convenient to establish the response by numerical techniques than by applying mathematical techniques to the response expressions.

Case 2: Response of double acoustical resonator for an excitation pressure made up of straight lines with finite number of discontinuities:

This excitation pressure can be illustrated graphically as in Figure 7 and can be expressed mathematically as follows:

$$P_1(t) = \sum_{i=1}^n [\alpha_i + \beta_i (t - \tau_i)] u(t - \tau_i); \quad (17)$$

where

$n$  = number of discontinuities on time axis,

$\alpha_i$  = pressure jump at time,  $t = \tau_i$ , and

$\beta_i$  = change in slope of pressure at time,  $t = \tau_i$ .

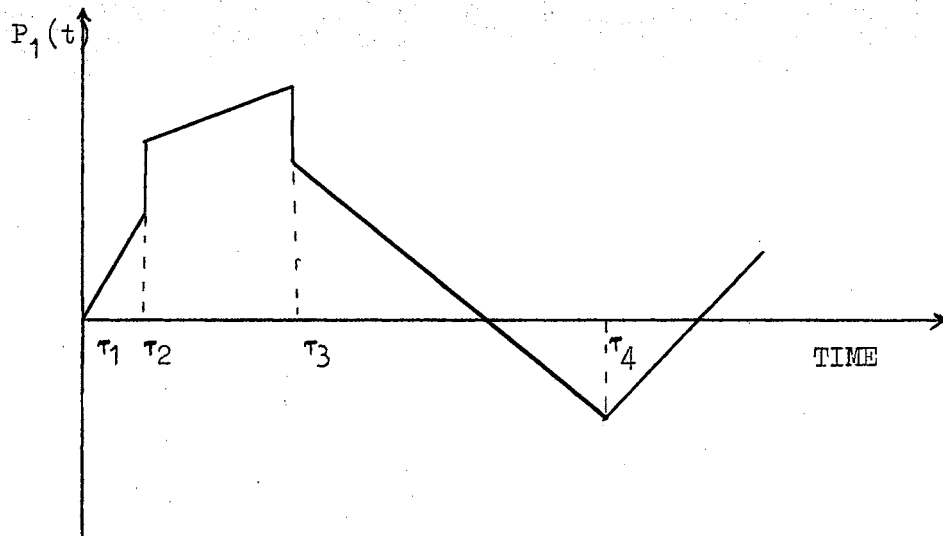


Figure 7. Excitation Pressure Made Up of Straight Lines

Laplace transform of  $P_1(t)$  is,

$$P_1(s) = \frac{1}{s^2} \sum_{i=1}^n [\alpha_i s + \beta_i] e^{-\tau_i s} \quad (18)$$

The excitation pressure on neck  $N_2$ ,

$$P_2(t) = 0, \text{ and hence } P_2(s) = 0.$$

The volume displacement response of the system for the excitation pressure of the type described in Figure 7 is (Appendix A),

$$X_1(t) = \frac{1}{\frac{\rho_0 l e_1}{A_1}} \sum_{i=1}^n \left\{ a_{1i} + b_{1i}(t - \tau_i) + \frac{e^{a(t - \tau_i)}}{b} \right. \\ \left. [\Phi_{1i} \sin b(t - \tau_i) + \Phi_{2i} \cos b(t - \tau_i)] + \frac{e^{c(t - \tau_i)}}{d} \right. \\ \left. [\Psi_{1i} \sin d(t - \tau_i) + \Psi_{2i} \cos d(t - \tau_i)] \right\} u(t - \tau_i), \text{ and}$$

$$X_2(t) = \frac{p_1^2}{\frac{\rho_0 l e_2}{A_2}} \sum_{i=1}^n \left\{ a_{2i} + b_{2i}(t - \tau_i) + \frac{e^{a(t - \tau_i)}}{b} \right. \\ \left. [\Phi_{3i} \sin b(t - \tau_i) + \Phi_{4i} \cos b(t - \tau_i)] + \frac{e^{c(t - \tau_i)}}{d} \right. \\ \left. [\Psi_{3i} \sin d(t - \tau_i) + \Psi_{4i} \cos d(t - \tau_i)] \right\} u(t - \tau_i). \quad (19)$$

The pressures in the cavities can be expressed in terms of volume displacements as follows:

$$P_1 = \frac{\rho_0 c^2}{V_1} (X_1 - X_2) = p_1^2 \sum_{i=1}^n \left\{ a_{xi} + b_{xi}(t - \tau_i) + \frac{e^{a(t - \tau_i)}}{b} \right. \\ \left. [\Phi_{xi} \sin b(t - \tau_i) + \Phi_{yi} \cos b(t - \tau_i)] + \frac{e^{c(t - \tau_i)}}{d} \right. \\ \left. [\Psi_{xi} \sin d(t - \tau_i) + \Psi_{yi} \cos d(t - \tau_i)] \right\} u(t - \tau_i).$$

$$\begin{aligned}
& [c_{xi} \sin b(t - \tau_i) + d_{xi} \cos b(t - \tau_i)] + \frac{e^{c(t - \tau_i)}}{d} \cdot \\
& [e_{xi} \sin d(t - \tau_i) + f_{xi} \cos d(t - \tau_i)] \left. \vphantom{[e_{xi} \sin d(t - \tau_i) + f_{xi} \cos d(t - \tau_i)]} \right\} u(t - \tau_i), \text{ and} \\
P_2 = \frac{\rho_0 c^2}{V_2} X_2 = p_1^2 p_2^2 \sum_{i=1}^n \left\{ a_{2i} + b_{2i}(t - \tau_i) + \frac{e^{a(t - \tau_i)}}{b} \right. \\
& [\phi_{3i} \sin b(t - \tau_i) + \phi_{4i} \cos b(t - \tau_i)] + \frac{e^{c(t - \tau_i)}}{d} \cdot \\
& \left. [\psi_{3i} \sin d(t - \tau_i) + \psi_{4i} \cos d(t - \tau_i)] \right\} u(t - \tau_i); \quad (20)
\end{aligned}$$

where

$$\begin{aligned}
a_{xi} &= a_{1i} - a_{2i} p_{12}^2, \\
b_{xi} &= b_{1i} - b_{2i} p_{12}^2, \\
c_{xi} &= c_{1i} - c_{2i} p_{12}^2, \\
d_{xi} &= d_{1i} - d_{2i} p_{12}^2, \\
e_{xi} &= e_{1i} - e_{2i} p_{12}^2, \text{ and} \\
f_{xi} &= f_{1i} - f_{2i} p_{12}^2.
\end{aligned}$$

These response expressions can be evaluated in the time domain for given uncoupled, undamped natural frequencies, coupling frequency and the damping factors.

#### Transmission of Energy From One Resonator to the Other

In the case of a dynamic system with more than one degree-of-freedom or multiple oscillators tightly coupled together, the feedback energy from the driven system to the driver cannot be neglected. For

illustration, in the case of two oscillators coupled together, both oscillators are on an equal footing, each is affected by the other. In the case of an undamped system subjected to transient excitation force of finite duration, the total energy of the system computed at the end of the forced era should remain constant for the rest of the period. However, the absolute maximum displacement (pressure in acoustical system) may occur in the residual era depending on the system parameters. The absolute displacements of masses or absolute pressures in the cavities of acoustical systems depends on the type of transient excitation force or pressure, the manner by which it is applied and the system parameters. If the excitation pressure is applied on neck  $N_1$  of the acoustical resonator (Figure 3), it is natural to expect that the pressure build up in cavity  $V_1$  is faster when compared to that in the cavity  $V_2$ . However, the maximum pressure amplitude can be in either one of the cavities depending on the dimensions of the necks and cavities.

One can anticipate the beating phenomenon in the residual era for the system with two degrees-of-freedom. In the case of mechanical elements coupled with acoustical elements forming a dynamic system with multiple degrees-of-freedom, the beating phenomenon exists both in pressure oscillations and the displacement oscillations of mechanical masses.

When a mechanical system with two degrees-of-freedom is subjected to finite duration driving force, both masses will have initial displacements and velocities at the end of the forced era. With these initial conditions, the displacement response in the residual era is the summation of two harmonic motions with the natural frequencies of



the system. When these two frequencies are different from each other, then the combination of these two motions is not harmonic. If the amplitude of this response varies periodically, then this phenomenon is known as the beating effect.

#### Merits and Demerits of Analog Computer

The analog computer solution of simultaneous differential equations is of a continuous form. Accuracy depends on the various elements of the analog computer. It is rather arduous in some cases, to make the system stable for the system of undamped physical systems. The individual elements of the system can be varied very conveniently and the response can be studied. It is well suited for the solution of the differential equations for particular configuration with numerical values. To study the effect of all the possible parameters, is rather tedious, particularly to study the maximax response of the dynamic system with multiple degrees-of-freedom. For example, in the expression for the pressure response of the double acoustical resonator, for excitation pressure of one cycle of sine wave, it is necessary to study the effect of two uncoupled frequencies and the coupling frequency on the maximax response. Since the analog form of the solution is in the time domain, it is necessary to solve for different combinations of coefficients of the differential equations in order to solve for maximax response. It is time consuming to study the maximax response for all the possible variables of the system. Also one should be extremely careful in selecting the numerical values for the parameters, so that the critical point will not be missed.

## CHAPTER IV

### THEORETICAL RESULTS

The pressures in the cavities of the system of the multiple acoustical resonator are functions of various system parameters such as uncoupled natural frequencies, coupling frequencies, and damping factors and the excitation pressures. The coupling frequencies are defined as the frequencies which couple two resonators. It is not possible to study the behavior of pressure response by the mathematical treatment of equation (14), for it is an extremely complicated function of system parameters and external pressure excitation. Also, since these expressions are functions of several variables, it is rather difficult to find the absolute maximum pressures in the time domain by applying the mathematical treatment. To represent the response spectra of the system, it is necessary to use a response surface instead of a response curve.

Before discussing the response of double acoustical resonators subjected to transient excitations, it is desirable to know the minimum number of independent parameters that affect the response. The response pressures in the cavities, when excited by a finite duration pressure, are the functions of the conductivities of the necks, volumes of the cavities and the period of excitation pressure. However, from the discussion in Chapter III, it is apparent that there are five independent parameters to represent the system, namely,  $P_1$ ,  $P_2$ ,  $P_{12}$ ,

$\xi_1$ , and  $\xi_2$ . The two parameters, amplitude and duration, represents the transient excitation pressure. It is desirable to use normalized system parameters to present the response spectra. The frequencies may be normalized by multiplying them by the period of excitation. Pressures may be normalized by dividing by the amplitude of the excitation pressure. The choice and number of parameters necessary to represent the system response are discussed in the next section by examining the governing equations.

### Governing Equations

The pressure response expressions are simpler in the case of the undamped system as compared to the damped system. Thus it is easier to understand the dynamic behavior of the system by discussing the undamped system exposed to external pressures.

The following are the expressions from Appendix A for the pressure response of an undamped double acoustical resonator in the forced era ( $0 < t < \tau$ ) for a one cycle sine wave pressure excitation of amplitude  $A_0$  and period  $\tau$ :

$$\frac{P_1}{A_0} = \frac{p_1^2}{(\omega^2 - p_+^2)(\omega^2 - p_-^2)} [a_z \sin \omega t + b_z \sin p_+ t + c_z \sin p_- t] , \quad \text{and} \quad (21)$$

$$\frac{P_2}{A_0} = \frac{p_1^2 p_2^2}{(\omega^2 - p_+^2)(\omega^2 - p_-^2)} [\sin \omega t + b_y \sin p_+ t + c_y \sin p_- t] ;$$

where  $p_+$  and  $p_-$  are two undamped natural frequencies of the system and are given by equation (18) in Appendix A as,

$$p_+^2 = \frac{(p_1^2 + p_2^2 + p_{12}^2) + \sqrt{(p_1^2 - p_2^2 - p_{12}^2)^2 + 4p_1^2 p_{12}^2}}{2} \quad (22)$$

$$p_-^2 = \frac{(p_1^2 + p_2^2 + p_{12}^2) - \sqrt{(p_1^2 - p_2^2 - p_{12}^2)^2 + 4p_1^2 p_{12}^2}}{2}$$

From these equations it appears that the pressure response can be reduced to a function of three variables; namely, two natural frequencies and the period of the excitation pressure, but the coefficients  $a_z, b_z, \dots, c_y$ , are functions of  $p_1, p_2, p_{12}$  and  $\omega$ , and cannot be reduced to a function of only coupled frequencies and  $\omega$ . Thus, the pertinent parameters for investigating the response are the uncoupled frequencies and the type of excitation pressure. It is of interest to note that the pressure response is not an implicit function of the elements of the systems, such as the volumes of cavities and conductivities or dimensions of the necks.

#### Uncoupled and Coupled Frequencies of the System

The coupled frequencies,  $p_+$  and  $p_-$  are functions of three variables  $p_1, p_2$ , and  $p_{12}$ . For the double acoustical resonator the frequencies  $p_1$  and  $p_2$  are defined as the frequencies of each of the resonators when the other resonator is absent. The coupling frequency is defined as the frequency of the system when the neck  $N_1$  is closed and the cavity  $V_2$  is removed. The following expressions for the frequencies are obtained from equations (7),

$$p_1 = c\sqrt{\frac{A_1}{v_1 l_1 e_1}},$$

$$p_2 = c\sqrt{\frac{A_2}{v_2 l_2 e_2}}, \text{ and}$$

$$p_{12} = \alpha \sqrt{\frac{A_2}{v_1 l}} e_2 \quad (23)$$

These frequencies are tabulated in Table I for buildings that can be idealized as double acoustical resonators. In this analysis the combination of two rooms with two doors open and all windows closed, as shown in Figure 8, is considered. For various values of areas of the door openings, volumes of the rooms, and keeping the actual length of the necks (doors) as six inches, the frequencies are calculated.

The equations (22) can be solved for uncoupled frequencies as functions of  $p_+$ ,  $p_-$  and  $p_{12}$  resulting in,

$$p_1^2 = \frac{(p_+^2 + p_-^2 - p_{12}^2) \pm \sqrt{[p_{12}^2 - (p_+^2 + p_-^2)]^2 - 4p_+^2 p_-^2}}{2},$$

and

$$p_2^2 = \frac{(p_+^2 + p_-^2 - p_{12}^2) \mp \sqrt{[p_{12}^2 - (p_+^2 + p_-^2)]^2 - 4p_+^2 p_-^2}}{2}.$$

Two combinations of  $p_1$  and  $p_2$  are obtained for given values of  $p_+$ ,  $p_-$  and  $p_{12}$ . For each set of  $p_1$  and  $p_2$  values the pressure response is different and hence  $p_+$  and  $p_-$  cannot be the pertinent system parameters to represent the response.

The pressures in the cavities were computed in time domain and plotted in Figure 9, for a short period sine pulse excitation. This illustrates the beating phenomenon of double acoustical resonator which was discussed in Chapter III.

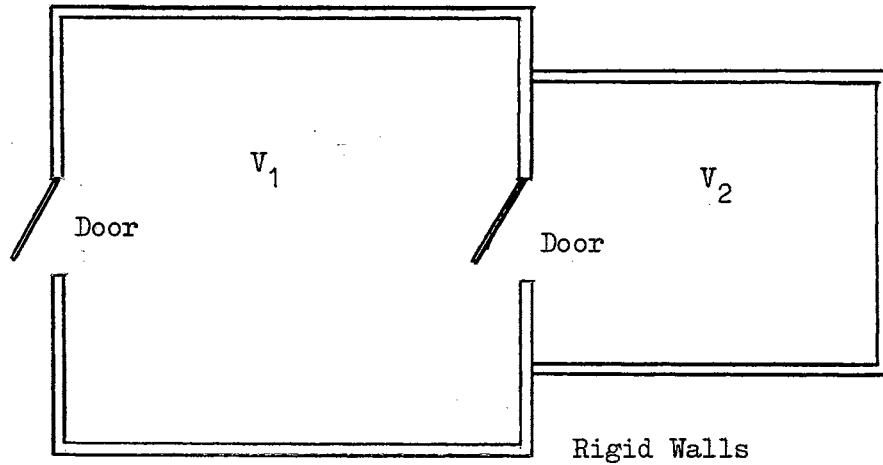


Figure 8. Building Structure That Can be Idealized as a Double Acoustical Resonator

#### Damped Acoustical Resonator

As it is stated in Chapter III, incorporation of damping makes the system more complicated to analyze. In this investigation it is assumed that the damping due to various mechanisms can be reduced to equivalent viscous damping which is a linear function of volume displacement. The governing pressure response equation for the excitation pressures of one cycle of sine pulse and the pressures made up of straight lines with finite discontinuities like finite duration N-waves and saw tooth waves are;

For sine pulse:

$$\frac{P_1}{A_0} = p_1^2 \omega \left\{ [A_x \cos \omega t + B_x \sin \omega t + \frac{e^{-at}}{b} (C_x \sin bt + D_x \cos bt)] \right. \\ \left. + \frac{e^{-ct}}{d} (E_x \sin dt + F_x \cos dt) \right\} u(t) - [A_x \cos \omega(t - \tau)]$$

TABLE I  
 NATURAL FREQUENCY OF TYPICAL ACOUSTIC STRUCTURES

$A_1$ (ft <sup>2</sup> )	$A_2$ (ft <sup>2</sup> )	$V_1$ (ft <sup>3</sup> )	$V_2$ (ft <sup>3</sup> )	$f_1$ (cps)	$f_2$ (cps)	$f_{12}$ (cps)
15	15	1000	1000	11.10	11.08	11.10
30	15	1000	1000	13.40	11.08	11.10
15	30	1000	1000	11.10	13.40	13.40
30	30	1000	1000	13.40	13.40	13.40
15	15	19000	1000	2.54	11.08	2.54
30	15	19000	1000	3.08	11.08	2.54
15	30	19000	1000	2.54	13.43	3.08
30	30	19000	1000	3.08	13.43	3.08
15	15	1000	19000	11.10	2.54	11.10
30	15	1000	19000	13.43	2.54	11.10
15	30	1000	19000	11.10	3.10	13.40
30	30	1000	19000	13.40	3.10	13.40
15	15	19000	19000	2.54	2.54	2.54
30	15	19000	19000	3.08	2.54	2.54
15	30	19000	19000	2.54	3.08	3.08
30	30	19000	19000	3.08	3.08	3.08

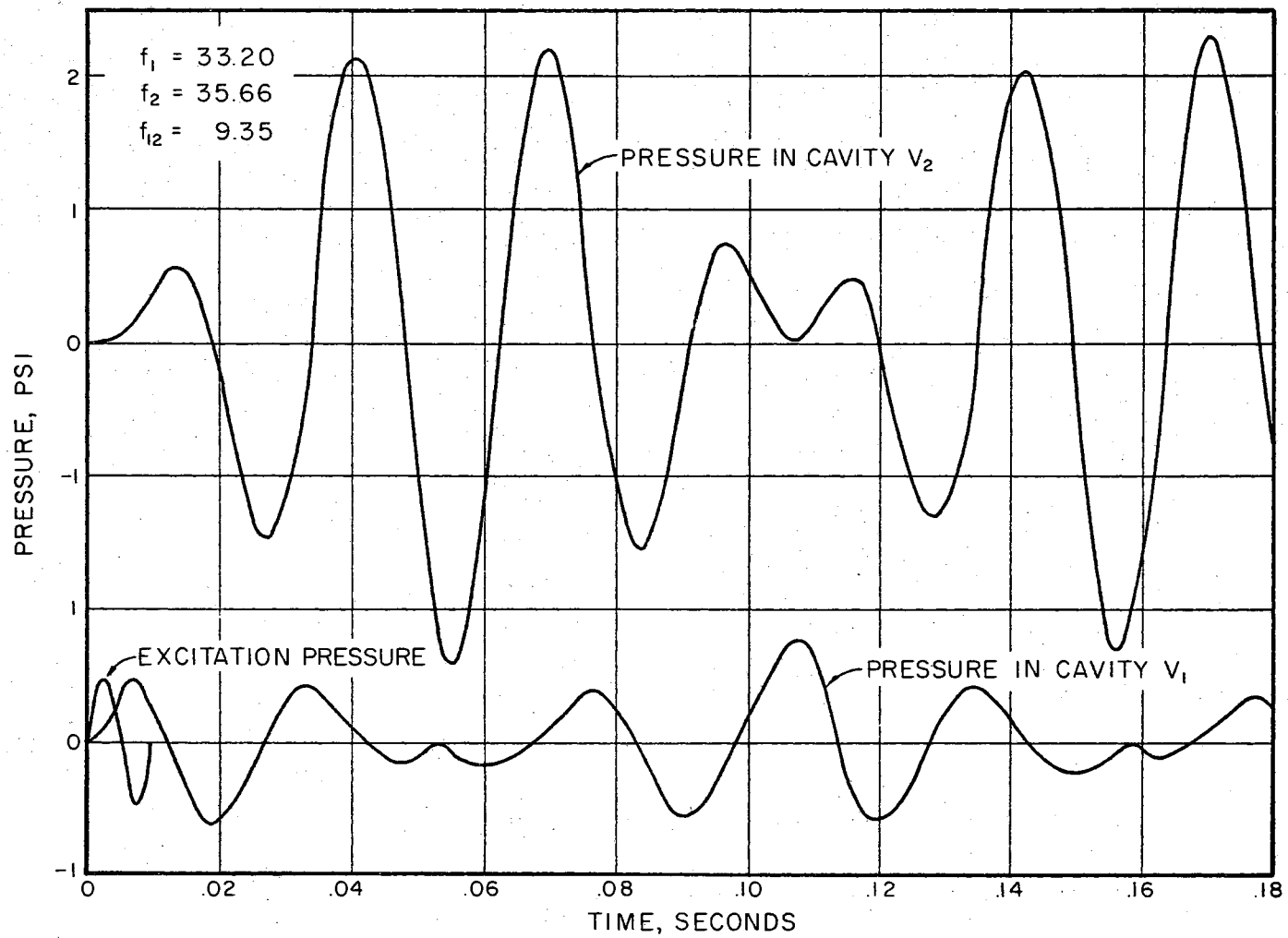


Figure 9. Pressure Beatings in a Double Acoustical Resonator



$$+ B_x \sin \omega(t - \tau) + \frac{e^{a(t - \tau)}}{b} (C_x \sin b(t - \tau) + D_x \cos b(t - \tau)) \\ + \frac{e^{c(t - \tau)}}{d} (E_x \sin d(t - \tau) + F_x \cos d(t - \tau)) \Big] u(t - \tau) \Big\} ,$$

and

$$\frac{P_2}{A_0} = p_1^2 p_2^2 \omega \left\{ \left[ a_2 \cos \omega t + \frac{b_2}{\omega} \sin \omega t + \frac{e^{at}}{b} (\Phi_3 \sin bt + \Phi_4 \cos bt) \right. \right. \\ \left. \left. + \frac{e^{ct}}{d} (\Psi_3 \sin dt + \Psi_4 \cos dt) \right] u(t) - \left[ a_2 \cos \omega(t - \tau) \right. \right. \\ \left. \left. + \frac{b_2}{\omega} \sin \omega(t - \tau) + \frac{e^{a(t - \tau)}}{b} (\Phi_3 \sin b(t - \tau) + \Phi_4 \cos b(t - \tau)) \right. \right. \\ \left. \left. + \frac{e^{c(t - \tau)}}{d} (\Psi_3 \sin d(t - \tau) + \Psi_4 \cos d(t - \tau)) \right] u(t - \tau) \right\}; \quad (24a)$$

and

For pressures with straight lines:

$$P_1 = p_1^2 \sum_{i=1}^n \left\{ a_{xi} + b_{xi}(t - \tau_i) + \frac{e^{a(t - \tau_i)}}{b} [c_{xi} \sin b(t - \tau_i) \right. \\ \left. + d_{xi} \cos b(t - \tau_i)] + \frac{e^{c(t - \tau_i)}}{d} [e_{xi} \sin d(t - \tau_i) \right. \\ \left. + f_{xi} \cos d(t - \tau_i)] \right\} u(t - \tau_i),$$

and

$$P_2 = p_1^2 p_2^2 \sum_{i=1}^n \left\{ a_{2i} + b_{2i}(t - \tau_i) + \frac{e^{a(t - \tau_i)}}{b} [\Phi_{3i} \sin b(t - \tau_i) \right. \\ \left. + \Phi_{4i} \cos b(t - \tau_i)] + \frac{e^{c(t - \tau_i)}}{d} [\Psi_{3i} \sin d(t - \tau_i) \right. \\ \left. + \Psi_{4i} \cos d(t - \tau_i)] \right\} u(t - \tau_i)$$

$$+ \Psi_{4i} \left. \begin{array}{l} \cos d(t - \tau_i) \\ \dots \end{array} \right\} u(t - \tau_i) \quad . \quad (24b)$$

These equations do not lend themselves to immediate conclusions as to the interactions of the system parameters due to complexity of the expressions. These expressions are computed numerically for different values of  $p_1$ ,  $p_2$ ,  $p_{12}$ ,  $\xi_1$ ,  $\xi_2$ , and period and type of excitation. The FORTRAN computer programs are written in such a way that the pressures in the cavities are computed in time domain for stated values of system parameters and the period of excitation pressures, and the printout is the maximum pressure that can occur in a given interval of time (Appendix C).

The response spectra of the transient response of the system are plotted in the frequency domain in Figures 10 to 18 for a sine pulse type excitation pressure. The system parameters used to represent responses are the frequencies of uncoupled resonators and damping factors. Since there are five system parameters in addition to the period of excitation, it is not possible to study the effect of each parameter on the response either from equations or from one representative curve. Hence, the results are presented in several figures such that the effect of two parameters can be studied in each of the figures. Figures 19a and 19b are the pressure response spectra of the same system for saw tooth and N-wave type excitations.

The frequencies are non-dimensionalized with respect to the frequencies corresponding to the period of excitation pressures. The pressures in the cavities are normalized with respect to the amplitude of the excitation pressures and thus correspond to pressure magnifications. In these figures  $P_1$  and  $P_2$  are the response pressures and

$\xi_1$  and  $\xi_2$  are the damping factors in the cavities  $V_1$  and  $V_2$ , respectively. The uncoupled frequencies are represented by  $f_1$  and  $f_2$ , and coupling frequency by  $f_{12}$ .  $A_0$  and  $\tau$  are the amplitude and the period of the excitation pressures.

From these spectra, it is not possible to conclude the critical circumstances under which the pressure magnification in the cavities will be maximum. However, by studying the numerical values of the maximum response for various values of frequencies and period of excitation pressures, it appears that the pressures will be magnified to a maximum possible value (maximax) whenever two natural frequencies are close to each other and also they are equal to both uncoupled frequencies and frequency of excitation. Ideally, this occurs when the two natural frequencies,  $p_+$  and  $p_-$ , are equal; however, this cannot happen because of the presence of the coupling term in the system.

A physical explanation for these large magnifications can be given in the following way: when two natural periods are equal, the plugs of air in the necks will attempt to move with the same frequency. If the two uncoupled natural periods are equal to the natural periods, then even a small amplitude of excitation pressure with the same period will reinforce the motion of air particles in the necks, thereby increasing the displacement magnification to a large extent.

Figures 10 and 11 illustrate the effect of the frequencies,  $f_1$  and  $f_2$  on pressure response in the cavity  $V_2$ , for an undamped system of double acoustical resonator. In Figure 10, the maximum pressure response in  $V_2$  to variable uncoupled frequency  $f_1$  of cavity  $V_1$ , with selected parametric values of uncoupled frequency  $f_2$  of cavity  $V_2$ , is

shown. In Figure 11, the maximum response pressure  $P_2$  to variable frequency of cavity  $V_2$ , with selected parametric values of frequency  $f_1$  of cavity  $V_1$ , is presented. In both these figures the other parameters of the system are held constant. The excitation pressure is a sine pulse with a period of 0.05 seconds, damping factors,  $\xi_1$  and  $\xi_2$  in the cavities are held zero, and the coupling frequency of the system,  $f_{12}$  retains a constant value of 2 cps. For each frequency  $f_2$  in Figure 10, and  $f_1$  in Figure 11, the maximum response curve shows the expected two humps of a two degree-of-freedom system. The family of curves is also a representative of classical dynamic absorber problem. As an illustration, as the difference between the uncoupled frequencies,  $f_1$  and  $f_2$  increases, the maximum response pressure  $P_2$  diminishes. As the difference between the uncoupled frequencies and the excitation frequency increases, the humps diminish and spread farther apart. When the difference is small the merging of the two humps reinforce each other to present a maximax response condition. This is shown by drawing the dotted envelope to the larger peak values.

Figures 12 and 13 demonstrate the effect of uncoupled frequencies of the system and the coupling frequency on response pressure in cavity  $V_2$ . In Figure 12, the maximum pressure response in cavity  $V_2$  to variable frequency  $f_1$ , with selected parametric values of coupling frequency  $f_{12}$ , is presented. The frequency of cavity  $V_2$ , is held constant at 20 cps. In Figure 13, the maximum pressure in cavity  $V_2$ , to variable uncoupled frequency,  $f_2$ , is shown for different values of coupling frequency  $f_{12}$ . The uncoupled frequency  $f_1$ , of the cavity  $V_1$ , is held constant at 20 cps. The other parameters of the system are held constant in these two figures. The damping factors are kept

at zero. The excitation pressure is a sine pulse with a period of 0.05 seconds. The maximum response pressure occurs when the frequencies of both the resonators are close together. As already stated in the earlier part of this section, it is clear from these figures that the pressure magnification in the cavity  $V_2$ , would increase as the coupling frequency  $f_{12}$ , decreased. As the difference between either of the natural periods,  $1/f_1$  or  $1/f_2$ , and the period of excitation pressure increases, the influence of  $f_{12}$  reduces, as can be seen in these figures for larger values of  $f_1$  or  $f_2$ .

Figure 14 is the description of the effect of coupling frequency  $f_{12}$  on the maximum response pressure in cavity  $V_2$ , for different parametric values of  $f_1$  and  $f_2$ . The damping factors,  $\xi_1$  and  $\xi_2$ , are kept at zero. The excitation pressure is a sine pulse with a period of 0.05 seconds. As illustrated in Figures 12 and 13, these curves also indicate that the maximum pressure in the cavity  $V_2$  will increase as the coupling frequency decreases. It can be observed from this figure that the pressure  $P_2$  is greater when the frequencies of two resonators are equal. This can also be seen from Figures 10 and 11.

Figures 15a and 15b are the pressure response spectra of cavity  $V_1$  for a double acoustical resonator system. The excitation pressure is a sine pulse with a period of 0.05 seconds. In Figure 15a, the maximum response pressure in cavity  $V_1$ , with two selected parametric values of frequency  $f_2$ , is shown. The coupling frequency  $f_{12}$ , is held constant and equal to 2 cps. These curves show that the influence of frequency  $f_2$ , of the cavity  $V_2$ , on the maximum pressure  $P_1$  in cavity  $V_1$  is very small. In Figure 15b the maximum pressure response in cavity  $V_1$  to variable frequency  $f_1$ , with selected values of coupling

frequency  $f_{12}$ , is shown. The frequency  $f_2$  of the cavity  $V_2$  is held constant at 20 cps. These curves indicate that the effect of coupling frequency on the response pressure in cavity  $V_1$ . From these two figures it can be observed that the frequency  $f_2$  of cavity  $V_2$ , and the coupling frequency  $f_{12}$ , have very small influence on the pressure  $P_1$  in cavity  $V_1$  so long as the difference between the frequency  $f_1$  and the excitation frequency corresponding to the period,  $\tau$ , is large.

Figure 16a is an illustration of the effect of the frequency  $f_2$  on the pressure magnification in cavity  $V_1$ . In this figure the variation of pressure  $P_2$  is shown as the frequency  $f_2$  varies for two parametric values of frequency  $f_1$  of cavity  $V_1$ . The damping factors,  $\xi_1$  and  $\xi_2$  are zero and the coupling frequency  $f_{12}$  is kept constant at 2 cps. The excitation pressure is a sine pulse with a period of 0.05 seconds. From the curves in this figure it can be inferred that the variation of frequency of cavity  $V_2$  does not affect the pressure in the cavity  $V_1$ . The significant effect of  $f_2$  can be seen mainly when the period of excitation is very close to the natural period  $1/f_2$  of cavity  $V_2$ .

In Figure 16b, the maximum pressure magnification in  $V_1$  to the coupling frequency  $F_{12}$  is shown for two parametric values of frequency  $f_1$  of cavity size  $V_1$ . The damping factors are zero and the frequency  $f_2$  is held constant at 20 cps. The excitation pressure is a sine pulse with a period of 0.05 seconds. From this figure it is not possible to conclude the general effect of the system parameters on the response pressures in cavity  $V_1$ . However, from Figures 16a and 16b it can be observed that the frequency  $f_1$  and coupling frequency  $f_{12}$  are the system parameters that affect the pressure magnification in

cavity  $V_1$ .

In Figures 17, 18a, and 18b, the maximum pressure response in cavity  $V_2$  to frequency  $f_1$ , with the parametric values of  $f_2$ , is shown for a damped double acoustical resonator. The coupling frequency  $f_{12}$  is kept constant at 2 cps. The excitation pressure is a sine pulse with a period of 0.05 seconds. But the damping factors are different in these three figures: In Figure 17, the damping factors,  $\xi_1$  and  $\xi_2$  are 0.05; In Figures 18a and 18b, these damping factors are 0.1 and 0.15, respectively. In these three figures the general trend of the maximum pressure response is the same as discussed earlier and given in Figure 10. However, comparison of these figures with Figure 10 indicates the effect of damping. It can be observed from these two figures that the maximum pressure magnification in cavity  $V_2$ , may be reduced to about three by incorporating the damping factors  $\xi_1$  and  $\xi_2$  equal to 0.1 in the system.

Figures 19a and 19b are the maximum pressure response spectra which illustrate the effect of frequencies  $f_1$  and  $f_2$  on the pressure in cavity  $V_2$ . The damping factors  $\xi_1$  and  $\xi_2$  of the cavities are held constant at 0.1. The coupling frequency in both the cases is kept at 2 cps. The variation of maximum pressure to frequency  $f_1$  with selected parametric values of frequency  $f_2$  of cavity  $V_2$  is shown. In Figure 19a, the excitation pressure is a saw tooth wave with amplitude of unity and period of 0.05 seconds. In Figure 19b, the excitation pressure is an N-wave with a period of 0.05 seconds and amplitude of unity. The general trend and behavior of the curves is the same as illustrated in Figure 18a, which is the response spectra of the system for a sine pulse type excitation. Comparison of these three figures

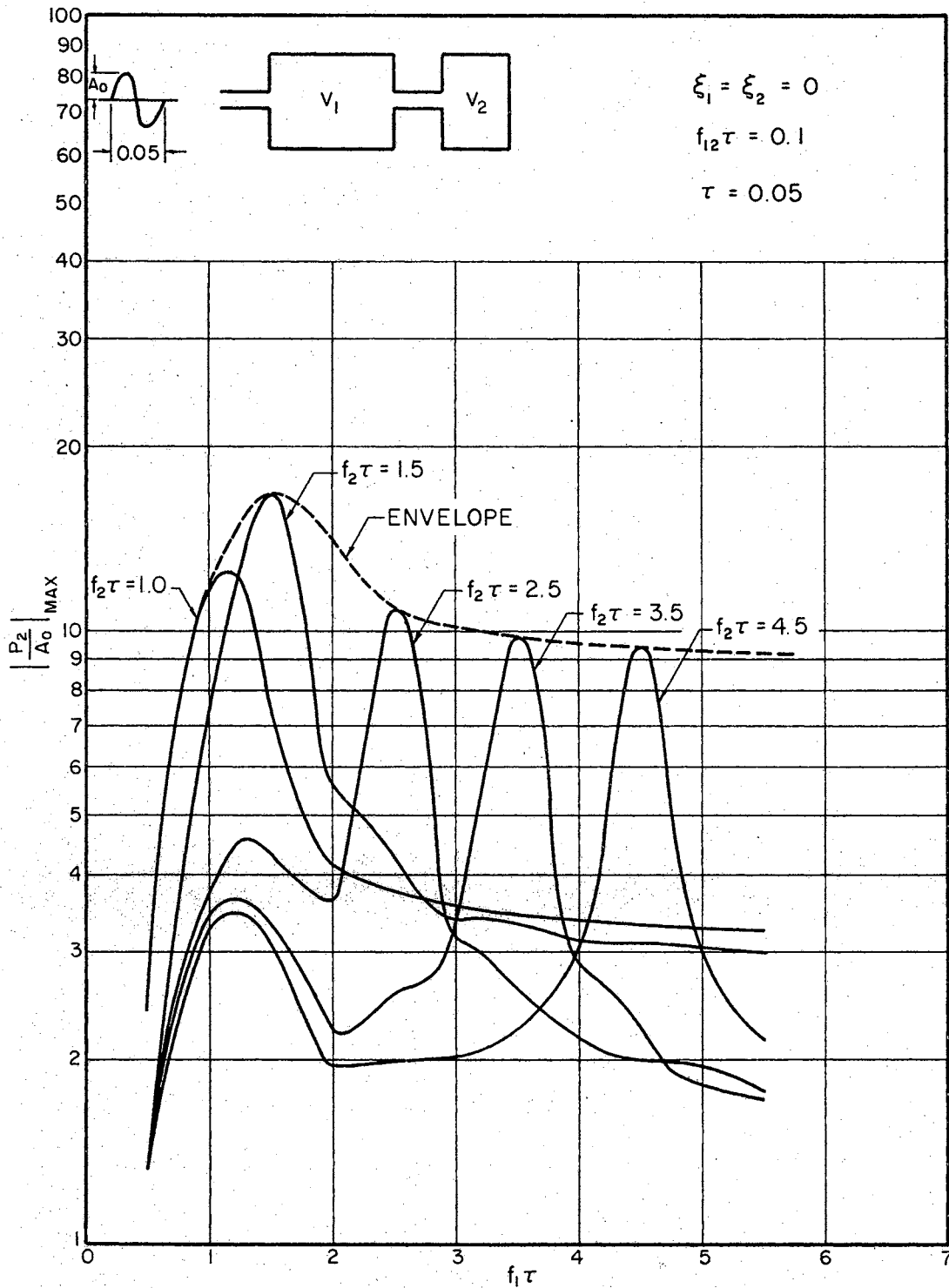


Figure 10. Pressure Response Spectra in  $V_2$  For a Constant Coupling Frequency (Effect of  $f_1$  on Undamped Resonator)



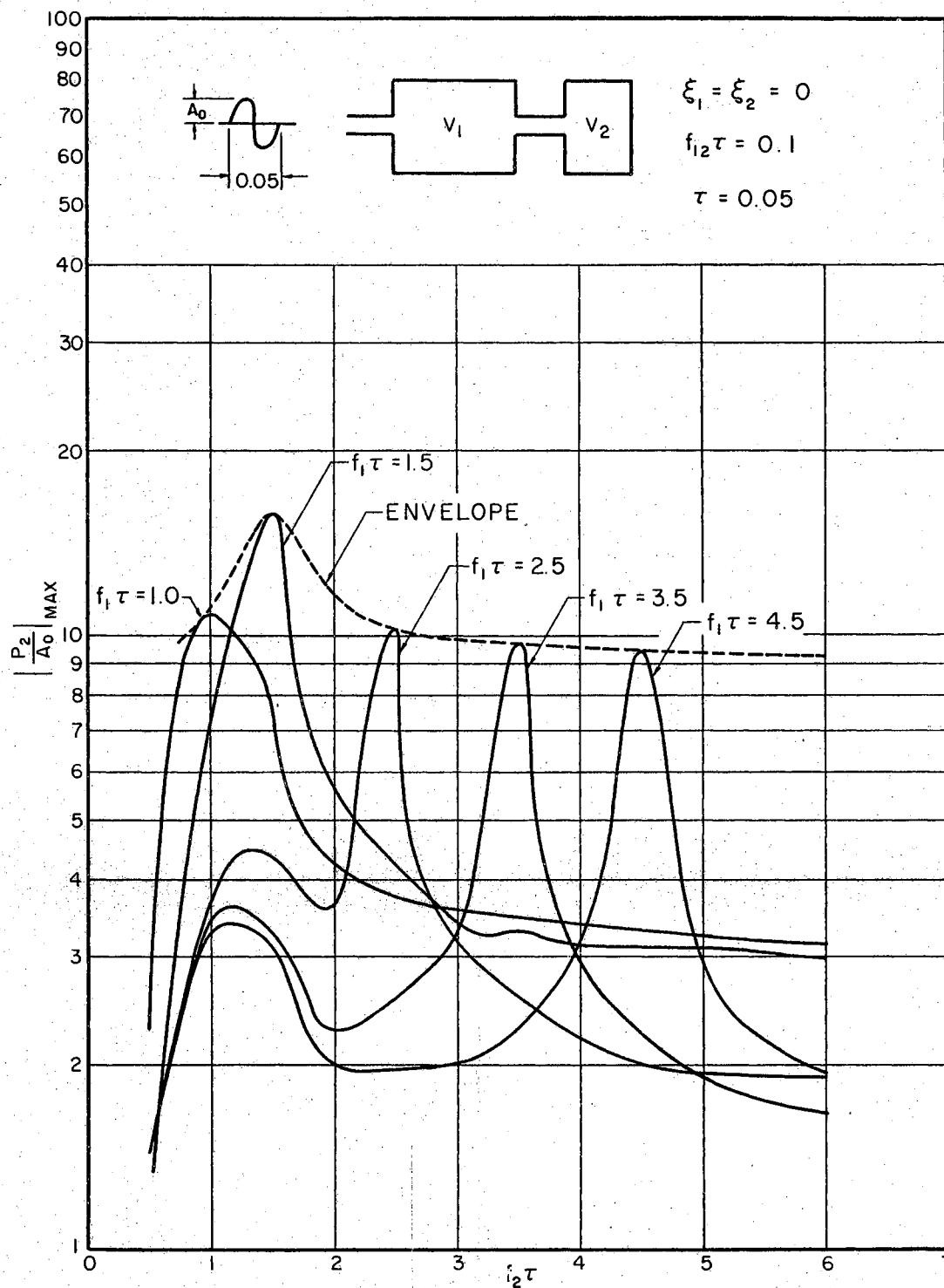


Figure 11. Pressure Response Spectra in  $V_2$  For a Constant Coupling Frequency (Effect of  $f_1$ )

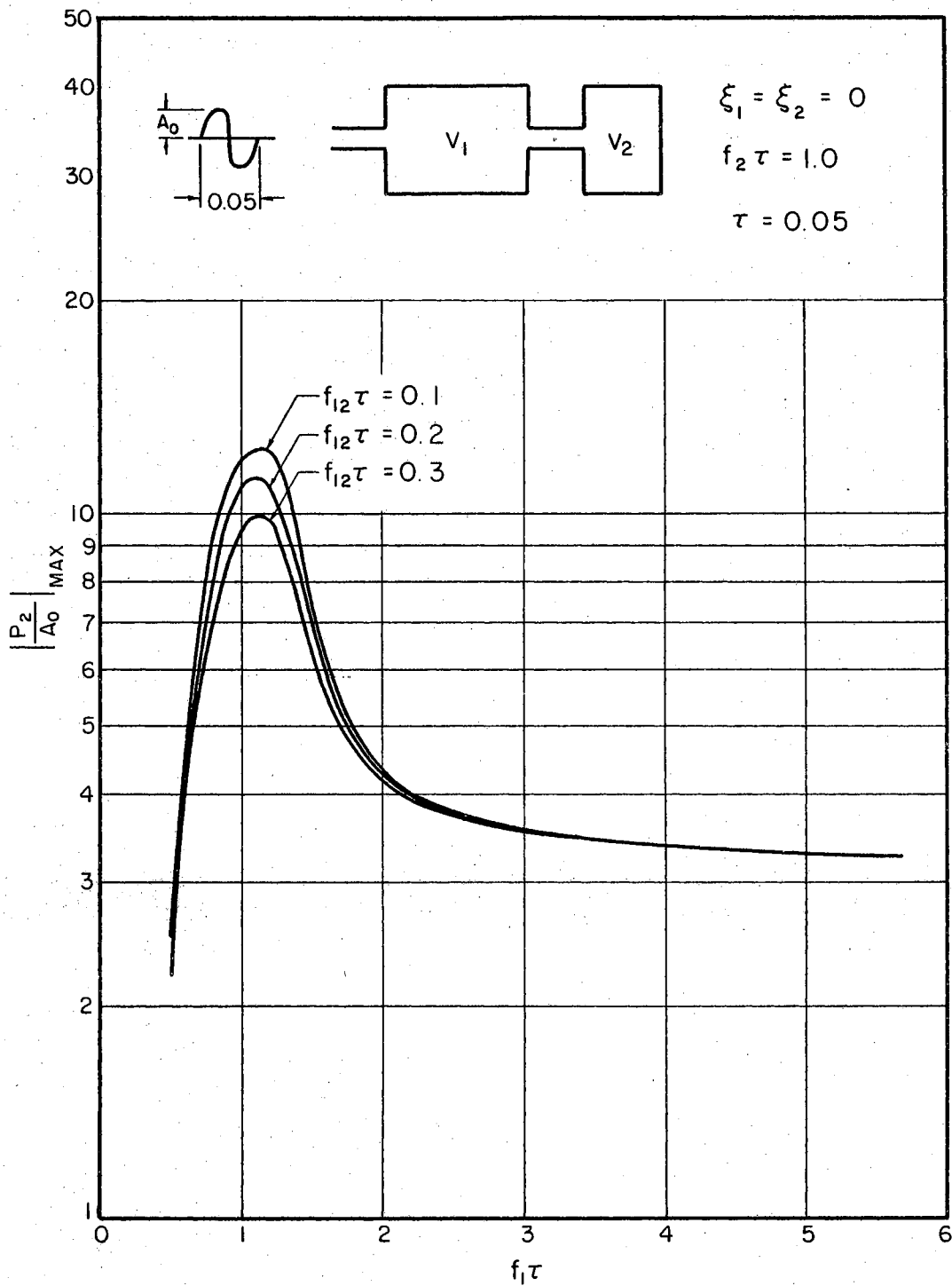


Figure 12. Pressure Response Spectra in  $V_2$  For a Constant  $f_2$   
(Effect of  $f_1$  and  $f_{12}$ )

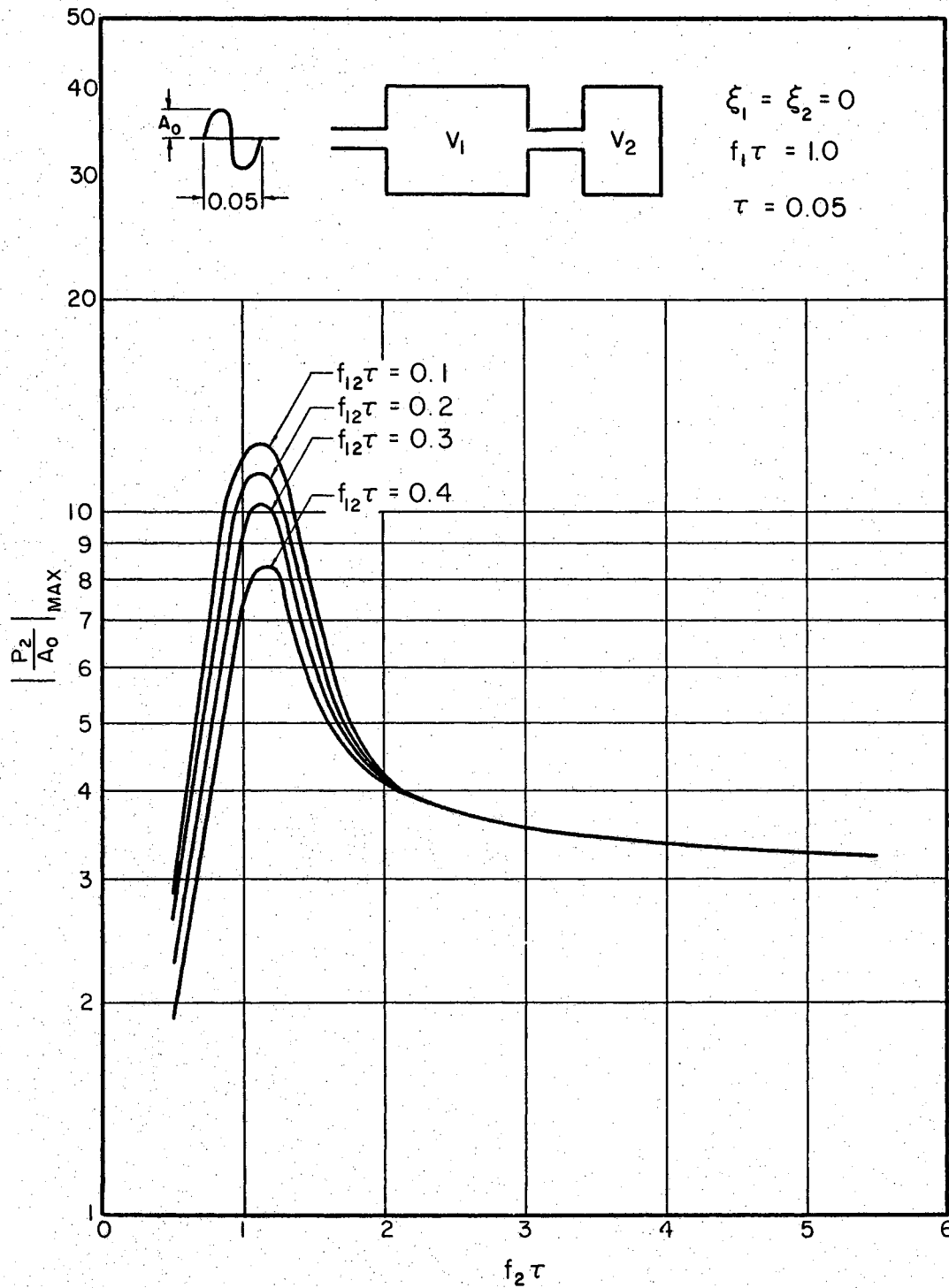


Figure 13. Pressure Response Spectra in  $V_2$  for a Constant  $f_1$   
(Effect of  $f_2$  and  $f_{12}$ )

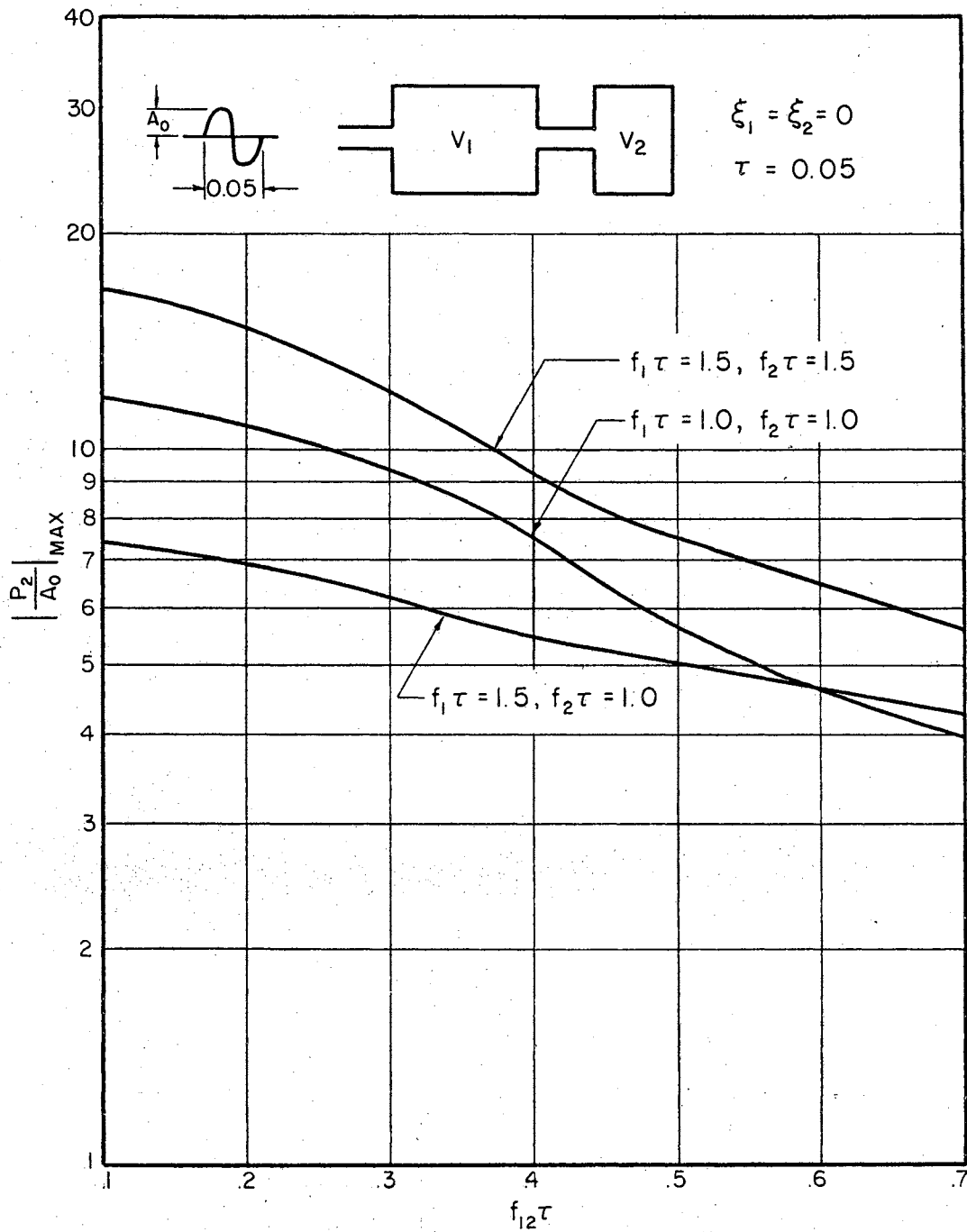


Figure 14. Pressure Response Spectra in  $V_2$  (Effect of  $f_{12}$ )

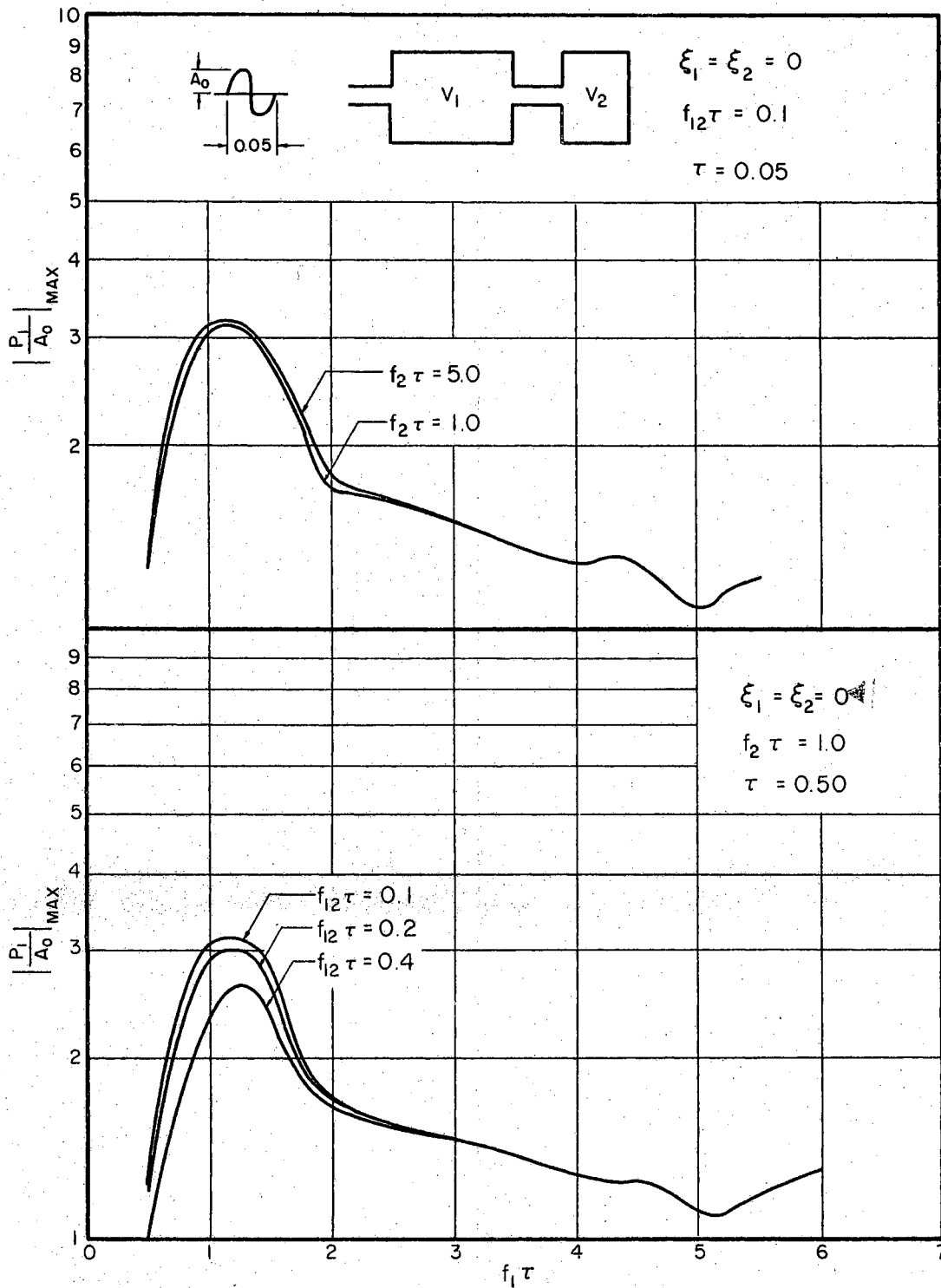


Figure 15a, 15b. Pressure Response Spectra in  $V_1$  For Constant  $f_{12}$  and  $f_2$  (Effect of  $f_1$ )

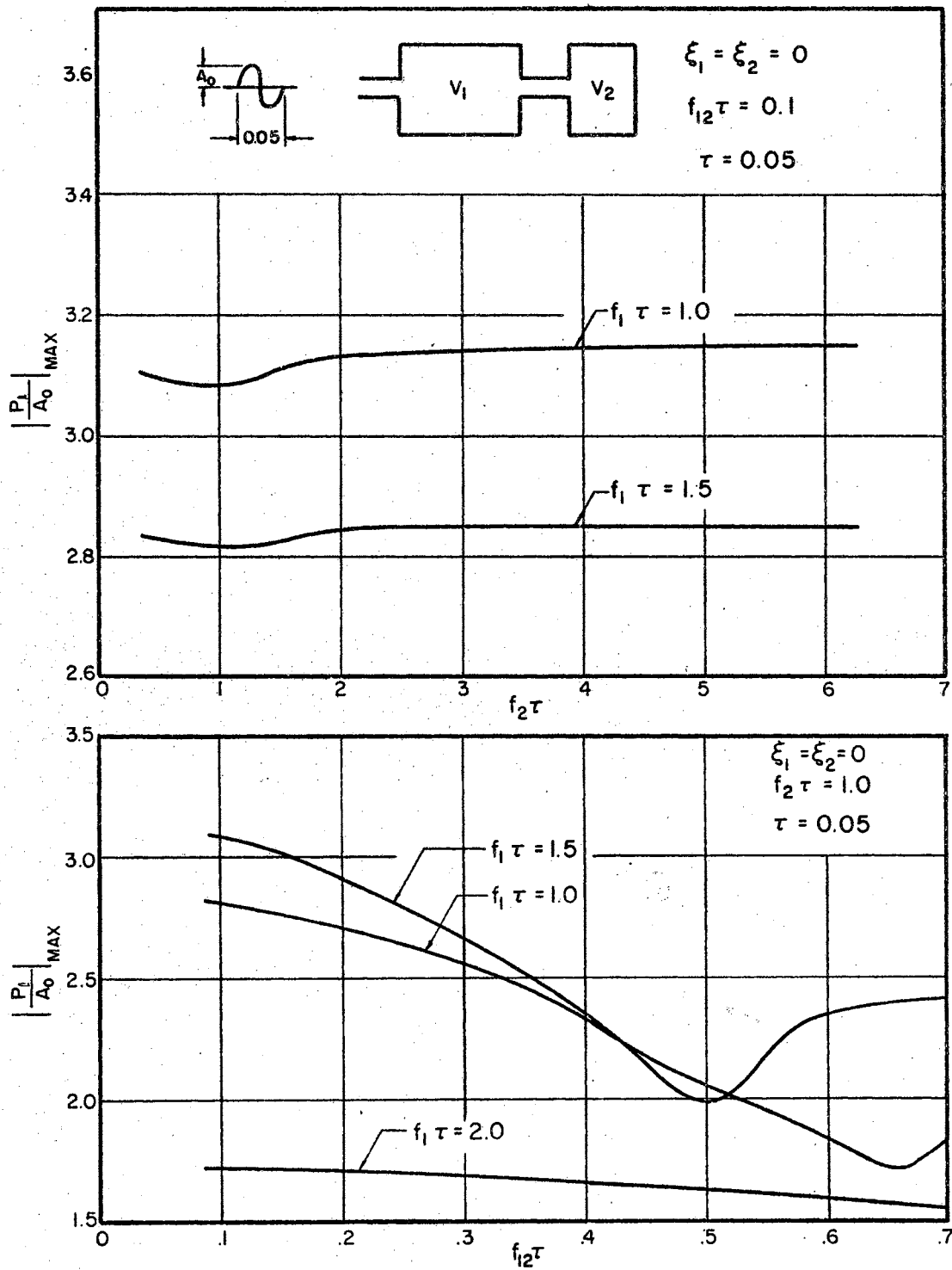


Figure 16a, 16b. Pressure Response Spectra in  $V_1$  For Constant  $f_{12}$  and  $f_2$  (Effect of  $f_2$  and  $f_{12}$ )

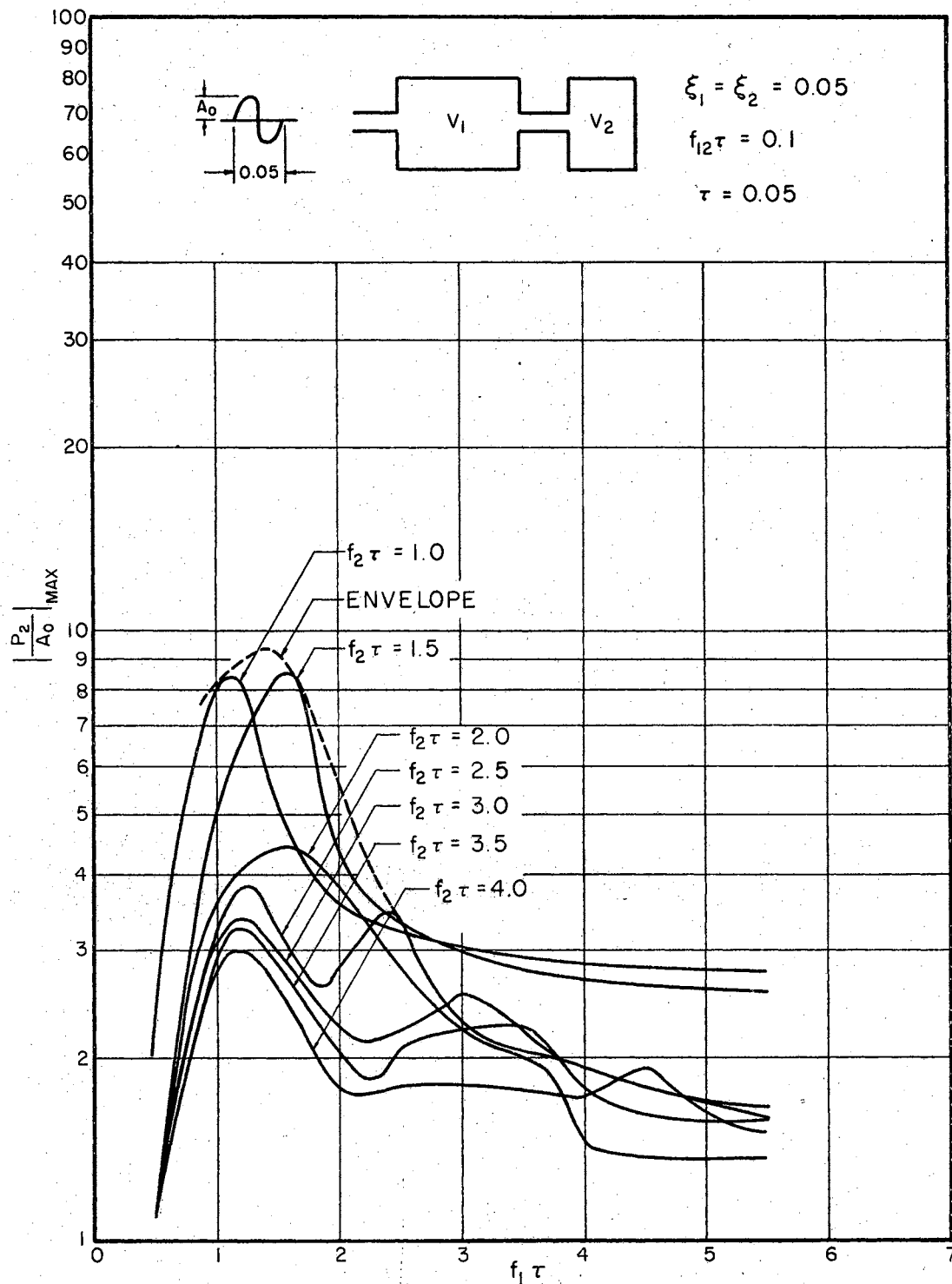


Figure 17. Pressure Response Spectra in  $V_2$  for Constant  $f_1$   
 (Effect of  $f_1$  With Damping Factors,  $\xi_1 = \xi_2 = 0.05$ )

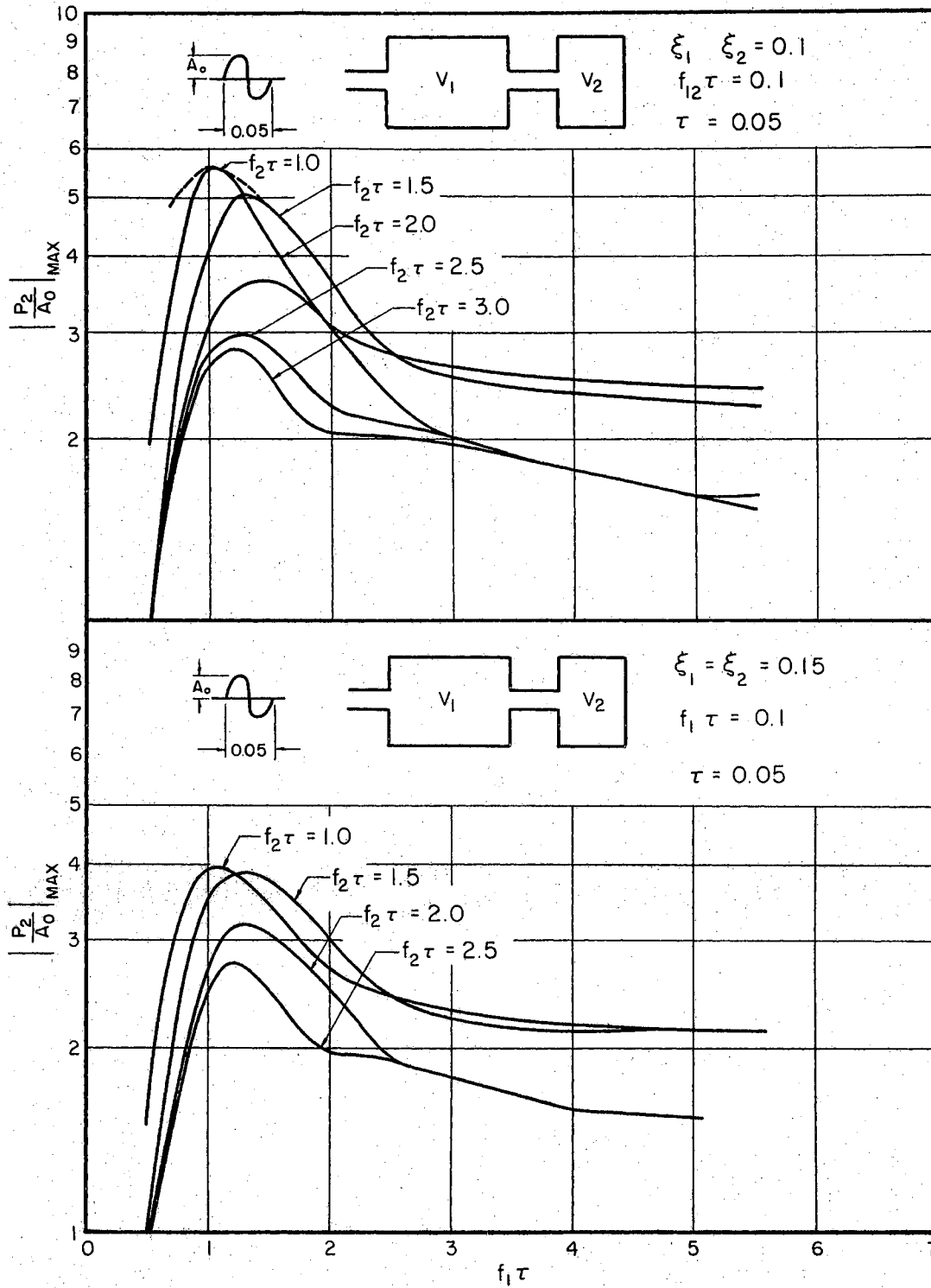
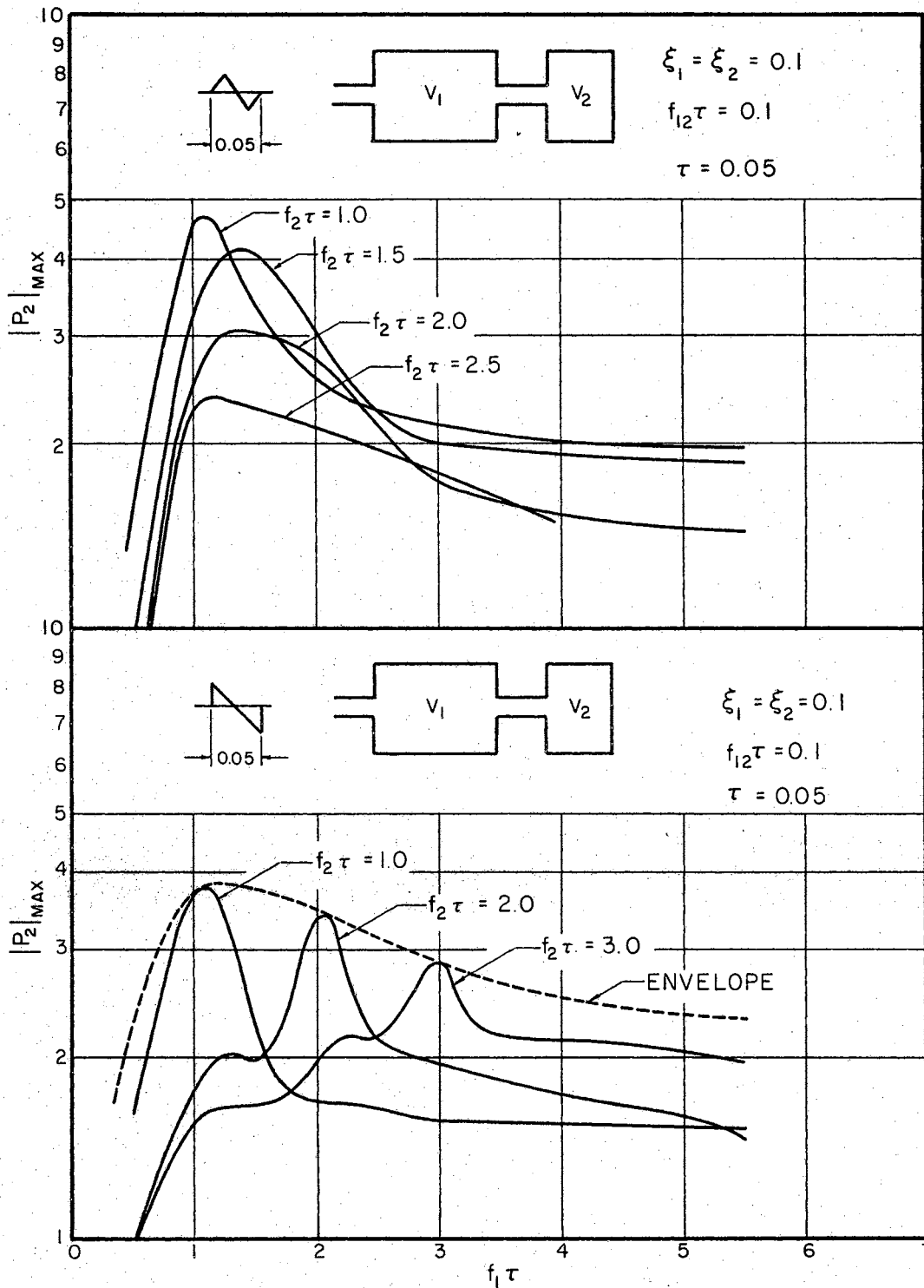


Figure 18a and 18b. Pressure Response for Constant  $f_{12}$   
(Effect of  $f_1$  and Damping Factors)





shows that the maximax pressure response will be greater for the excitation of a sine pulse, when the other parameters are held same.

From the pressure response spectra of the double acoustical resonator to an excitation pressure of one sine pulse, it is apparent that the uncoupled natural frequency  $f_2$  has little effect on the pressure in cavity  $V_1$ . The prime controlling parameters of this response pressure are  $f_1$ ,  $f_{12}$  and the period of excitation pressure. However, the pressure in the cavity  $V_2$  is affected by both the frequencies  $f_1$  and  $f_2$ . The coupling frequency  $f_{12}$  has a considerable effect on the pressures in both the cavities when the normalized frequencies,  $f_1 \tau$  and  $f_2 \tau$ , are close to unity. The damping factor of 0.1 reduces the maximax pressure magnification in the cavities from 16.7 to 5.1 as can be seen by comparing Figures 10 and 18a. From Figure 14, it appears that the pressure magnification in cavity  $V_2$  can be as high as 18 for a system having a coupling frequency of 2 cps, uncoupled frequencies  $f_1 = f_2 = 30$  cps, and damping factors  $\xi_1 = \xi_2 = 0$ . However, these values are not the highest possible maximax pressures, since in certain cases where the system is tuned properly by varying the system parameters and the period of excitation pressures, these pressures can be magnified theoretically to the order of about 50. Since in physical systems the damping is inevitable and the coupling is limited, the highest actual maximax magnifications would be of the order of about 15.

#### Mechanical System

In certain cases, an acoustical system coupled to a mechanical system can be idealized to a simple mechanical system. The physical

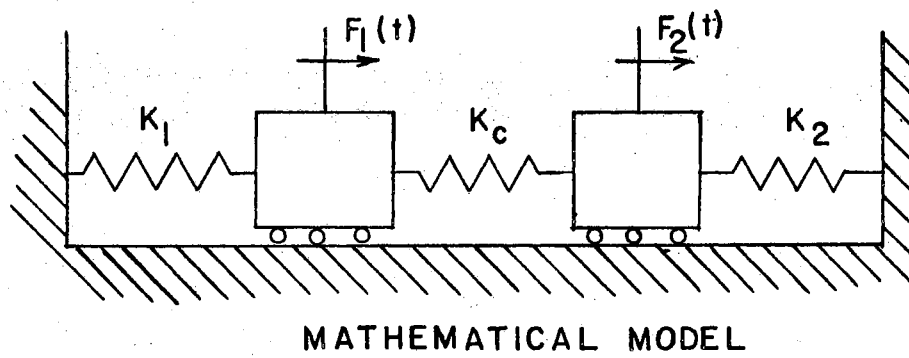
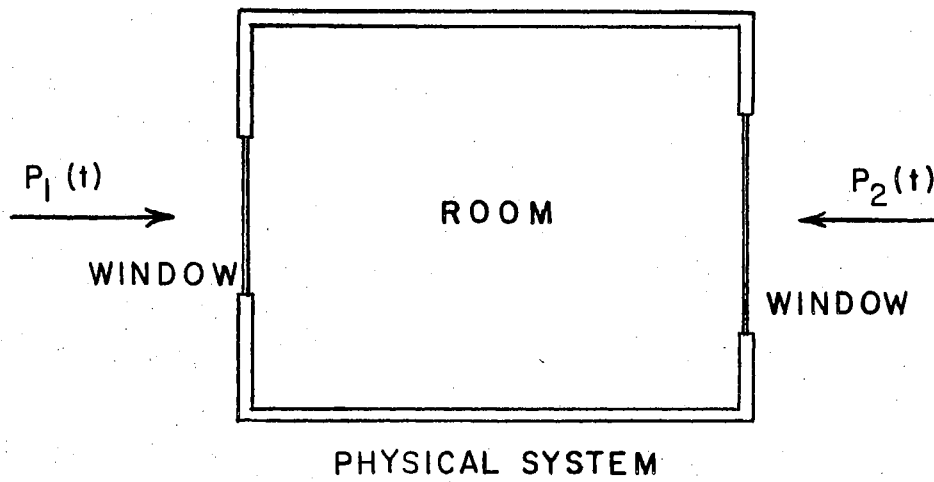


Figure 20. Mechano-acoustic System

and mathematical models of this type of system are shown in Figure 20. With the assumption of no dissipation of energy in the system, the following equations of motion may be derived:

$$M_1 \ddot{x}_1 + (k_1 + k_c) x_1 - k_c x_2 = F_1(t) ,$$

and

$$M_2 \ddot{x}_2 + (k_2 + k_c) x_2 - k_c x_1 = F_2(t) ; \quad (25)$$

where  $F_1(t)$  and  $F_2(t)$  are the external forces acting on masses  $M_1$  and  $M_2$ , respectively. The response solution discussed in this chapter can be extended to this system since the differential equations (25) are of the same type as equations (8).

The displacement response spectra of the system shown in Figure 20 are plotted for a particular configuration in Figures 21 to 23. The system parameters selected for this study are that of a typical commercial building of a large size warehouse, and the sonic boom type of excitation pressure with a period of 0.135 seconds. The effect of one uncoupled frequency  $f_1$  was studied, keeping the other two frequencies constant for three kinds of application of excitation force of one sine pulse: 1) external force only on one mass, 2) external force on both the masses in the same direction (in phase), and 3) external force on both the masses in opposite direction to each other (phase opposition). The response displacement,  $x_1$ , was normalized with respect to displacement,  $x_{st_1}$ .  $x_{st_1}$  is defined as the static displacement of mass  $M_1$ , when a static force equal to the amplitude of excitation force  $F_0$  is applied on mass  $M_1$  while mass  $M_2$  is held stationary. Similarly, the displacement  $x_2$  is normalized with respect to static displacement  $x_{st_2}$ . These normalizing quantities are given by,

$$x_{st_1} = \frac{F_o}{k_1 + k_c} ,$$

$$x_{st_2} = \frac{F_o}{k_2 + k_c} .$$

In many practical cases the excitation pressures such as sonic booms and blastings would be on all external sides of buildings which can be idealized as the force acting on both the masses in opposite directions.

Figure 21 is the displacement response of the mechanical system when only one mass is excited with transient force of a sine pulse. The displacement of mass  $M_2$ , which is not excited by the external force, is much less than that of the mass  $M_1$ . Both the modes of the system are excited and the maximax of  $x_1$  and  $x_2$  occur at  $f_1$  equals 8.3 and 8.8, respectively.

Figure 22 is the displacement magnifications plotted when both the masses are excited with the force of sine pulses in the opposite direction. In this case, primarily the second mode of the system is excited. The displacements  $x_1$  and  $x_2$  are maximum when the frequency  $f_1$  equals 7.4 and 8.2, respectively. Figure 23 is the displacement response when both the masses are excited with forces of sine pulses in the same direction. In this case the system is excited mainly with its first mode. The maximum displacements  $x_1$  and  $x_2$  occur at  $f_1$  equals 6.9 and 8.9, respectively.

When both the masses of the system are excited by the forces in the opposite direction as in Figure 22, the potential energy would be stored in all the three springs. But when the forces are applied in

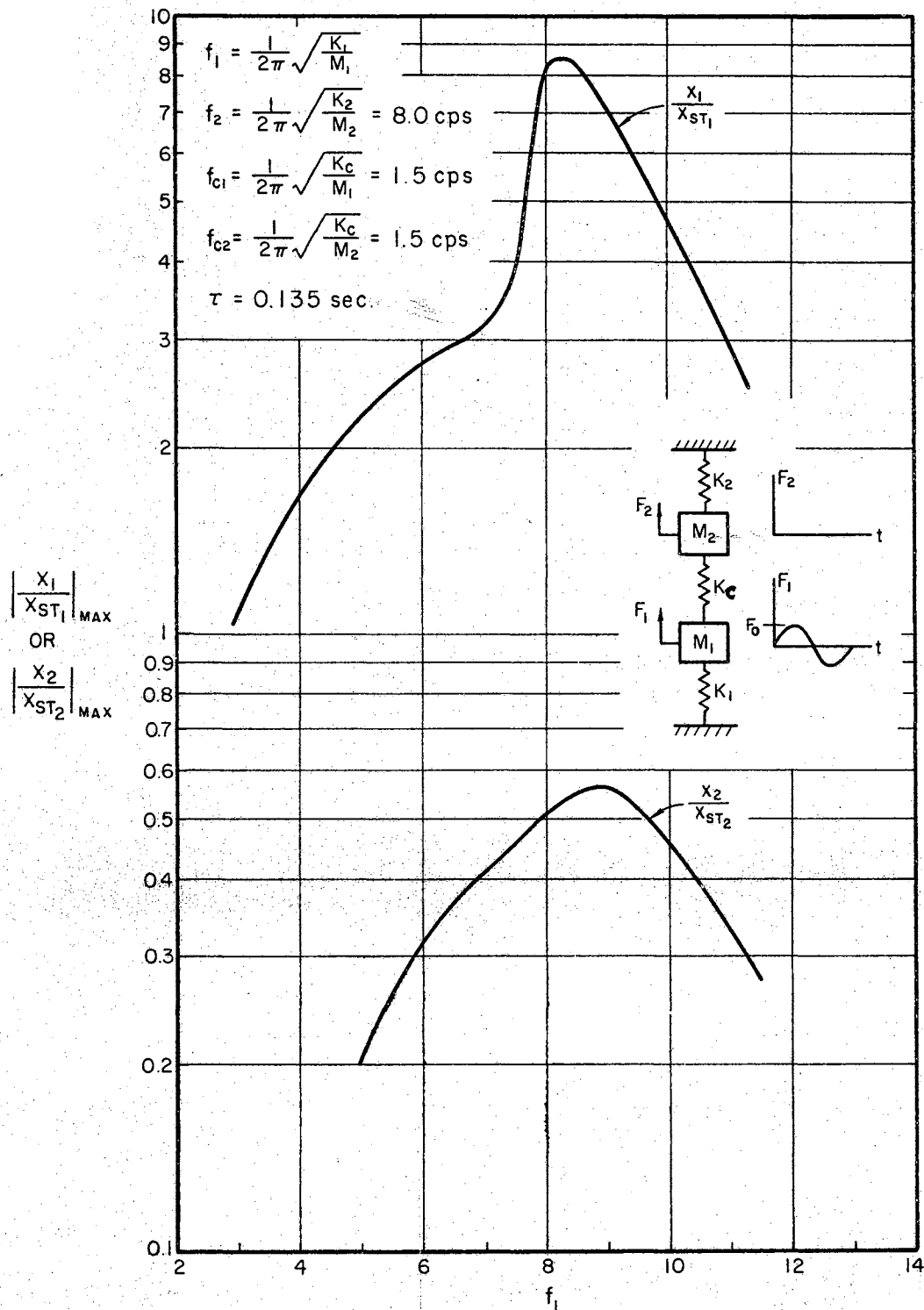


Figure 21. Displacement Response Spectra of Two Degrees-of-Freedom System (Mass  $M_1$  is Excited by a Force of Sine Pulse)

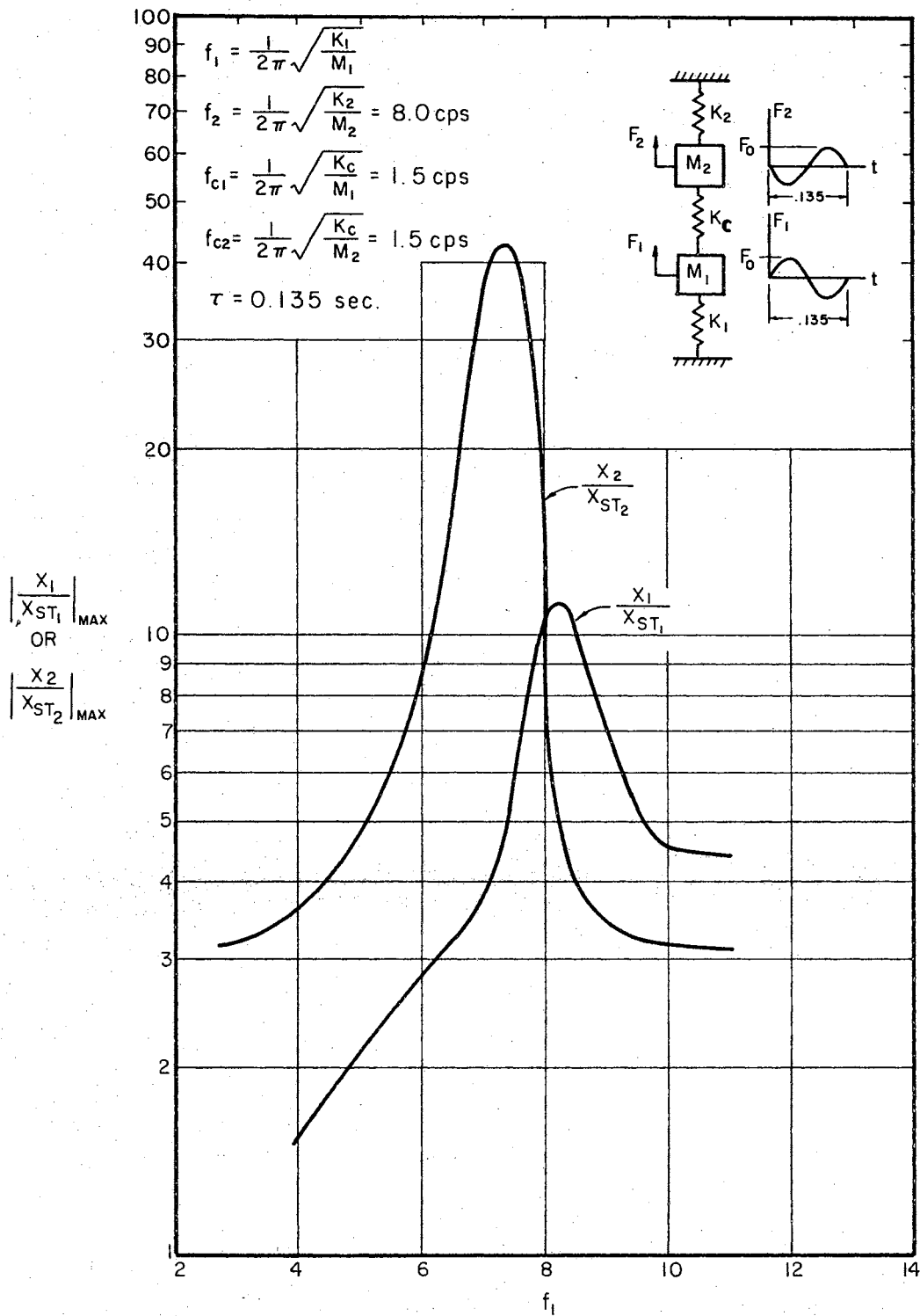


Figure 22. Displacement Response Spectra of Two Degrees-of-Freedom System (Both the Masses are Excited by the Forces of Sine Pulses in the Opposite Direction)

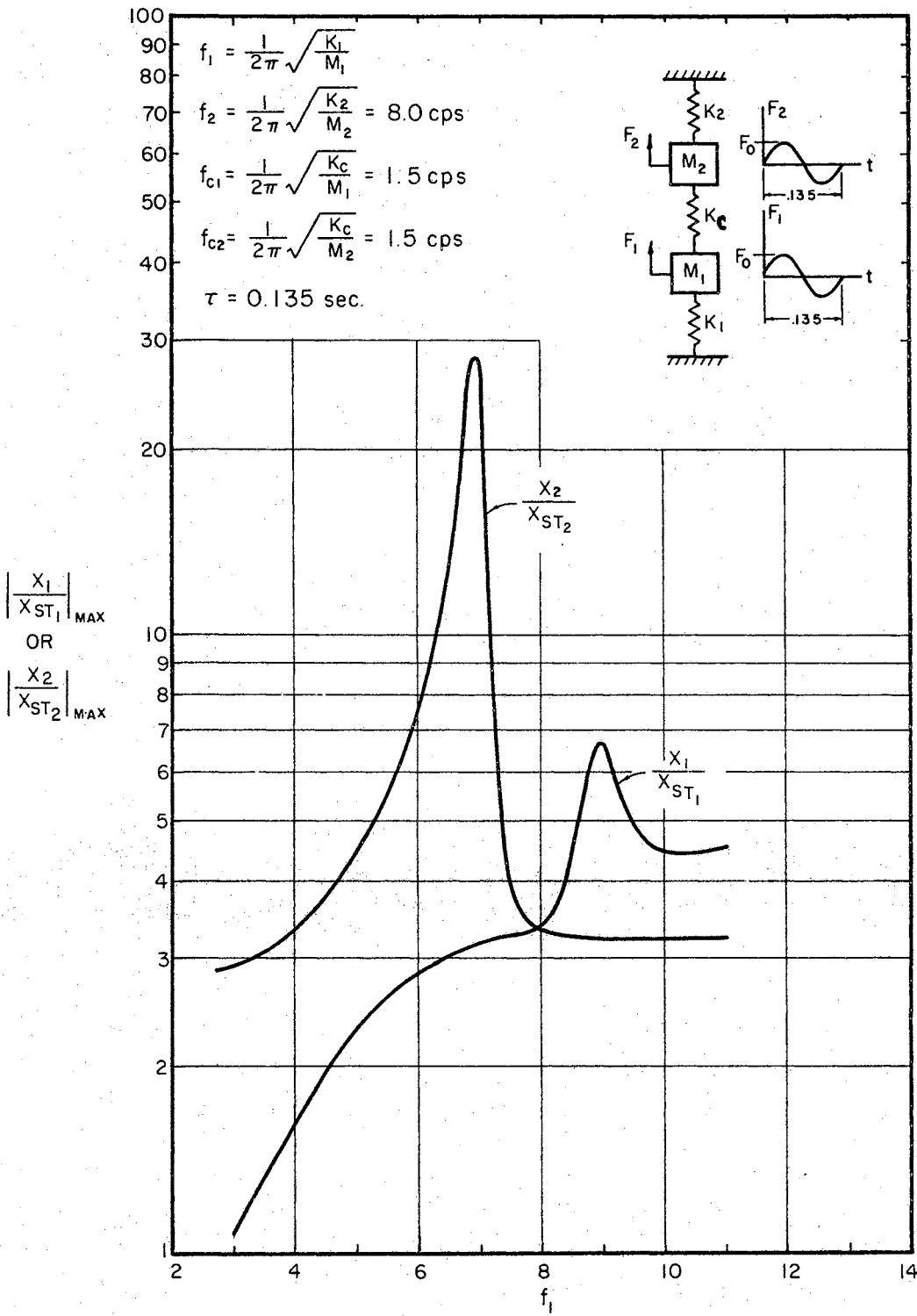


Figure 23. Displacement Response Spectra of Two Degrees-of-freedom System (Both the Masses are Excited by the Forces of Sine Pulses in the Same Direction)



the same direction as in Figure 23, the potential energy would be stored essentially in springs  $k_1$  and  $k_2$ . Therefore, the system can store more energy in the first case than in the second case for a given force and in a given interval of time. The displacement magnifications are large in the first case. In a properly tuned system, the displacements can be large enough to damage the structures. However, the presence of damping reduces the displacements to some extent, as discussed in the previous section.

## CHAPTER V

### EXPERIMENTAL MODEL AND INSTRUMENTATION

In order to substantiate the theory established and verify the validity of the assumptions made in the previous chapters, it was necessary to build an experimental model of a double acoustical resonator and devise an apparatus capable of producing appropriate finite duration pressures whose shape, amplitude, and time duration were within the limits which permit easy study. A small scale model of two resonators coupled through the neck was built so that the system parameters could be changed easily.

#### Description of the Model

The test resonator which was used to study the response of the double acoustical resonator in the laboratory consisted of two cylindrical tubes with cylindrical necks made up of plexiglass. The two resonators were of different sizes as shown in Figure 24. A photograph of this assembled model is shown in Figure 25. The dimensions of the model were dictated by the frequencies of the excitation pressures. The diameters of the necks were mainly dictated by the coupling frequency. To have a small value of coupling frequency, it was desirable to have a smaller cross sectional area and larger length for the neck,  $N_2$ , which coupled the two resonators. It was essential to have a large volume for cavity  $V_1$  and small volume for  $V_2$  for both of the uncoupled

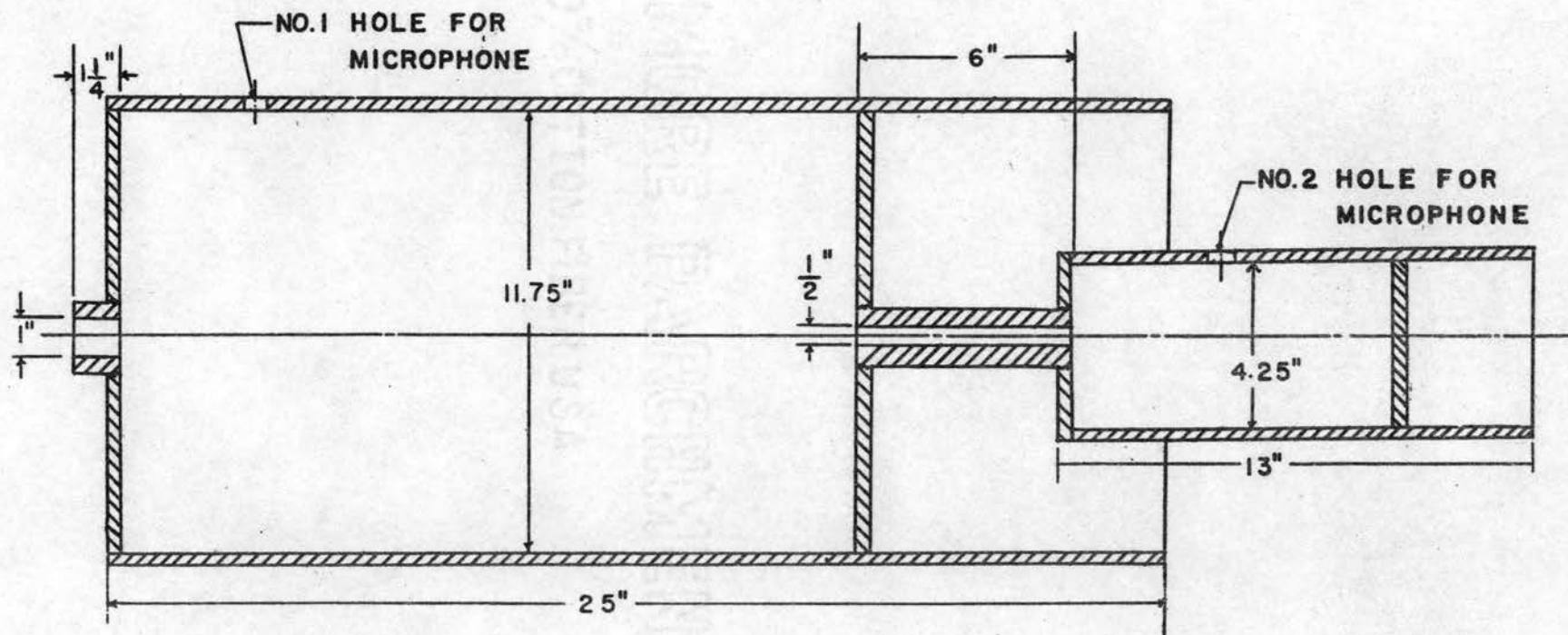


Figure 24. Configuration of Test Resonator (Double Acoustical Resonator)

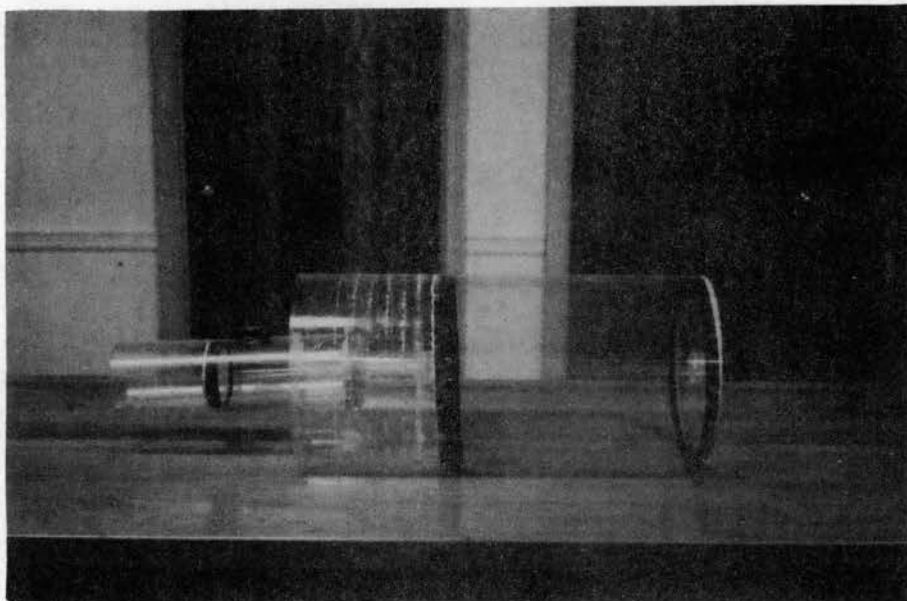


Figure 25. Test Resonator Assembly

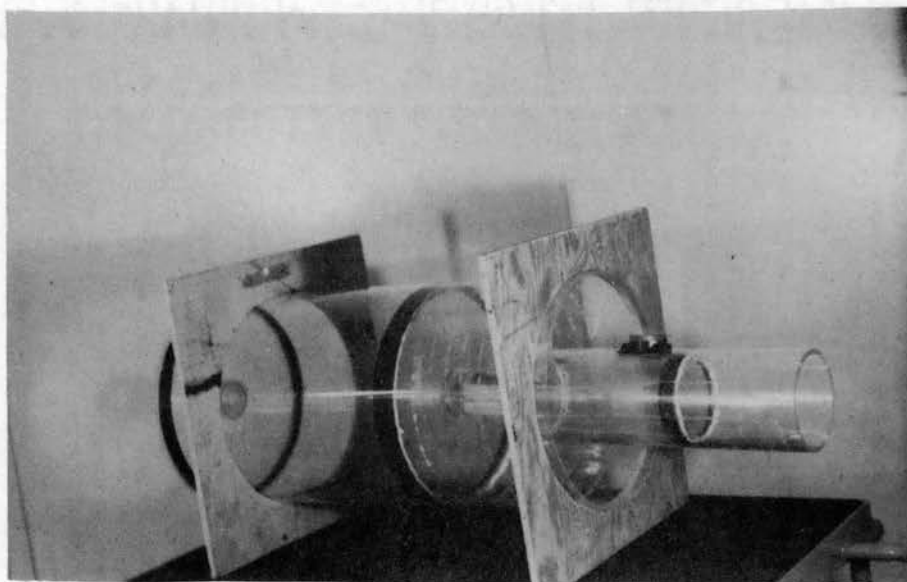


Figure 26. Test Resonator Mounted in Wooden Frame

frequencies to be of the same order of magnitude, since the cross sectional area of neck,  $N_2$ , is small. The inside diameters of the cavities were 11.75 inches and 4.25 inches. The length of the larger resonator could be varied from zero to 24 inches and the smaller one from zero to 12 inches by varying the positions of the respective pistons. The necks were threaded to the pistons so that these could be replaced easily by the cylindrical necks of the required dimensions. By changing the volumes of the cavities and dimensions of the necks, the system parameters  $p_1$ ,  $p_2$ , and  $p_{12}$  could be easily varied. Holes, measuring  $5/16$  of an inch, were drilled on the walls to install Altec microphones to measure the pressures inside the cavities. The cavities were sealed by using  $1/16$  inch felt on the circumference of the pistons. The resonators were mounted in a wooden framework as shown in Figure 26, which served two purposes, 1) as a reinforcement to make the walls rigid, and 2) as a stand for the resonator system while testing.

#### Simulation of Finite Duration Transient Pressures

The plane wave tube which was available in the Oklahoma State University Acoustic Laboratory was used as an acoustic delay line to produce transient pressures which were used as excitation pressures on the system. This apparatus had a cross sectional area of about 14 inches square and was 32 feet long. A photograph of this tube is shown in Figure 27. To have a plane wave at the test end of the tube, the length had to be much larger than either of the cross sectional dimensions and at the input end it needed to be driven in an evenly distributed manner. The first requirement was satisfied by the available dimensions of the tube, and the second requirement was accomplished by driving with a

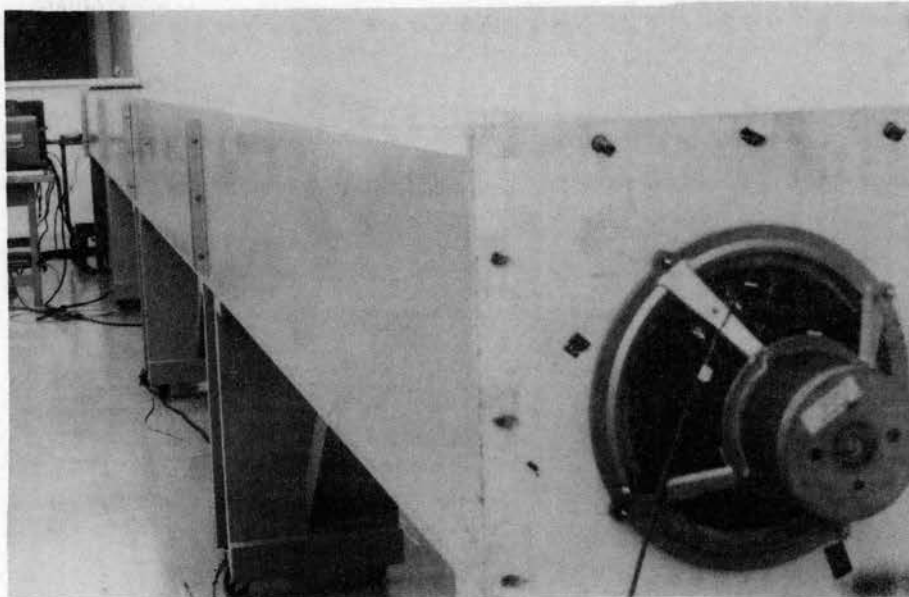


Figure 27. Plane Wave Tube

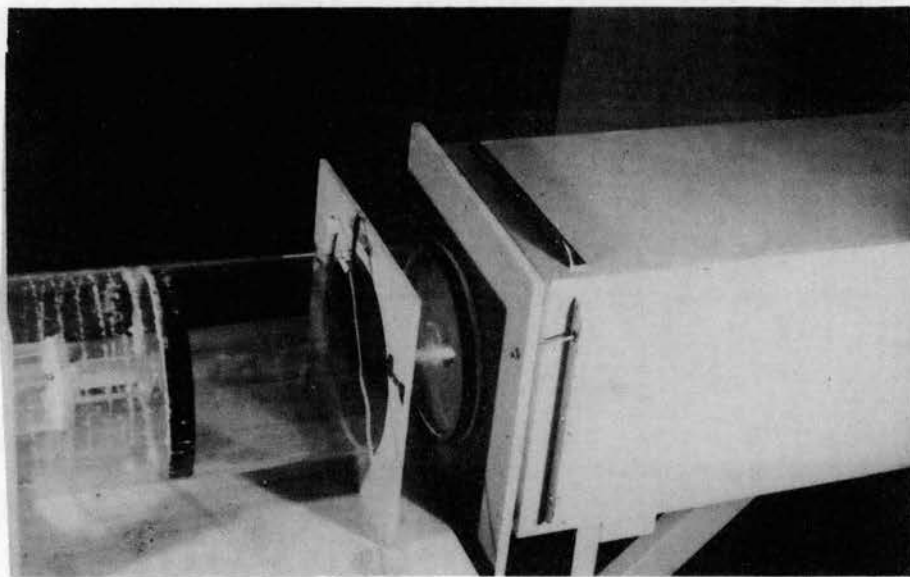


Figure 28. Resonator Arranged with  
Plane Wave Tube



14 inch loud speaker, as shown in Figure 27.

A low frequency function generator which was capable of producing sine, triangular, or square wave signals from 0.02 cps to 1000 cps was used. The voltage signal from the function generator was fed to the Tone Burst generator which was a coherent gate and served to convert the signal from steady state to a transient of required duration. The signal from the gate, after being amplified, was fed to the loud speaker, as shown in the upper part of Figure 29. The pressure pulses produced by the loud speaker driven by gated signals were sent through the plane wave tube to the test end.

#### Testing and Instrumentation

The loud speaker produced good transients in the frequency range from 15 to 300 cycles per second. The microphone (Altec, 21 BR 150) response was flat for frequencies above 10 cycles per second. Test resonators with natural frequencies from 20 to 50 cycles per second, which were described earlier in this chapter, are compatible with these requirements. The plane wave tube was long enough so that the reflected wave took a long time to travel and to affect the response of the system.

The block diagram of the instrumentation used to measure and record the pressures is shown in Figure 29. The arrangement of the resonator with the plane wave tube is shown in Figure 28. The three factory-calibrated microphones were arranged at the end of the plane wave tube, as shown in Figure 31, to compare the sensitivities.

The excitation pressure and the response pressures in the two cavities were measured through microphones (Altec, 21 BR 150) and recorded through a C.E.C. oscillograph and also viewed on an oscillo-

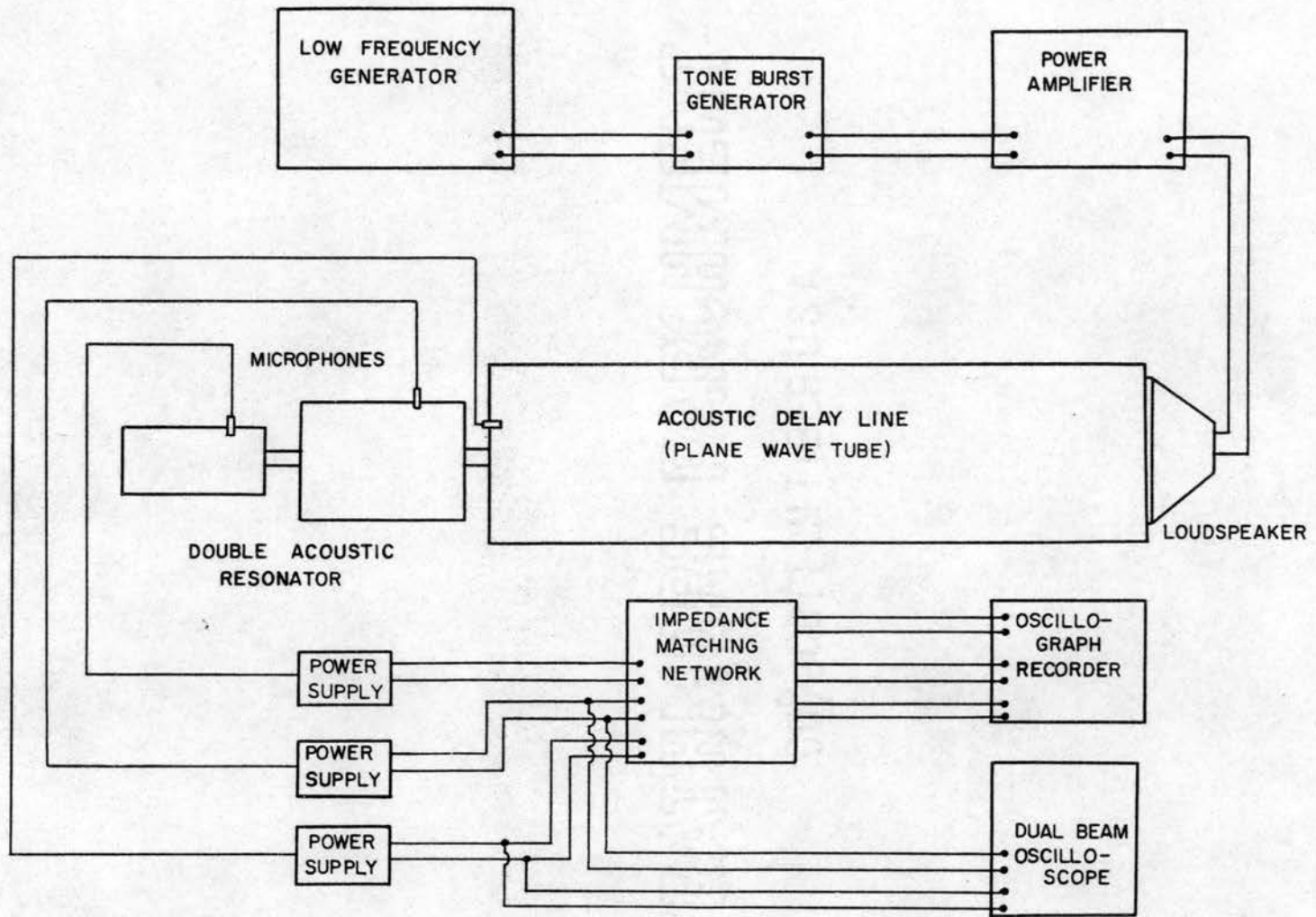


Figure 29. Block Diagram of the Instrumentation



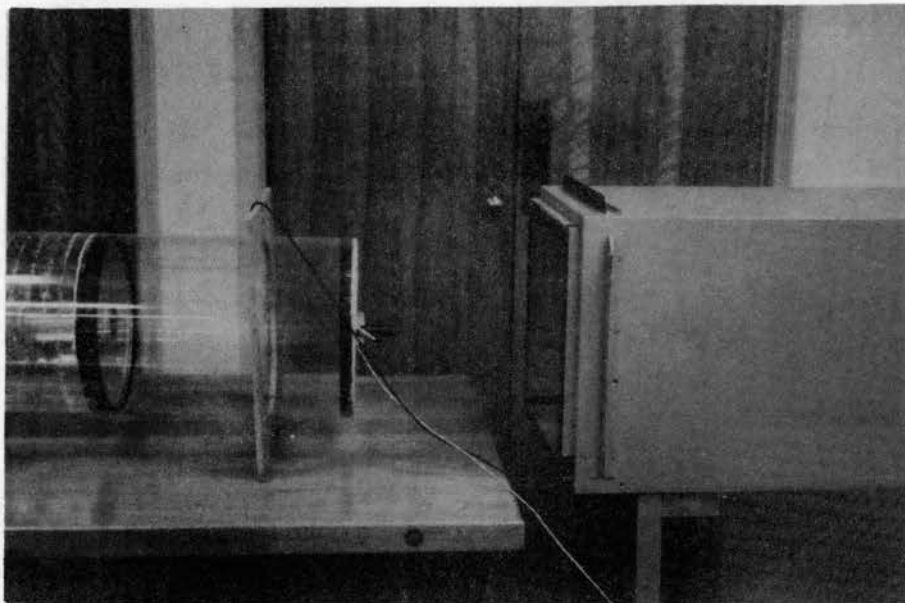


Figure 30. Arrangement of the Resonator  
to Test the Effect of Loading  
Due to the Impedance of the  
Plane Wave Tube

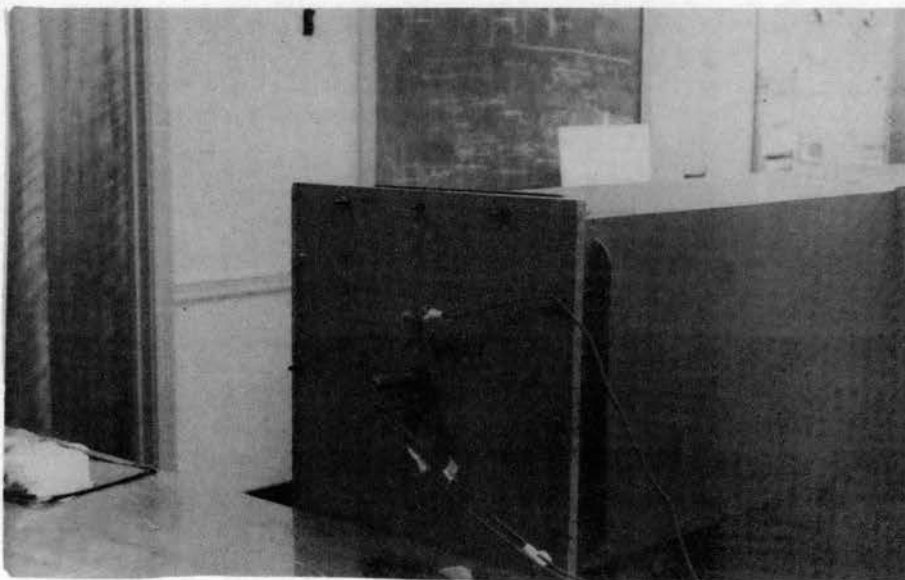


Figure 31. Arrangement of Microphones with  
Plane Wave Tube for Comparative  
Calibration

scope screen. Since the output impedance of the microphone power supply was much larger than the input impedance of the oscillograph, it was necessary to build an impedance match network. The sensitivity of the galvanometers were adjusted through the matching network so that all the channels had the same deflection for the same voltage signals in the frequency range of 20 to 60 cycles per second.

The effect of impedance of the plane wave tube on the response of the resonator was checked experimentally by measuring the response pressures when the model was about one foot away from the test end of the tube, as shown in Figure 30. These measurements were not much different from the pressures measured in the cavities with the test end closed as in Figure 28 and excited with the same type of pressure. Since the cross-sectional area of the plane wave tube was large compared to that of the neck, there was a little effect of the tube on the response of the resonator. However, the impedance of the tube did affect the excitation pressures produced by the loud speaker. Very distinct sine pulses could be produced when the end of the tube was closed except for the neck of the resonator.

## CHAPTER VI

### EXPERIMENTAL PROCEDURE AND RESULTS

The test model and the instrumentation described in Chapter V were used to test the theoretical response of the system of the double acoustical resonator in time domain. The laboratory testing also yielded a better understanding of the physical parameters and damping mechanism of the system and the general validity of the theoretical assumptions made in the analysis.

#### Natural Frequency and Damping Measurements

The natural frequencies of the two uncoupled resonators were measured by two methods: 1) by exciting the resonator with a short duration transient pulse and observing or recording the free relaxation pressure oscillations in the cavities; and, 2) by sweeping the steady state excitation pressure and observing the maximum pressure magnification. Both of these methods give the same values of natural frequencies. The damped natural frequency,  $p_d$ , is a function of undamped natural frequency,  $p$ , and the damping factor  $\xi$  and is given as,

$$p_d = \sqrt{1 - \xi^2} p \quad (26)$$

Since the damping factor is of the order of 0.05,  $p_d$  and  $p$  are approximately equal.

The undamped natural frequencies were estimated from equation (23).

The end correction for the neck was taken as  $0.785 R$  for each end of the neck assuming an infinite baffle termination. This end correction seems to be a little high, and resulted in calculated frequencies a little low when compared with the experimentally evaluated values. For each set-up two values were taken, one while sweeping the frequency from low values to high and another while decreasing. Generally, the difference was only two to three percent. Table II gives the comparison of measured natural frequencies, when the joints of the resonator were sealed to the theoretically determined values for different volumes of the cavities.

When the joints of the resonator were not sealed well, the measured frequencies were higher than that of the theoretically estimated values. The air motion through the small holes has the effect of increasing the area of the neck. Since the natural frequency is proportional to the square root of the area of the neck, the presence of air leaks would result in higher measured frequencies.

The damping characteristics are readily evaluated from the free vibration tests. These test procedures consisted of exciting the resonator with a transient pressure pulse of short duration and observing the free pressure oscillations in the residual era. Many types of pulses were tried to excite the resonator with no control maintained over the pulse shape or period. The free pressure oscillation records always displayed the smooth decay curves of a typical simple oscillator. Figures 32 and 33 are typical traces of pressure signals obtained by exciting with a sudden impulse by waving a hand across the neck of the resonator. The damping factors measured from the logarithmic decrement of free oscillations were in the range of 0.05 to 0.065. For a smaller

TABLE II

## THEORETICAL AND EXPERIMENTAL NATURAL FREQUENCIES OF RESONATORS

Cavity diameter — 11.75 inches  
 Neck diameter — 1 inch  
 Neck length —  $1\frac{1}{2}$  inch

Length of the cavity inches	Calculated frequency cps	Experimentally determined frequency cps
21.5	27.6	27.8
20.5	28.3	28.5
19.5	29.0	30.0
18.5	29.8	30.2
17.5	30.6	30.5
16.5	31.6	32.0
15.5	32.6	33.2
14.5	33.7	34.3
13.5	34.8	35.5

Cavity diameter — 4.25 inches  
 Neck diameter — 0.5 inch  
 Neck length — 6 inches

13.25	27.4	28.6
12.25	28.6	29.8
11.25	29.8	31.2
10.25	31.2	32.2
9.25	32.8	33.9
8.25	34.8	35.7
7.5	36.4	37.0



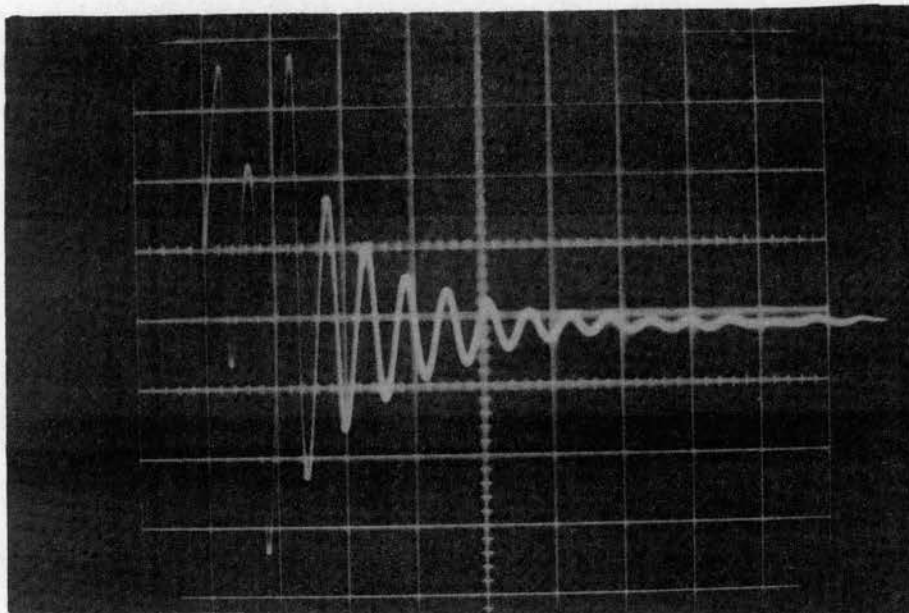


Figure 32. Free Pressure Oscillations in the Resonator of 11.75 inches Diameter, (Neck: 1 inch Diameter and 1.25 inches Length)

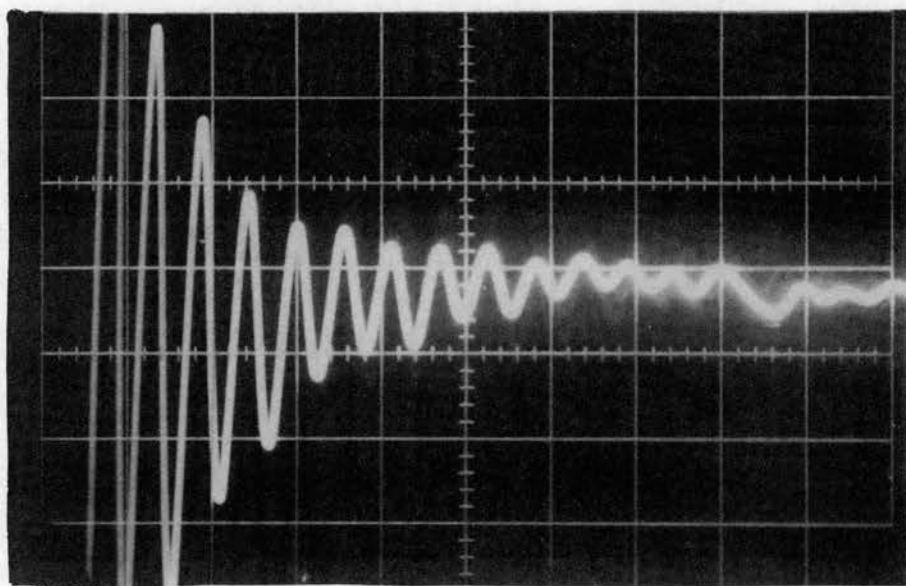


Figure 33. Free Pressure Oscillations in the Resonator of 4.25 inches Diameter, (Neck: 0.5 inches Diameter and 6 inches Length)

resonator with a longer neck, the damping was found to be slightly higher. Damping could also be estimated from steady state tests by measuring the amplitudes near resonance. The results were in close agreement with those obtained from the transient or free vibration tests.

These tests were conducted also to establish the mechanism of damping and the response due to higher modes. The energy dissipation could be due to the following reasons: 1) wall vibrations, 2) leakage through the felt which is used for sealing purposes, and 3) friction and reradiation through the necks. Since the 11.75 inch resonator had a wall of thickness 1/16 inch, it was suspected that wall vibrations might be the main cause of energy dissipation. These free vibration tests were conducted before and after stiffening the resonator both with circumferential and longitudinal reinforcements. The damping measurements from these tests indicated that the energy dissipation was not due to wall vibrations. To establish the damping due to leak through the felt, all the leaks were sealed well with a calking compound and tested for damping factor. It was found that the energy was not dissipated through the felt because there were no leaks even without the calking compound applied. From these tests it was inferred that the damping is only due to friction and reradiation through the necks. One could also conclude from these tests that the higher mode frequencies of the resonator were not present since the amplitude of these higher modes did not appear in the transient response oscillations, as is apparent from Figures 32 and 33.

#### Pressure Responses in Time Domain

The best method to establish the validity of the assumptions made

in the theoretical study is to test the model for the simulated excitation pressures and compare the theoretical results with the measured values. This was done by measuring the response of the double acoustical resonator system in the time domain for the transient pressure of one sine pulse. This study was performed for several configurations of the system, all of which showed excellent agreement between the recorded traces and analytically predicted response results. These results further demonstrated the relatively minor importance of higher mode responses. The analysis was made in obtaining theoretical response curves by using an excitation pressure of one cycle of an ideal sine wave and straight line approximation. The calculated values of uncoupled natural frequencies and coupling frequency and measured values of damping factors were used to define the resonator system. The equations of motion were derived as discussed in Chapter III and solved for the response using Laplace transformation techniques and a digital computer. The pressure response in the cavities as a function of complex frequencies is given by,

$$P_1(s) = G_{A1}(s) \cdot P_A(s) + G_{B1}(s) \cdot P_B(s)$$

$$P_2(s) = G_{A2}(s) \cdot P_A(s) + G_{B2}(s) \cdot P_B(s) \quad (27)$$

where  $G_{A1}$ ,  $G_{A2}$ ,  $G_{B1}$  and  $G_{B2}$  are the transfer functions of the system and are defined as functions of uncoupled natural frequencies and damping factors;  $P_A(s)$  and  $P_B(s)$  are the external pressures applied on necks  $N_1$  and  $N_2$ , respectively. In the present analysis there is no external pressure on neck  $N_2$ , thus, in equation (27)  $P_B(s)$  is equal to zero. The correction factors for the neck length were taken as 1.57 R,



where  $R$  is the radius of the neck.

Figure 34 shows the comparison between the experimentally measured and theoretically computed pressures in cavity  $V_1$ . Also, the excitation pressure at the test end of the plane wave tube (very close to resonator neck  $N_1$ ) and an ideal sine pulse are plotted in the same figure. A damping factor,  $\xi_1 = \xi_2 = 0.06$ , was used in the computation. There is a very close agreement between the measured and the theoretical pressures in the forced era. There is a discrepancy in the residual era, since the measured or actual external pressure was not exactly the same as that of the ideal pressure assumed in computations. Figure 35 shows the measured response and excitation pressures, computed response, and an ideal excitation pressure of sine pulse.

Figure 36 is the pressure recording inside the cavities and the excitation pressure. The trace of excitation pressure was obtained with the microphone placed close to the neck,  $N_1$ , of the resonator at the test end of the plane wave tube. The response traces were obtained with the microphones fixed through the side walls of the resonator. The amplitude of pressure in  $V_2$  is larger than that of  $V_1$ .

These pressures were compared with the theoretically calculated pressure responses in the cavities. Figure 37 gives the comparison between the measured pressures in the cavities and the computed values by assuming the excitation pressure as a sine pulse. The agreement between theory and experiment is excellent in the forced era. In the residual era they deviate. This is because of the difference between the actual and ideal pressure pulses as shown in Figure 37. Figure 38 is the computed response to an idealized wave of straight lines. These results are compared with the measured values. The trend of the

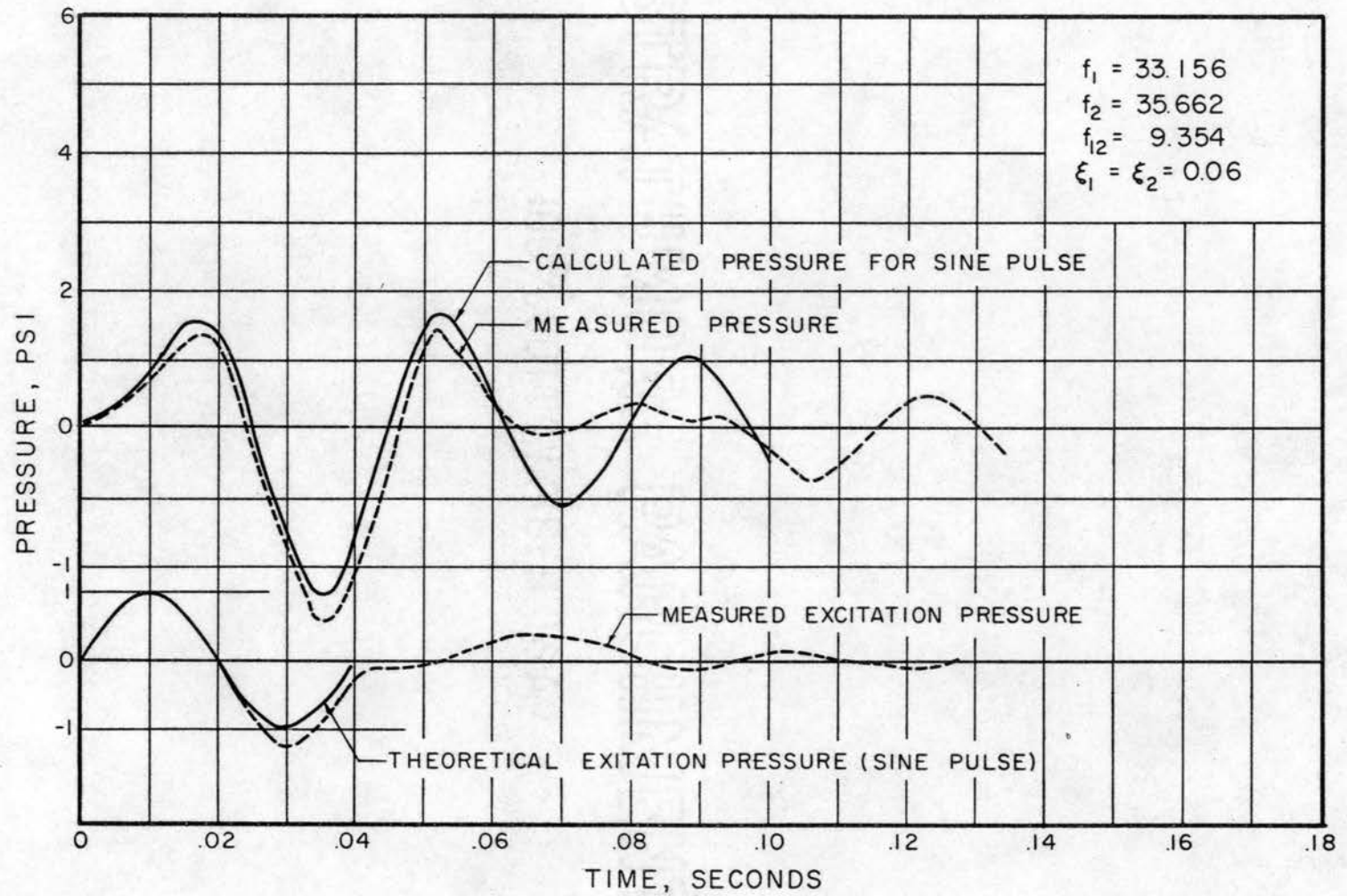


Figure 34. Pressure Response in Cavity  $V_1$

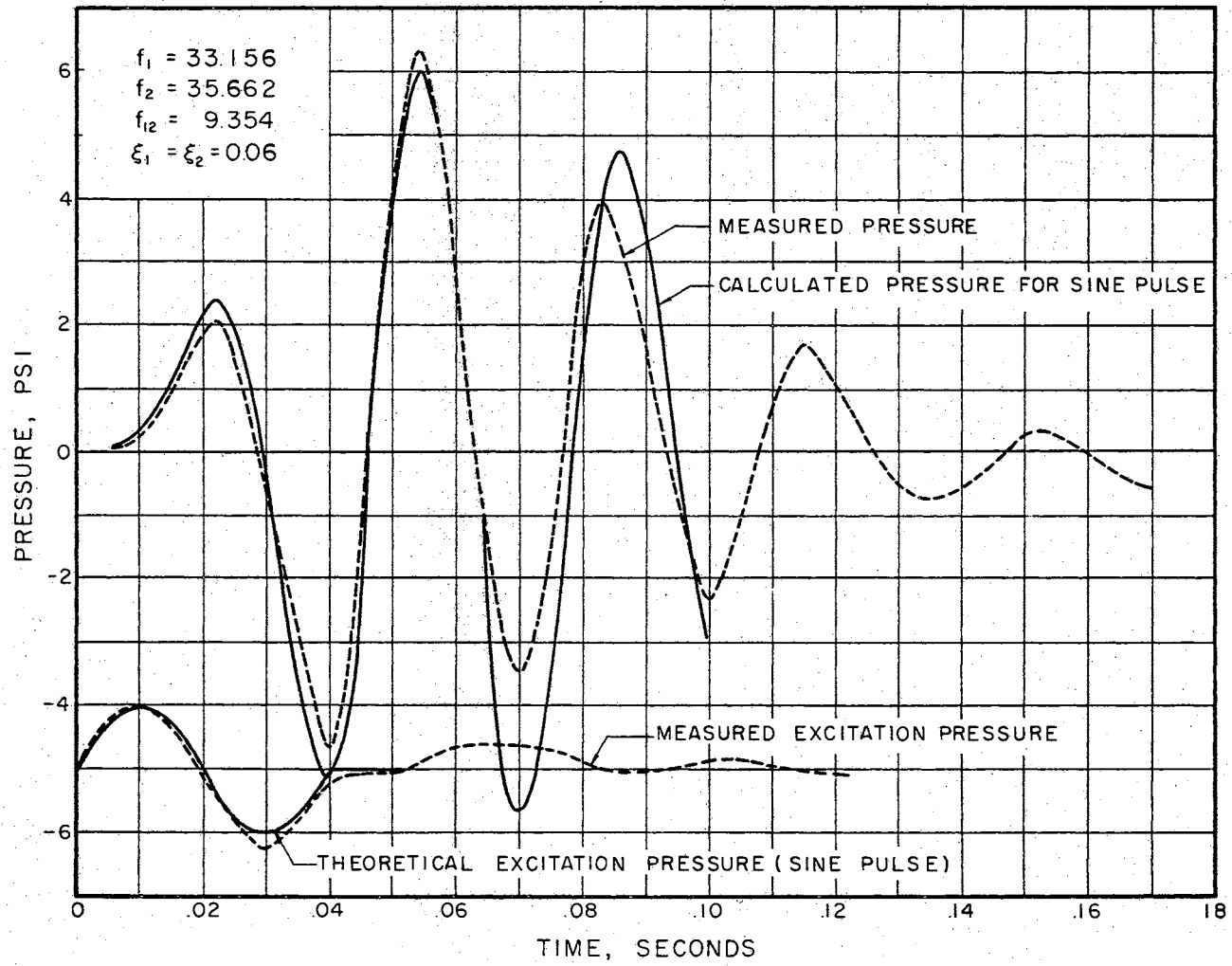


Figure 35. Pressure Response in Cavity  $V_2$

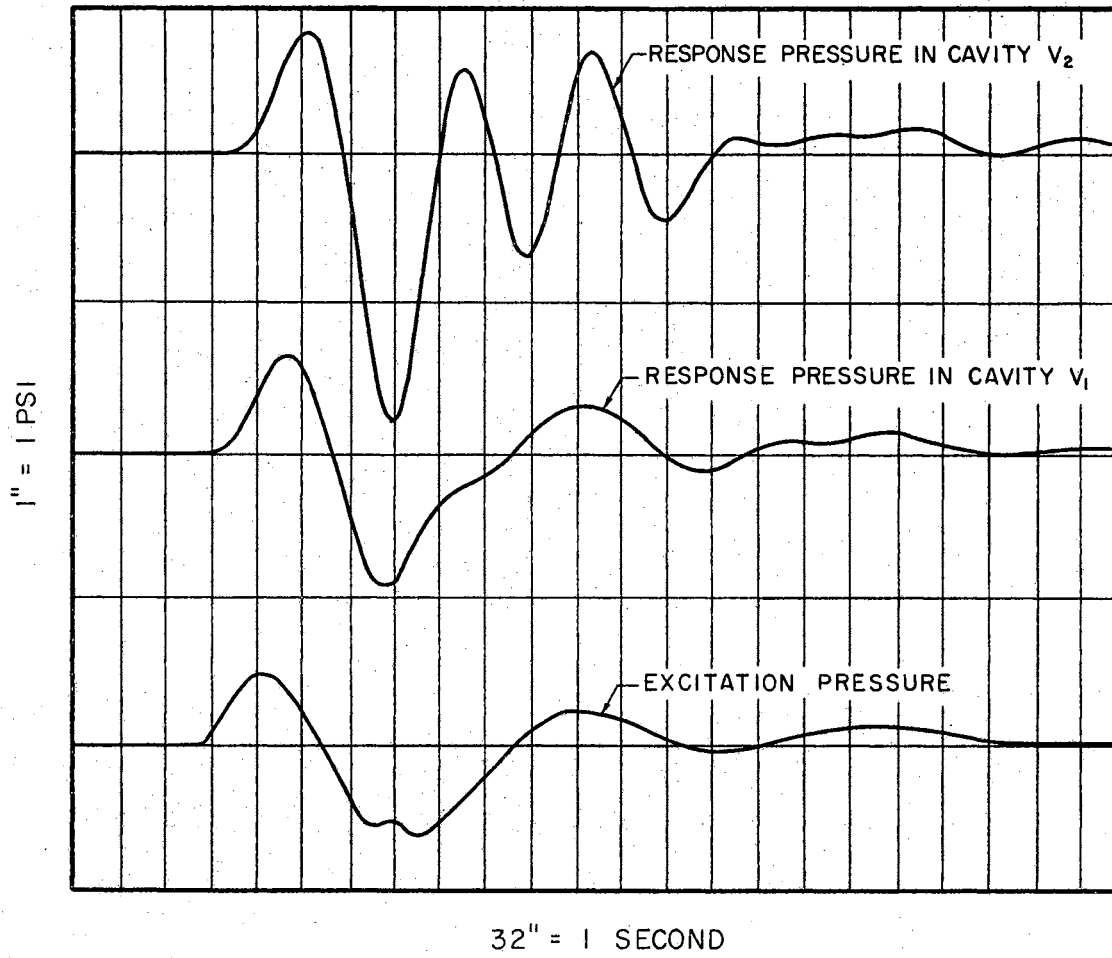


Figure 36. Time Response Measurements

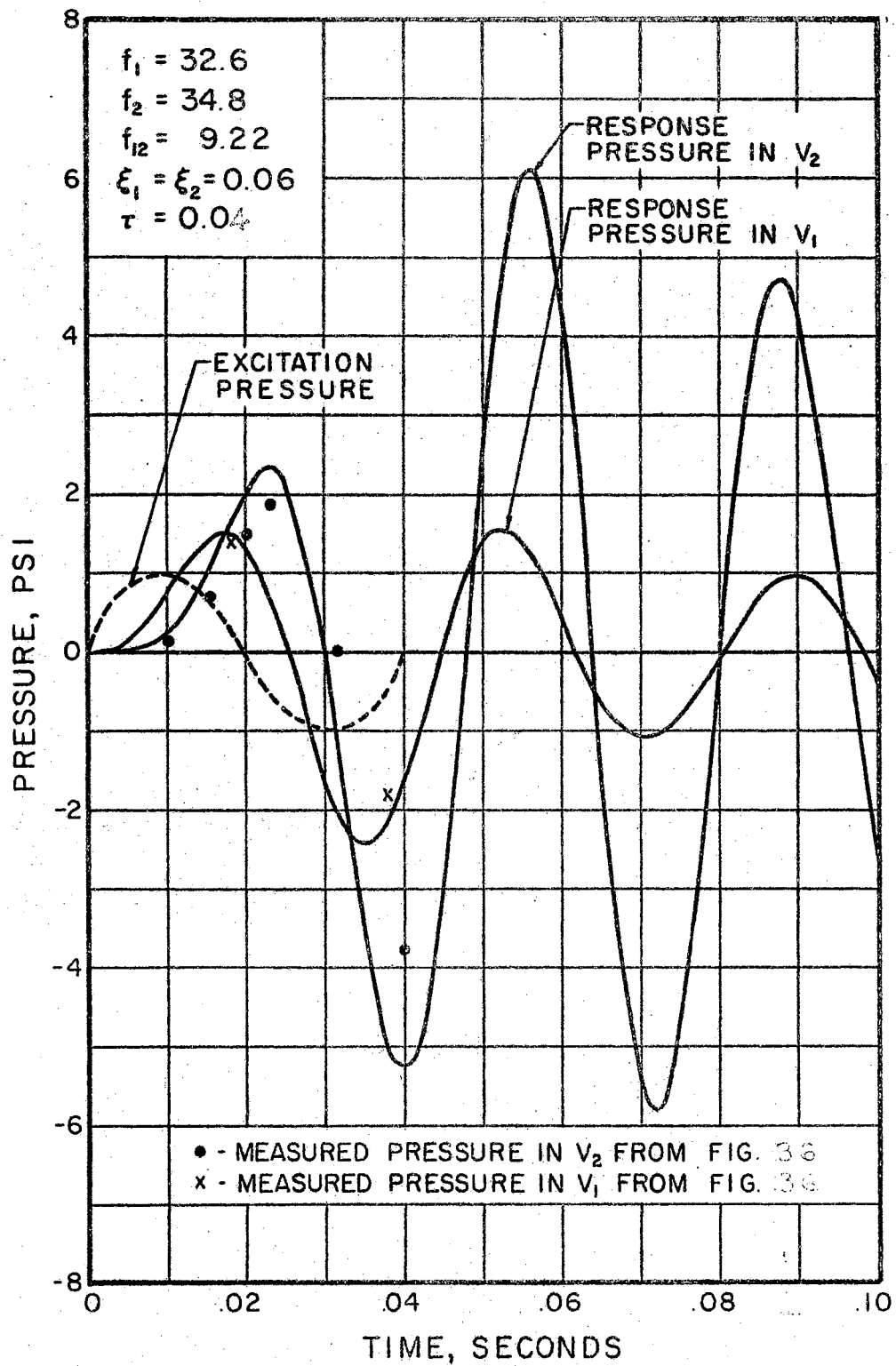


Figure 37. Response Pressures From Idealized Sine Pulse

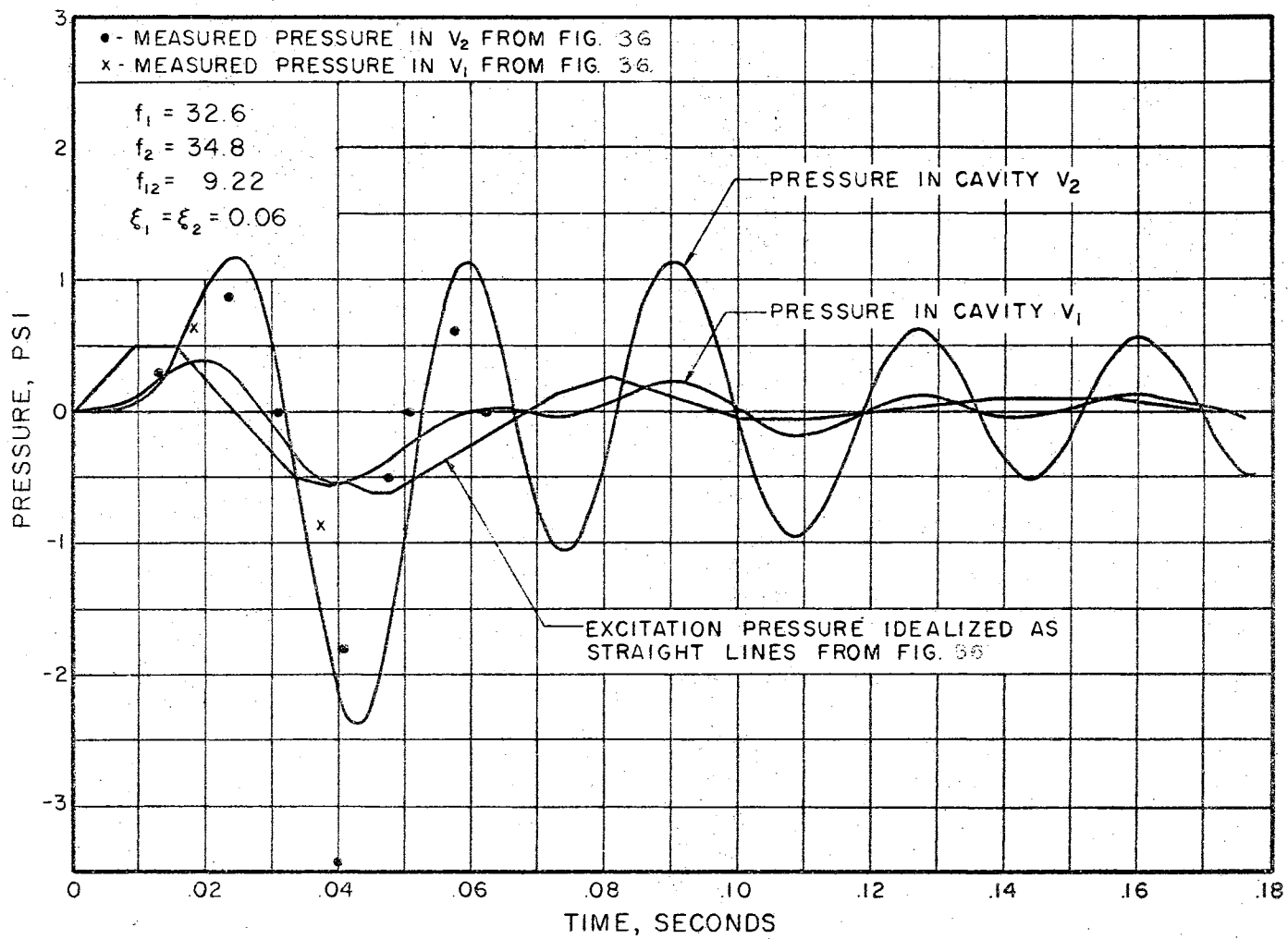


Figure 38. Response Pressures by Straight Line Approximation

responses of both calculated and measured pressures are the same, but the absolute values are not in agreement. This may be due to the shape of the measured excitation pressure being quite different from the idealized excitation pressure.

The study of this particular time response indicates that the assumptions made in the mathematical model are valid. The higher modes are not important in the response analysis. Thus, the results obtained in the theoretical analysis may be accepted.

## CHAPTER VII

### CONCLUSIONS AND RECOMMENDATIONS

The conclusions drawn as a consequence of this investigation may be divided into two groups depending on the phase of the investigation.

I. The following deductions have been attained from the experimental investigation:

1. The lumped parameter representation of coupled acoustical resonators is adequate for the response analysis.
2. The presence of air leaks will have a large effect on the natural frequencies and on the response of the system.
3. In actual physical systems such as buildings, it is rather difficult to estimate the amount of leakage and damping; and thus, it is necessary to use the measured estimates of natural frequencies and damping factors in the response analysis.
4. The assumptions made in the derivation of the mathematical model are valid.
5. The damping of a resonator with rigid walls is due probably to the friction and re-radiation at the necks.
6. In a physical system the higher mode response is not important, since the small amount of damping present in the system reduces the amplitude of higher modes in a short time.



II. From the theoretical analysis and response spectra, the following conclusions have been attained:

1. The pressure magnification of a double acoustical resonator can be as large as 50 when the undamped system is tuned properly and the coupling frequency is very small. However, since in a physical system the damping is inevitable and the coupling frequency is limited by the elements of the system, the pressures can only be magnified to the order of about 15.
2. The pressure oscillations associated with acoustic response in the structure may possibly act as a secondary source driving other properly tuned elements of the system to large amplitudes.
3. Mathematical modeling by use of lumped parameters is an excellent method, which is amenable for the transient response analysis.
4. If the walls are rigid such that there is no contribution of response due to wall vibrations, the response can be predicted analytically within four percent, by using measured values for damping.
5. From this analysis, it is possible to predict the response of double acoustical resonators to any type of finite duration transient excitation pressures which can either be approximated by straight lines or sine pulses.
6. The damage to the acoustic structures exposed to transient pressures can be reduced by incorporating damping. A damping factor of about 0.1 reduces the maximum pressures by about three times.

7. The two uncoupled frequencies of the system are parameters which affect the response of the cavity of the resonator which is excited by external pressure.
8. The uncoupled natural frequency related to the resonator excited with external pressure is the parameter which mainly affects the response of this cavity.
9. Pressure magnifications can be reduced to about unity by designing the structures in such a way that the natural frequencies are apart from each other and also apart from the frequency of excitation pressure.

#### Suggestions for Future Study

It is recommended that further study be conducted in the area of dynamic response of mechano-acoustic structures in transient conditions. It appears that the transient response of the acoustical systems by lumped parameter representation is more fruitful; however, in certain cases where lumped parameters may not fulfill the requirements, it would be advantageous to explore the continuous systems.

Specifically the following recommendations are made for further study in this area:

1. The conclusions stated concerning the mechanism of damping in the resonator are primarily based on experimental tests. It would be useful if additional effort would be put on mathematical analysis. It appears that the damping due to various mechanisms can be separated and analyzed as a function of system parameters.

2. The influence of non-rigid wall vibrations on the response of the system should be investigated. These wall vibrations might cause dissipation of energy in the system.
3. It is necessary to determine the influence of higher mode response for larger resonators where the critical dimension is not less than 16 times the wave length corresponding to the natural frequency. From the experimental study of this investigation, it seems that this restriction is not strictly necessary.
4. There are many acoustical structures which may not be idealized to the system of the double acoustical resonator. Hence, it is worthwhile to analyze the multiple coupled resonators with three or more degrees of freedom.
5. The study of the response of continuous mechanical systems such as windows and ceilings coupled to an acoustical resonator needs to be investigated.
6. The correction factors for neck lengths of Helmholtz resonator, as a function of dimensions of the necks and of the flanges at the ends of the neck needs to be examined.

## BIBLIOGRAPHY

- (1) McGinnis, C. S., V. F. Albert. "Multiple Helmholtz Resonators." The Journal of the Acoustical Society of America, July, 1952, Vol. 24.
- (2) Rayleigh, J. W. S. The Theory of Vibrations, Volume II. Dover Publications, New York, 1945.
- (3) Olson, H. F. Dynamical Analogies. D. Van Nostrand Company, Princeton, New Jersey, 1958.
- (4) Simpson, J. D. "The Transient Response of a Helmholtz Resonator with Application to Sonic Boom Response Studies." Ph.D. Thesis, Oklahoma State University, May, 1966.
- (5) Morse, P. M. Vibration and Sound. McGraw-Hill Book Company, 1948.
- (6) Beranek, L. L. Acoustics. McGraw-Hill Book Company, 1954.
- (7) Kinsler, L. E., A. R. Frey. Fundamentals of Acoustics. John Wiley & Sons, Inc., New York, 1962.
- (8) Ingard, Uno. "The Near Field of a Helmholtz Resonator Exposed to a Plane Wave." The Journal of the Acoustical Society of America, Vol. 25, Number 6, November, 1953, pp 1062-1067.
- (9) Paris, E. T. "The Magnification of Acoustic Vibrations by Single and Double Resonance." Science Progress, XX, Number 77, 1925.
- (10) Von Max Wein. "Over the Reaction of a Resonant System." Physik, 1894.
- (11) Christian, Von E. "Zur Theorie Allgemeiner Schwach Gekoppler Akustischer Resonatoren." Acustica, Vol. 5, 1955.
- (12) Ingard, Uno. "On the Theory and Design of Acoustic Resonators." The Journal of the Acoustical Society of America, Vol. 5, 1953.
- (13) Hartig, H. E., R. F. Lambert. "Attenuation in a Rectangular Slotted Tube of (1,0) Transverse Acoustic Waves." The Journal of the Acoustical Society of America, Vol. 23, January, 1950.

- (14) Ingard, Uno. "On the Radiation of Sound into a Circular Tube with an Application to Resonators." The Journal of the Acoustical Society of America, Vol. 20, September, 1948.
- (15) Lambert, R. F. "A Study of the Factors Influencing the Damping of an Acoustic Cavity Resonator." The Journal of the Acoustical Society of America, Vol. 25, November, 1953.
- (16) Lamb, H. The Dynamical Theory of Sound. Dover Publications Inc., New York.
- (17) Crandall, I. B. Theory of Vibrating Systems and Sound. D. Van Nostrand Company, Inc., New York, 1927.
- (18) Andrews Associates, Inc., and Hudgins, Thompson and Bell Associates, Inc. Final Report on Studies of Structural Response to Sonic Booms, for the Federal Aviation Agency, Vol. 1, February, 1965.
- (19) Cheng, D. H. "Some Dynamic Effects of Sonic Booms on Building Structural Elements." Langley Working Paper, No. 25, NASA.
- (20) Air Research and Development Command, Wright Patterson Air Force Base, Ohio. Response of Structures to Aircraft Generated Shock Waves.
- (21) Ingles, A. R. "Pressure Reduction and Temperature Variation on the Performance of a Double Form of Helmholtz Resonator." The Journal of the Acoustical Society of America, Vol. 35, May, 1953.
- (22) Rsevkin, S. N. A Course of Lectures on Theory of Sound. Translated from Russian by O. M. Blunn, The Macmillan Company, New York.
- (23) Bauer, B. B. "Transfer Couplings for Equivalent Network Synthesis." The Journal of the Acoustical Society of America, Vol. 25, No. 5.
- (24) Scanlan, R. H., and R. Rosenbaum. Introduction to the Study of Aircraft Vibration and Flutter. The Macmillan Company, New York.
- (25) Timoshenko. Vibration Problems in Engineering. D. Van Nostrand Company, Inc.
- (26) Den Hartog, J. P. Mechanical Vibrations. McGraw Hill Book Company, Inc., 1956.
- (27) Oldenburger, Rufus. "Algebraic Approach to Design of Automatic Controls." Transactions of the A.S.M.E., February, 1958, pp 433-443.

- (28) Ormondroyd, J., and J. P. Den Hartog. "The Theory of the Dynamic Vibration Absorber." Transactions of the A.S.M.E., Applied Mechanics, APM SO-7, pp 9-22.
- (29) Thompson, W. T. Laplace Transformation, Second Edition. Prentice Hall, Inc., Englewood Cliffs, New Jersey.
- (30) Jacobsen, L. S. and R. S. Ayre. Engineering Vibrations. McGraw Hill Book Company, Inc., New York, 1958, pp 160-183 and 317-350.
- (31) Baker, A. F. "Contact Chatter Characteristics of a Linear Viscous Damped Contact Systems." Ph.D. Thesis, Oklahoma State University, May, 1966.
- (32) Kryter, K. D. "Laboratory Tests of Physiological-Psychological Reactions to Sonic Booms." Journal of the Acoustical Society of America, Vol. 39, No. 5, May, 1966, Part 2 Sonic Boom Symposium, pp 565-572.

APPENDIX A

RESPONSE SOLUTION OF THE DOUBLE ACOUSTICAL RESONATOR

The equations of motion for the system of double acoustical resonator shown in Figure 2 are derived in complex frequency domain in Chapter III as,

$$\left[ \frac{\rho_o l_{e1}}{A_1} s^2 + c_1 s + \frac{\rho_o c^2}{V_1} \right] X_1(s) - \left[ c_1 s + \frac{\rho_o c^2}{V_1} \right] X_2(s) = P_1(s) ,$$

$$\left[ \frac{\rho_o l_{e2}}{A_2} s^2 + (c_1 + c_2) s + \frac{\rho_o c^2}{V_1} + \frac{\rho_o c^2}{V_2} \right] X_2(s) - \left[ c_1 s + \frac{\rho_o c^2}{V_1} \right] .$$

$$X_1(s) = P_2(s). \quad (1)$$

The characteristic determinant of this equation is

$$\Delta = \begin{vmatrix} \frac{\rho_o l_{e1}}{A_1} s^2 + c_1 s + \frac{\rho_o c^2}{V_1} & - \left[ c_1 s + \frac{\rho_o c^2}{V_1} \right] \\ - \left[ c_1 s + \frac{\rho_o c^2}{V_1} \right] & \frac{\rho_o l_{e2}}{A_2} s^2 + (c_1 + c_2) s + \frac{\rho_o c^2}{V_1} + \frac{\rho_o c^2}{V_2} \end{vmatrix} \quad (2)$$

This equation can be simplified to

$$\Delta = \frac{\rho_o^2 l_{e1} l_{e2}}{A_1 A_2} s^4 + 2(p_2^2 s_2 + p_1^2 s_1 + p_2^2 s_{12}) s^3 + (p_1^2 + p_2^2)$$

$$+ p_{12}^2 + 4p_1 p_2 \xi_1 \xi_2) s^2 + 2p_1 p_2 (\xi_1 p_2 + \xi_2 p_1) s + p_1^2 p_2^2 ; (3)$$

where the damping factors  $\xi_1$ ,  $\xi_2$  and  $\xi_{12}$  are defined as,

$$\xi_1 = \frac{c_1}{2M_1 p_1} ,$$

$$\xi_2 = \frac{c_2}{2M_2 p_2} , \text{ and}$$

$$\xi_{12} = \frac{c_1}{2M_2 p_2} = \xi_1 \frac{p_{12}^2}{p_1 p_2} .$$

Solution of equation (1) for volume displacements,  $X_1(s)$  and  $X_2(s)$ , are,

$$X_1(s) = \frac{P_1(s) \frac{\rho_0 l e_2}{A_2} \left[ s^2 + 2p_2 (\xi_2 + \xi_{12}) s + p_2^2 + p_{12}^2 \right]}{\Delta}$$

$$+ \frac{P_2(s) \frac{\rho_0 l e_1}{A_1} \left[ 2\xi_1 p_1 s + p_1^2 \right]}{\Delta} , \text{ and}$$

$$X_2(s) = \frac{P_2(s) \frac{\rho_0 l e_1}{A_1} \left[ s^2 + 2\xi_1 p_1 s + p_1^2 \right]}{\Delta}$$

$$+ \frac{P_1(s) \frac{\rho_0 l e_1}{A_1} p_1^2 \left[ \frac{2\xi_1}{p_1} s + 1 \right]}{\Delta} . \quad (4)$$

For the excitation pressures of one cycle of sine wave (Figure 6) on neck,  $N_1$ , and no excitation on neck,  $N_2$ , the equation(4) can be reduced to,



$$X_1(s) = \frac{A_0 \omega [s^2 + g_1 s + g_0] [1 - e^{-T}s]}{\frac{\rho_0^l e_1}{A_1} (s^2 + \omega^2) [s^4 + B_3 s^3 + B_2 s^2 + B_1 s + B_0]}, \quad \text{and} \quad (5)$$

$$X_2(s) = \frac{A_0 \omega p_1^2 [h_1 s + 1] [1 - e^{-T}s]}{\frac{\rho_0^l e_2}{A_2} (s^2 + \omega^2) [s^4 + B_3 s^3 + B_2 s^2 + B_1 s + B_0]};$$

where

$$\begin{aligned} g_1 &= 2p_2 (\xi_2 + \xi_{12}), \\ g_0 &= p_2^2 + p_{12}^2, \\ B_3 &= 2 p_1 \xi_1 + p_2 \xi_2 + p_2 \xi_{12}, \\ B_2 &= p_1^2 + p_2^2 + p_{12}^2 + 4p_1 p_2 \xi_1 \xi_2, \\ B_1 &= 2p_1 p_2 [\xi_1 p_2 + \xi_2 p_1], \\ B_0 &= p_1^2 p_2^2, \quad \text{and} \\ h_1 &= \frac{2\xi_1}{p_1}. \end{aligned} \quad (5a)$$

Equation (5) may be transformed into time domain from the complex frequency domain by the technique of partial fractions. It is necessary to find the roots of the characteristic equation (3). The characteristic equation,

$$s^4 + B_3 s^3 + B_2 s^2 + B_1 s + B_0, \quad (7)$$

is a fourth degree, linear polynomial equation. For a stable system, the real parts of the roots of this equation should be negative.

With this assumption, the equation can have one of the following three combinations of the roots:

1. All four of the roots may be complex with negative real part,

2. All of the roots may be real negative numbers, and
3. Two roots may be complex and two may be real negative numbers.

If the system has to have at least some roots with pure real numbers, the response of the system is not oscillatory, but it is overdamped. Assuming that the system has an oscillatory motion for which the roots of the characteristic equation must be of the form  $a \pm jb$  where  $a$  and  $b$  are real numbers and  $j = \sqrt{-1}$ .

If the roots of the polynomial equation are  $a \pm jb$  and  $c \pm jd$ , the following identity can be written:

$$\begin{aligned} s^4 + B_3s^3 + B_2s^2 + B_1s + B_0 &= [s - (a + jb)][s - (a - jb)] \\ &\quad [s - (c + jd)][s - (c - jd)] \quad (8) \\ &= [(s - a)^2 + b^2][(s - c)^2 + d^2] . \end{aligned}$$

Equation (5) can be reduced to the following form by utilizing the identity (8),

$$X_1(s) = \frac{\frac{A_0 \omega}{\frac{\rho_0 l e_1}{A_1}} [s^2 + g_1s + g_0][1 - e^{-\tau s}]}{(s^2 + \omega^2)[(s - a)^2 + b^2][(s - c)^2 + d^2]} , \text{ and} \quad (9)$$

$$X_2(s) = \frac{\frac{A_0 \omega}{\frac{\rho_0 l e_2}{A_2}} p_1^2 (h_1s + 1)(1 - e^{-\tau s})}{(s^2 + \omega^2)[(s - a)^2 + b^2][(s - c)^2 + d^2]} .$$

The following expressions may be obtained by factoring the right hand side of equation (9) in terms of partial fractions, so that each term can be reduced to known form:

$$\frac{s^2 + g_1s + g_0}{(s^2 + \omega^2)[(s - a)^2 + b^2][(s - c)^2 + d^2]} = \frac{a_1s + b_1}{s^2 + \omega^2}$$

$$+ \frac{c_1 s + d_1}{(s - a)^2 + b^2} + \frac{e_1 s + f_1}{(s - c)^2 + d^2}, \text{ and}$$

$$\frac{h_1 s + 1}{(s^2 + \omega^2)[(s - a)^2 + b^2][(s - c)^2 + d^2]} = \frac{a_2 s + b_2}{s^2 + \omega^2}$$

$$+ \frac{c_2 s + d_2}{(s - a)^2 + b^2} + \frac{e_2 s + f_2}{(s - c)^2 + d^2} . \quad (10)$$

When the right side of equation (10) is reduced to a common denominator and the numerators of both sides of the equations are equated, the following will result:

$$\begin{aligned} s^2 + g_1 s + g_0 &= (a_1 s + b_1)[(s - a)^2 + b^2][(s - c)^2 + d^2] \\ &+ (c_1 s + d_1)[s^2 + \omega^2][(s - c)^2 + d^2] \\ &+ (e_1 s + f_1)[s^2 + \omega^2][(s - a)^2 + b^2], \text{ and} \quad (11) \end{aligned}$$

$$\begin{aligned} h_1 s + h_0 &= (a_2 s + b_2)[(s - a)^2 + b^2][(s - c)^2 + d^2] \\ &+ (e_2 s + d_2)(s^2 + \omega^2)[(s - c)^2 + d^2] \\ &+ (e_2 s + f_2)(s^2 + \omega^2)[(s - a)^2 + b^2] . \end{aligned}$$

The equations (11) can be simplified and the like powers of  $s$  on both sides are equated to obtain the two sets of simultaneous equations (12) and (13) written in matrix form.

Equations (5) can be rewritten in the following form, by utilizing equations (9) and (11) and the solution of equations

$$\begin{bmatrix}
 1 & 0 & 1 & 0 & 1 & 0 \\
 2(a+c) & -1 & 2c & -1 & 2a & -1 \\
 (a+c)^2 + b^2 & -2(a+c) & c^2 + d^2 + \omega^2 & -2c & a^2 + b^2 + \omega^2 & -2a \\
 + d^2 + 2ac & & & & & \\
 2[a(c^2 + d^2) & -[(a+c)^2 & 2\omega^2 c & -(c^2 + d^2 & 2\omega^2 a & -(a^2 + b^2 \\
 + c(a^2 + b^2)] & + b^2 + d^2 & + \omega^2) & + \omega^2) & + \omega^2) & \\
 + 2ac] & & & & & \\
 (a^2 + b^2) \cdot & -2[a(c^2 + d^2) & \omega^2(c^2 + d^2) & -2c\omega^2 & \omega^2(a^2 + b^2) & -2a\omega^2 \\
 (c^2 + d^2) & + c(a^2 + b^2)] & & & & \\
 0 & (a^2 + b^2) \cdot & 0 & \omega^2(c^2 + d^2) & 0 & \omega^2(a^2 + b^2) \\
 & (c^2 + d^2) & & & & 
 \end{bmatrix}
 \begin{bmatrix}
 a_1 \\
 b_1 \\
 c_1 \\
 d_1 \\
 e_1 \\
 f_1
 \end{bmatrix}
 =
 \begin{bmatrix}
 0 \\
 0 \\
 0 \\
 -1 \\
 g_1 \\
 g_0
 \end{bmatrix}
 \tag{12}$$

$$\begin{bmatrix}
 1 & 0 & 1 & 0 & 1 & 0 \\
 2(a+c) & -1 & 2c & -1 & 2a & -1 \\
 (a+c)^2 + b^2 + d^2 + 2ac & -2(a+c) & c^2 + d^2 + \omega^2 & -2c & a^2 + b^2 + \omega^2 & -2a \\
 2[a(c^2 + d^2) + c(a^2 + b^2)] & -[(a+c)^2 + b^2 + d^2 + 2ac] & 2\omega^2 c & -(c^2 + d^2 + \omega^2) & 2\omega^2 a & -(a^2 + b^2 + \omega^2) \\
 (a^2 + b^2) \cdot (c^2 + d^2) & -2[a(c^2 + d^2) + c(a^2 + b^2)] & \omega^2(c^2 + d^2) & -2c\omega^2 & \omega^2(a^2 + b^2) & -2a\omega^2 \\
 0 & (a^2 + b^2) \cdot (c^2 + d^2) & 0 & \omega^2(c^2 + d^2) & 0 & \omega^2(a^2 + b^2)
 \end{bmatrix}
 \begin{bmatrix}
 a_2 \\
 b_2 \\
 c_2 \\
 d_2 \\
 e_2 \\
 f_2
 \end{bmatrix}
 =
 \begin{bmatrix}
 0 \\
 0 \\
 0 \\
 0 \\
 h_1 \\
 1
 \end{bmatrix}
 \tag{13}$$

(12) and (13):

$$X_1(s) = \frac{\frac{A_0 \omega}{\rho_0 l e_1}}{A_1} \left[ \frac{a_1 s + b_1}{s^2 + \omega^2} + \frac{c_1 s + d_1}{(s - a)^2 + b^2} + \frac{e_1 s + f_1}{(s - c)^2 + d^2} \right] \cdot$$

(1 - e<sup>-τs</sup>) , and (14)

$$X_2(s) = \frac{\frac{A_0 \omega}{\rho_0 l e_2}}{A_2} \left[ \frac{a_2 s + b_2}{s^2 + \omega^2} + \frac{c_2 s + d_2}{(s - a)^2 + b^2} + \frac{e_2 s + f_2}{(s - c)^2 + d^2} \right] \cdot$$

(1 - e<sup>-τs</sup>) .

Inverse Laplace transformation of functions of the type,

$$\frac{c_1 s + d_1}{(s - a)^2 + b^2}$$

is discussed below.

A function  $\Phi(s)$  is defined as,

$$\Phi(s) = c_1 s + d_1,$$

then

$$\Phi(a + jb) = c_1(a + jb) + d_1.$$

This identity may be reduced to the following form:

$$\Phi_1 + j\Phi_2 = c_1 a + d_1 + jc_1 b.$$

The real and imaginary parts of both sides are equated to obtain the following equations:

$$\Phi_1 = c_1 a + d_1, \text{ and}$$

$$\Phi_2 = c_1 b.$$

Solution of these two equations yield the following expressions,

$$c_1 = \frac{\Phi_2}{b}, \text{ and}$$

$$d_1 = \Phi_1 - \frac{a}{b} \Phi_2.$$

Hence

$$\begin{aligned} \frac{c_1 s + d_1}{(s-a)^2 + b^2} &= \frac{\frac{\Phi_2}{b} s + (\Phi_1 - \frac{a}{b} \Phi_2)}{(s-a)^2 + b^2} = \frac{\Phi_2}{b} \frac{(s-a)}{(s-a)^2 + b^2} \\ &+ \frac{\Phi_1}{b} \frac{b}{(s-a)^2 + b^2}. \end{aligned}$$

The inverse transformation is as follows:

$$L^{-1} \left[ \frac{c_1 s + d_1}{(s-a)^2 + b^2} \right] = e^{at} \left[ \frac{1}{b} \sqrt{\Phi_1^2 + \Phi_2^2} \sin(bt + \theta) \right],$$

where

$$\tan \theta = \frac{\Phi_2}{\Phi_1}.$$

Equations (14) may be transformed to time domain and written as,

$$\begin{aligned} X_1(t) &= \frac{A_0 \omega}{\rho_0 l e_1 A_1} \left\{ [a_1 \cos \omega t + \frac{b_1}{\omega} \sin \omega t + \frac{e^{at}}{b} (\sqrt{\Phi_1^2 + \Phi_2^2} \right. \\ &\quad \left. \sin (bt - \theta_1)) + \frac{e^{ct}}{d} (\sqrt{\Psi_1^2 + \Psi_2^2} \sin (dt - \theta_2))] u(t) \right. \\ &\quad \left. - [a_1 \cos \omega(t - \tau) + \frac{b_1}{\omega} \sin \omega(t - \tau) + \frac{e^{a(t - \tau)}}{b} \right. \\ &\quad \left. (\sqrt{\Phi_1^2 + \Phi_2^2} \sin (b(t - \tau) - \theta_1)) + \frac{e^{c(t - \tau)}}{d} (\sqrt{\Psi_1^2 + \Psi_2^2} \right. \end{aligned}$$

$$\left. \begin{aligned} & \left. \sin (d(t-\tau) - \theta_2)) \right] u(t-\tau) \right\} , \text{ and} \quad (15) \\ X_2(t) = & \frac{A_0 \omega}{\rho_0 l e_2} \left\{ \left[ a_2 \cos \omega t + \frac{b_2}{\omega} \sin \omega t + \frac{e^{at}}{b} (\sqrt{\Phi_3^2 + \Phi_4^2} \cdot \right. \right. \\ & \left. \left. \sin (bt - \theta_3)) + \frac{e^{ct}}{d} (\sqrt{\Psi_3^2 + \Psi_4^2} \sin (dt - \theta_4)) \right] u(t) \right. \\ & \left. - \left[ a_2 \cos \omega (t-\tau) + \frac{b_2}{\omega} \sin \omega (t-\tau) + \frac{e^{a(t-\tau)}}{b} \cdot \right. \right. \\ & \left. \left. (\sqrt{\Phi_3^2 + \Phi_4^2} \sin (b(t-\tau) - \theta_3)) \right] + \frac{e^{ct}}{d} (\sqrt{\Psi_3^2 + \Psi_4^2} \cdot \right. \\ & \left. \left. \sin (d(t-\tau) - \theta_4)) \right] u(t-\tau) \right\} ; \end{aligned}$$

where

$$\begin{aligned} \theta_1 &= \tan^{-1} \frac{\Phi_2}{\Phi_1} , & \Phi_3 &= c_2 a + d_2 , \\ \theta_2 &= \tan^{-1} \frac{\Psi_2}{\Psi_1} , & \Phi_3 &= c_2 b , \\ \theta_3 &= \tan^{-1} \frac{\Phi_4}{\Phi_3} , & \Psi_1 &= e_1 c + f_1 , \\ \theta_4 &= \tan^{-1} \frac{\Psi_4}{\Psi_3} , & \Psi_2 &= e_1 d , \\ & & \Psi_3 &= e_2 c + f_2 , \text{ and} \\ & & \Psi_4 &= e_2 d . \end{aligned}$$

The volume displacements  $X_1(t)$  and  $X_2(t)$  at necks  $N_1$  and  $N_2$ , respectively, can be evaluated using numerical techniques.

If there is no energy dissipation (damping) in the system of double acoustical resonator, the characteristic determinant may be simplified to



$$\Delta = \frac{\rho_o^2 l e_1 l e_2}{A_1 A_2} [(s^2 + p_+^2)(s^2 + p_-^2)]; \quad (17)$$

where  $p_+$  and  $p_-$  are two undamped, coupled natural frequencies of the system and are given by

$$p_+^2 = \frac{(p_1^2 + p_2^2 + p_{12}^2) + \sqrt{(p_1^2 - p_2^2 - p_{12}^2)^2 + 4 p_1^2 p_{12}^2}}{2}, \quad (18)$$

and

$$p_-^2 = \frac{(p_1^2 + p_2^2 + p_{12}^2) - \sqrt{(p_1^2 - p_2^2 - p_{12}^2)^2 + 4 p_1^2 p_{12}^2}}{2}.$$

The volume displacement response for excitation pressure of one cycle of sine wave on neck  $N_1$  of the system can be expressed as a function of natural frequencies,  $p_+$  and  $p_-$ , as follows:

$$X_1(s) = \frac{A_o \omega}{\frac{\rho_o^2 l e_1}{A_1}} \frac{(s^2 + p_2^2 + p_{12}^2)(1 - e^{-\tau s})}{(s^2 + \omega^2)(s^2 + p_+^2)(s^2 + p_-^2)}, \text{ and}$$

$$X_2(s) = \frac{A_o \omega}{\frac{\rho_o^2 l e_1 l e_2}{A_1 A_2}} \frac{(1 - e^{-\tau s})}{(s^2 + \omega^2)(s^2 + p_+^2)(s^2 + p_-^2)}. \quad (19)$$

The expressions in equations (19) may be factored by partial fractions and can be simplified to

$$X_1(s) = \frac{A_o \omega}{\frac{\rho_o^2 l e_1}{A_1}} \left[ \frac{a_1 s + b_1}{s^2 + \omega^2} + \frac{c_1 s + d_1}{s^2 + p_+^2} + \frac{e_1 s + f_1}{s^2 + p_-^2} \right] (1 - e^{-\tau s}),$$

and

$$X_2(s) = \frac{A_o \omega}{\frac{\rho_o^2 l e_1 l e_2}{A_1 A_2}} \left[ \frac{a_2 s + b_2}{s^2 + \omega^2} + \frac{c_2 s + d_2}{s^2 + p_+^2} + \frac{e_2 s + f_2}{s^2 + p_-^2} \right] (1 - e^{-\tau s}); \quad (20)$$

where

$$a_1 = c_1 = e_1 = a_2 = c_2 = e_2 = 0,$$

$$b_1 = \frac{p_2^2 + p_{12}^2 - \omega^2}{(\omega^2 - p_+^2)(\omega^2 - p_-^2)},$$

$$d_1 = \frac{p_2^2 + p_{12}^2 + p_+^2}{(\omega^2 - p_+^2)(p_-^2 - p_+^2)},$$

$$f_1 = \frac{(\omega^2 - p_+^2)(\omega^2 - p_-^2)(p_-^2 - p_+^2) - (p_1^4 - p_+^4)(p_2^2 + p_{12}^2 + \omega^2)}{(\omega^4 - p_+^4)(\omega^2 - p_-^2)(p_-^2 - p_+^2)}$$

$$- \frac{(\omega^4 - p_-^4)(p_2^2 + p_{12}^2 - p_1^2)}{(\omega^4 - p_+^4)(\omega^2 - p_-^2)(p_-^2 - p_+^2)},$$

$$b_2 = \frac{1}{(p_+^2 - \omega^2)(p_-^2 - \omega^2)},$$

$$f_2 = \frac{(\omega^4 - p_+^4)}{(p_+^4 - \omega^4)(p_-^4 - \omega^4)(p_+^2 - p_-^2)}, \text{ and}$$

$$d_2 = \frac{1}{(p_+^2 - \omega^2)(p_+^2 - p_-^2)}.$$

Transformation of equation (20) into time domain yields

$$X_1(t) = \frac{A_0}{\frac{\rho_0 l e_1}{A_1} (\omega^2 - p_+^2)(\omega^2 - p_-^2)} \left\{ [a_x \sin \omega t + b_x \sin p_+ t + c_x \sin p_- t]u(t) - [a_x \sin \omega(t - \tau) + b_x \sin p_+(t - \tau) + c_x \sin p_-(t - \tau)]u(t - \tau) \right\}, \text{ and}$$

$$\begin{aligned}
 X_2(t) = & \frac{A_0 \frac{\rho_0 c^2}{V_1}}{\frac{\rho_0^2 l e_1 l e_2}{A_1 A_2} (\omega^2 - p_+^2)(\omega^2 - p_-^2)} \left\{ [\text{Sin } \omega t + b_y \text{ Sin } p_+ t \right. \\
 & + c_y \text{ Sin } p_- t] u(t) - [\text{Sin } \omega(t - \tau) + b_y \text{ Sin } p_+(t - \tau) \\
 & \left. + c_y \text{ Sin } p_-(t - \tau)] u(t - \tau) \right\} ; \quad (21)
 \end{aligned}$$

where the coefficients are defined as

$$a_x = p_2^2 + p_{12}^2 - \omega^2 ,$$

$$b_x = \frac{(p_2^2 + p_{12}^2 - p_+^2)(\omega^2 - p_-^2) \omega}{(p_-^2 - p_+^2) p_+} ,$$

$$c_x = \frac{(\omega^2 - p_+^2)(\omega^2 - p_-^2)(p_-^2 - p_+^2) - (p_2^2 + p_{12}^2 - \omega^2)(p_-^4 - p_+^4)}{(\omega^2 + p_+^2)(p_-^2 - p_+^2)p_-}$$

$$- \frac{(\omega^4 - p_-^4)(p_2^2 + p_{12}^2 - p_+^2) \omega}{(\omega^2 + p_+^2)(p_-^2 - p_+^2)p_-} ,$$

$$b_y = \frac{(\omega^2 - p_-^2) \omega}{(p_-^2 - p_+^2) p_+} , \quad \text{and}$$

$$c_y = \frac{(\omega^4 - p_+^4) \omega}{(p_+^2 - p_-^2)(\omega^2 + p_+^2)p_-} .$$

Because of absence of the damping in the system the volume displacement equations (21) are very much simpler as compared to the equations (15). From these equations, the effect of undamped natural frequencies on the response can be evaluated.

Excitation Pressure Made up of Straight Lines on Neck  $N_1$   
and No Pressure on Neck  $N_2$

The excitation pressure  $P_1(t)$  is defined in Chapter III as

$$P_1(t) = \sum_{i=1}^n [\alpha_i + \beta_i(t - \tau_i)] u(t - \tau_i) \quad (22)$$

where

$n$  = number of discontinuities of  $P_1(t)$  on time axis,

$\alpha_i$  = jump in pressure,  $P_1(t)$  at time,  $t = \tau_i$ ,

$\beta_i$  = change in slope of pressure at time,  $t = \tau_i$ , and

$u(t - \tau_i)$  = unit step function such that  $P(t)$  multiplied by  $u(t - \tau_i)$  will have a value of zero for  $t < \tau_i$  and  $P(t)$  in the region  $t > \tau_i$ .

The Laplace transform of  $P_1(t)$  is

$$P_1(s) = \frac{1}{s^2} \sum_{i=1}^n [\alpha_i s + \beta_i] e^{-\tau_i s} \quad (23)$$

The excitation pressure on neck  $N_2$ ,

$$P_2(t) = 0, \quad \text{and hence} \quad P_2(s) = 0.$$

The expressions for the volume displacement response of the system may be reduced to the following form after substitution of equation (23) in equation (4):

$$X_1(s) = \frac{(s^2 + g_1 s + g_0) \sum_{i=1}^n (\alpha_i s + \beta_i) e^{-\tau_i s}}{\frac{\rho_0 l e_1}{A_1} s^2 [s^4 + B_3 s^3 + B_2 s^2 + B_1 s + B_0]}, \quad \text{and}$$

$$X_2(s) = \frac{p_1^2 (h_1 s + 1) \sum_{i=1}^n (\alpha_i s + \beta_i) e^{-\tau_i s}}{\frac{\rho_0 l e_2}{A_1} s^2 [s^4 + B_3 s^3 + B_2 s^2 + B_1 s + B_0]}; \quad (24)$$

where the coefficient of  $s$  in the denominator is defined by the equation (5a).

For the stable oscillatory response of the system, equation (24) can be reduced to the following form after utilizing equation (8)

$$X_1(s) = \frac{(s^2 + g_1 s + g_0) \sum_{i=1}^n (\alpha_i s + \beta_i) e^{-\tau_i s}}{\frac{\rho_0 l e_1}{A_1} s^2 [(s-a)^2 + b^2][(s-c)^2 + d^2]}, \text{ and}$$

$$X_2(s) = \frac{p_1^2 (h_1 s + 1) \sum_{i=1}^n (\alpha_i s + \beta_i) e^{-\tau_i s}}{\frac{\rho_0 l e_2}{A_2} s^2 [(s-a)^2 + b^2][(s-c)^2 + d^2]} ; \quad (25)$$

where  $(a \pm jb)$  and  $(c \pm jd)$  are the roots of polynomial equation (8).

These equations can be expanded in terms of the partial fractions as follows:

$$\frac{(s^2 + g_1 s + g_0)(\alpha_i s + \alpha_i)}{s^2 [(s-a)^2 + b^2][(s-c)^2 + d^2]} = \frac{a_i s + b_i}{s^2} + \frac{c_i s + d_i}{(s-a)^2 + b^2}$$

$$+ \frac{e_i s + f_i}{(s-c)^2 + d^2}, \quad \text{and}$$

$$\frac{(h_1 s + 1)(\alpha_i s + \beta_i)}{s^2 [(s-a)^2 + b^2][(s-c)^2 + d^2]} = \frac{A_i s + B_i}{s^2} + \frac{C_i s + D_i}{(s-a)^2 + b^2}$$

$$+ \frac{E_i s + F_i}{(s-c)^2 + d^2}. \quad (26)$$

The right side of this equation is reduced to a common denominator, and the like powers of  $s$  on both sides of the equation are

equated to obtain the following two sets of simultaneous matrix equations, (27) and (28).

Solution of these equations for the co-efficients is utilized along with equation (26) to reduce the response equation into the following form:

$$X_1(s) = \frac{1}{\frac{\rho_0 l e_1}{A_1}} \sum_{i=1}^n \left[ \frac{a_i s + b_i}{s^2} + \frac{c_i s + d_i}{(s-a)^2 + b^2} + \frac{e_i s + f_i}{(s-c)^2 + d^2} \right] e^{-\tau_i s}, \text{ and}$$

$$X_2(s) + \frac{p_1^2}{\frac{\rho_0 l e_2}{A_2}} \sum_{i=1}^n \left[ \frac{A_i s + B_i}{s^2} + \frac{C_i s + D_i}{(s-a)^2 + b^2} + \frac{E_i s + F_i}{(s-c)^2 + d^2} \right] e^{-\tau_i s}. \quad (29)$$

Transformation of the equations (29) into time domain by inverse transformation yields the following equations:

$$X_1(t) = \frac{1}{\frac{\rho_0 l e_1}{A_1}} \left\{ a_i + b_i(t - \tau_i) + \frac{e^{a(t - \tau_i)}}{b} \right.$$

$$\left. [ \Phi_2 \cos b(t - \tau_i) + \Phi_1 \sin b(t - \tau_i) \right.$$

$$\left. + \frac{e^{c(t - \tau_i)}}{d} [ \Psi_2 \cos d(t - \tau_i) + \Psi_1 \sin d(t - \tau_i) ] \right\}, \text{ and}$$

$$\begin{aligned}
 X_2(t) = \frac{p_1^2}{\frac{\rho_0 l e_2}{A_2}} & \left\{ A_i + B_i (t - \tau_i) + \frac{e^{a(t - \tau_i)}}{b} \right. \\
 & [\Phi_3 \sin b(t - \tau_i) + \Phi_4 \cos b(t - \tau_i)] \\
 & \left. + \frac{e^{c(t - \tau_i)}}{d} [\Psi_3 \sin d(t - \tau_i) + \Psi_4 \cos d(t - \tau_i)] \right\} ; (30)
 \end{aligned}$$

where

$$\Phi_1 = c_i a + d_i ,$$

$$\Phi_2 = c_i b ,$$

$$\Psi_1 = e_i c + f_i ,$$

$$\Psi_2 = e_i d ,$$

$$\Phi_3 = C_i a + D_i ,$$

$$\Phi_4 = C_i b ,$$

$$\Psi_3 = E_i c + F_i , \text{ and}$$

$$\Psi_4 = E_i d .$$

$$\begin{bmatrix}
 1 & 0 & 1 & 0 & 1 & 0 \\
 2(a+c) & -1 & 2c & 1 & -2a & 1 \\
 a^2 + b^2 + c^2 + d^2 + 4ac & -2(a+c) & d^2 & -2c & b^2 & -2a \\
 2[a(c^2 + d^2) + c(a^2 + b^2)] & -[a^2 + b^2 + c^2 + d^2 + 4ac] & 0 & -d^2 & 0 & -b^2 \\
 (a^2 + b^2)(c^2 + d^2) & -2[a(c^2 + d^2) + c(a^2 + b^2)] & 0 & 0 & 0 & 0 \\
 0 & (a^2 + b^2)(c^2 + d^2) & 0 & 0 & 0 & 0
 \end{bmatrix}
 \begin{bmatrix}
 a_i \\
 b_i \\
 c_i \\
 d_i \\
 e_i \\
 f_i
 \end{bmatrix}
 =
 \begin{bmatrix}
 0 \\
 0 \\
 \alpha_i \\
 a_i \alpha_i + \beta_i \\
 a_i \alpha_i + a_i \beta_i \\
 a_i \beta_i
 \end{bmatrix}
 \quad (27)$$



$$\begin{bmatrix}
 1 & 0 & 1 & 0 & 1 & 0 \\
 2(a+c) & 1 & -2c & -1 & 2a & 1 \\
 a^2+b^2+c^2 & -2(a+c) & -d^2 & -2c & b^2 & -2a \\
 \quad + d^2 + 4ac & & & & & \\
 -2[a(c^2+d^2) & a^2+b^2+c^2 & 0 & d^2 & 0 & b^2 \\
 \quad + c(a^2+b^2)] & \quad + d^2 + 4ac & & & & \\
 (a^2+b^2) \cdot & -2[a(c^2+d^2) & 0 & 0 & 0 & 0 \\
 (c^2+d^2) & \quad + c(a^2+b^2)] & & & & \\
 0 & (a^2+b^2) \cdot & 0 & 0 & 0 & 0 \\
 & (c^2+d^2) & & & & 
 \end{bmatrix}
 \begin{bmatrix}
 A_i \\
 B_i \\
 C_i \\
 D_i \\
 E_i \\
 F_i
 \end{bmatrix}
 =
 \begin{bmatrix}
 0 \\
 0 \\
 0 \\
 -c_1 \alpha_i \\
 c_1 \beta_i + \alpha_i \\
 \beta_i
 \end{bmatrix}
 \quad (28)$$

## APPENDIX B

### CALIBRATIONS AND LIST OF MAJOR INSTRUMENTATION

Three Altec condenser microphones, Tektronic dual beam oscilloscope, and C.E.C. oscillograph were used to measure and record the pressures. All the microphones were calibrated at the factory and the sensitivities are given by manufacturers as -54.5 DB (reference 1 volt per dyne per centimeter) for the frequencies of 10 to 4000 cycles per second. Conversion of these sensitivities into pressures gives 1.095 psf/volt. A test was conducted by arranging all the three microphones at the test end of the plane wave tube as shown in Figure 31 and measuring the responses for steady state pressures. It was found that there was a slight difference in the sensitivities. Table III shows the relative sensitivities at various frequencies. However, while recording in the oscillograph the sensitivities of all the three channels were compensated by adjusting the matching network so that all the response traces are to the same scale. They were not calibrated for the absolute sensitivities, since that was not necessary for this investigation.

The amplitude calibration was checked with the internal square wave calibrator of the scope and found to be satisfactory. In short, the calibrations of the recording instrumentation was satisfactory for the relative pressure response measurements.

TABLE III  
RELATIVE SENSITIVITIES OF MICROPHONES

Frequency cps	Microphone #1	Microphone #2	Microphone #3
20	0.50	0.51	0.50
30	0.49	0.52	0.50
40	0.54	0.58	0.57
50	0.56	0.56	0.55
60	0.45	0.48	0.47
70	0.62	0.66	0.63
80	0.38	0.40	0.39
90	0.81	0.87	0.84
100	0.34	0.37	0.36
110	0.71	0.76	0.73
120	0.37	0.40	0.40
130	0.31	0.34	0.32
140	0.62	0.65	0.66
150	0.30	0.31	0.30
160	0.75	0.80	0.77
170	0.28	0.31	0.30
180	0.35	0.36	0.36
190	0.34	0.35	0.35
200	0.24	0.25	0.24

## List of Major Instrumentation

Microphone System: Model 21BR150 condenser microphones; 165A bases;  
Model 526B power supply; manufacturer - Altec Lansing Corporation.

Dual Beam Oscilloscope: Model 502; manufacturer - Tektronix; serial  
number - 022893.

Low Frequency Function Generator: Model 202A; manufacturer -  
Hewlett-Packard; serial number - 037-09559.

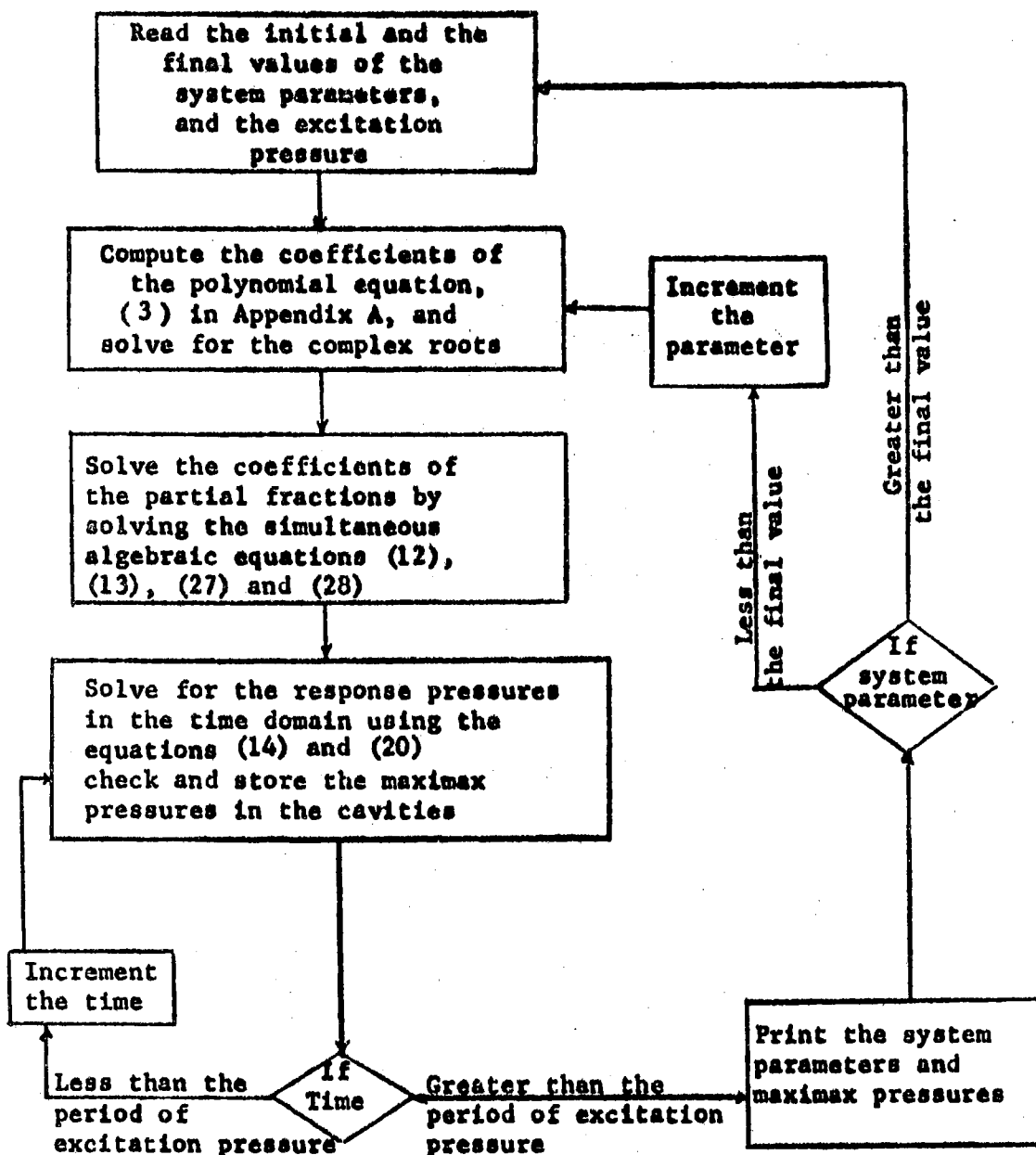
Tone Burst Generator: Type 1396-A; manufacturer - General Radio  
Company; serial number 354.

Power Amplifier: Model MC75; manufacturer - McIntosh.

Oscillograph: Model 5-124; manufacturer - Consolidated Electrodynamics  
Corporation; serial number 6307.

APPENDIX C

FLOW DIAGRAM OF COMPUTER PROGRAM FOR THE MAXIMAX RESPONSE  
OF DOUBLE ACOUSTICAL RESONATOR



VITA

Narayana N. Reddy

Candidate for the Degree of

Doctor of Philosophy

**Thesis:** RESPONSE SPECTRA OF COUPLED ACOUSTICAL RESONATOR TO  
TRANSIENT EXCITATION

**Major Field:** Mechanical Engineering

**Biographical:**

**Personal Data:** Born in Settahally, Mysore State, India,  
February 5, 1938, the son of Nanja Reddy and Veeramma.

**Education:** Graduated from Municipal High School, Anekal,  
Mysore, 1953; earned the Bachelor of Engineering degree  
in Mechanical Engineering from the University of Mysore,  
Mysore, 1960; earned the Master of Engineering degree in  
Aeronautical Engineering from the Indian Institute of  
Science, Bangalore, India, 1962; completed the requirements  
for the Doctor of Philosophy degree in Mechanical Engineer-  
ing in October, 1966.

**Professional Experience:** Aeronautical Engineer, Hindustan  
Aircraft Ltd., August, 1962, to January, 1964; Graduate  
Assistant, Oklahoma State University, September, 1964,  
to August, 1966.

**Organizations:** Member of Pi Tau Sigma, American Society of  
Mechanical Engineers, Acoustical Society of America.